Material Properties of Cold In-Place Recycled and Full-Depth Reclamation Asphalt Concrete

DETAILS

97 pages | 8.5 x 11 | PAPERBACK
ISBN 978-0-309-46580-9 | DOI 10.17226/24902

CONTRIBUTORS

Charles W. Schwartz, Brian K. Diefenderfer, and Benjamin F. Bowers; National Cooperative Highway Research Program; Transportation Research Board; National Academies of Sciences, Engineering, and Medicine

NATIONAL COOPERATIVE HIGHWAY RESEARCH PROGRAM

NCHRP RESEARCH REPORT 863

Material Properties of Cold In-Place Recycled and Full-Depth Reclamation Asphalt Concrete

Charles W. Schwartz
UNIVERSITY OF MARYLAND
College Park, MD

AND

Brian K. Diefenderfer
Benjamin F. Bowers
VIRGINIA TRANSPORTATION RESEARCH COUNCIL
Charlottesville, VA

Subscriber Categories
Construction • Maintenance and Preservation • Materials

Research sponsored by the American Association of State Highway and Transportation Officials
in cooperation with the Federal Highway Administration

The National Academies of
SCIENCES • ENGINEERING • MEDICINE

TRB
TRANSPORTATION RESEARCH BOARD

2017

NATIONAL COOPERATIVE HIGHWAY RESEARCH PROGRAM

Systematic, well-designed research is the most effective way to solve many problems facing highway administrators and engineers. Often, highway problems are of local interest and can best be studied by highway departments individually or in cooperation with their state universities and others. However, the accelerating growth of highway transportation results in increasingly complex problems of wide interest to highway authorities. These problems are best studied through a coordinated program of cooperative research.

Recognizing this need, the leadership of the American Association of State Highway and Transportation Officials (AASHTO) in 1962 initiated an objective national highway research program using modern scientific techniques—the National Cooperative Highway Research Program (NCHRP). NCHRP is supported on a continuing basis by funds from participating member states of AASHTO and receives the full cooperation and support of the Federal Highway Administration, United States Department of Transportation.

The Transportation Research Board (TRB) of the National Academies of Sciences, Engineering, and Medicine was requested by AASHTO to administer the research program because of TRB's recognized objectivity and understanding of modern research practices. TRB is uniquely suited for this purpose for many reasons: TRB maintains an extensive committee structure from which authorities on any highway transportation subject may be drawn; TRB possesses avenues of communications and cooperation with federal, state, and local governmental agencies, universities, and industry; TRB's relationship to the National Academies is an insurance of objectivity; and TRB maintains a full-time staff of specialists in highway transportation matters to bring the findings of research directly to those in a position to use them.

The program is developed on the basis of research needs identified by chief administrators and other staff of the highway and transportation departments, by committees of AASHTO, and by the Federal Highway Administration. Topics of the highest merit are selected by the AASHTO Special Committee on Research and Innovation (R&I), and each year R&I's recommendations are proposed to the AASHTO Board of Directors and the National Academies. Research projects to address these topics are defined by NCHRP, and qualified research agencies are selected from submitted proposals. Administration and surveillance of research contracts are the responsibilities of the National Academies and TRB.

The needs for highway research are many, and NCHRP can make significant contributions to solving highway transportation problems of mutual concern to many responsible groups. The program, however, is intended to complement, rather than to substitute for or duplicate, other highway research programs.

NCHRP RESEARCH REPORT 863

Project 09-51
ISSN 2572-3766 (Print)
ISSN 2572-3774 (Online)
ISBN 978-0-309-44671-6
Library of Congress Control Number 2017960991

COPYRIGHT INFORMATION

NOTICE

The research report was reviewed by the technical panel and accepted for publication according to procedures established and overseen by the Transportation Research Board and approved by the National Academies of Sciences, Engineering, and Medicine.

The opinions and conclusions expressed or implied in this report are those of the researchers who performed the research and are not necessarily those of the Transportation Research Board; the National Academies of Sciences, Engineering, and Medicine; or the program sponsors.

The Transportation Research Board; the National Academies of Sciences, Engineering, and Medicine; and the sponsors of the National Cooperative Highway Research Program do not endorse products or manufacturers. Trade or manufacturers' names appear herein solely because they are considered essential to the object of the report.

Published research reports of the

NATIONAL COOPERATIVE HIGHWAY RESEARCH PROGRAM

are available from

Transportation Research Board
Business Office
500 Fifth Street, NW
Washington, DC 20001

and can be ordered through the Internet by going to

http://www.national-academies.org

and then searching for TRB

Printed in the United States of America

The National Academies of
SCIENCES • ENGINEERING • MEDICINE

The **National Academy of Sciences** was established in 1863 by an Act of Congress, signed by President Lincoln, as a private, non-governmental institution to advise the nation on issues related to science and technology. Members are elected by their peers for outstanding contributions to research. Dr. Marcia McNutt is president.

The **National Academy of Engineering** was established in 1964 under the charter of the National Academy of Sciences to bring the practices of engineering to advising the nation. Members are elected by their peers for extraordinary contributions to engineering. Dr. C. D. Mote, Jr., is president.

The **National Academy of Medicine** (formerly the Institute of Medicine) was established in 1970 under the charter of the National Academy of Sciences to advise the nation on medical and health issues. Members are elected by their peers for distinguished contributions to medicine and health. Dr. Victor J. Dzau is president.

The three Academies work together as the **National Academies of Sciences, Engineering, and Medicine** to provide independent, objective analysis and advice to the nation and conduct other activities to solve complex problems and inform public policy decisions. The National Academies also encourage education and research, recognize outstanding contributions to knowledge, and increase public understanding in matters of science, engineering, and medicine.

Learn more about the National Academies of Sciences, Engineering, and Medicine at **www.national-academies.org**.

The **Transportation Research Board** is one of seven major programs of the National Academies of Sciences, Engineering, and Medicine. The mission of the Transportation Research Board is to increase the benefits that transportation contributes to society by providing leadership in transportation innovation and progress through research and information exchange, conducted within a setting that is objective, interdisciplinary, and multimodal. The Board's varied committees, task forces, and panels annually engage about 7,000 engineers, scientists, and other transportation researchers and practitioners from the public and private sectors and academia, all of whom contribute their expertise in the public interest. The program is supported by state transportation departments, federal agencies including the component administrations of the U.S. Department of Transportation, and other organizations and individuals interested in the development of transportation.

Learn more about the Transportation Research Board at **www.TRB.org**.

COOPERATIVE RESEARCH PROGRAMS

CRP STAFF FOR NCHRP RESEARCH REPORT 863

NCHRP PROJECT 09-51 PANEL
Field of Materials and Construction—Area of Bituminous Materials

AUTHOR ACKNOWLEDGMENTS

The research reported herein was performed under NCHRP Project 09-51 by the Department of Civil and Environmental Engineering at the University of Maryland—College Park, MD (UMD), with the Virginia Transportation Research Council (VTRC), Wirtgen GmbH, and Colas Solutions Inc. The report was authored by Dr. Charles W. Schwartz, UMD (Principal Investigator), Dr. Brian K. Diefenderfer, Associate Principal Research Scientist, VTRC (Co-Principal Investigator), and Dr. Benjamin F. Bowers, Research Scientist, VTRC. Mr. Mike Marshall (Wirtgen GmbH) and Mr. Todd Thomas (Colas Solutions Inc.) also contributed to the work described in this report. The work was done under the general supervision of Dr. Schwartz at UMD.

The authors greatly appreciate the efforts of those who assisted with collecting field cores for this study. They include personnel from the following state departments of transportation: Colorado; Delaware; Illinois; Kansas; Maine; New York State; Utah; and Washington State; along with the West Virginia Division of Highways; Los Angeles County Department of Public Works; City of San Jose Department of Public Works; City of Edmonton Transportation Services; FHWA Eastern and Central Federal Lands Highway Divisions; Ministry of Transportation of Ontario; Blount Construction, S&ME, and Road Science Georgia (Georgia); S. Drain Engineering of Illinois; AMEC Environment and Infrastructure (Ontario); and Pavement Recycling Systems (California).

FOREWORD

By Edward Harrigan
Staff Officer
Transportation Research Board

This report presents procedures for determining material properties of cold-recycled asphalt mixtures for input to structural design and analysis programs and suggested Level 3 modulus values for these materials for use in pavement structural analyses with Pavement ME Design. The report will be of immediate interest to engineers in state highway agencies and industry with responsibility for structural design and analysis of pavements incorporating cold-recycled, asphalt-stabilized materials.

Highway agencies are placing increasing emphasis on sustainability, recycling, and making maximum use of existing pavement assets in rehabilitation strategies. Such emphasis has led agencies to explore the advantages of producing asphalt mixtures using cold-recycling technology, particularly cold in-place recycling (CIR), cold central-plant recycling (CCPR), and full-depth reclamation (FDR).

Recent improvements in asphalt emulsion chemistry that enable better aggregate coating, shorter curing times, and the elimination of solvents have substantially increased the applicability of mixtures produced by CIR, CCPR, and FDR. Unfortunately, minimal information is available on the material properties of these asphalt mixtures to facilitate the structural design of pavements incorporating stabilized base materials produced with these processes. In particular, the *Mechanistic-Empirical Pavement Design Guide (MEPDG)* developed under NCHRP Project 1-37A and now available as AASHTOWare Pavement ME Design provides only minimal guidance for using these processes and materials.

The objective of this research was to determine relevant properties of CIR, CCPR, and FDR materials with emulsified or foamed asphalt recycling/stabilizing agents for input into pavement structural design programs. The research was conducted by the University of Maryland, College Park, Maryland, with support from the Virginia Transportation Research Council, Charlottesville, Virginia. The project developed a small-scale testing procedure that permits the measurement of the dynamic modulus and repeated load permanent deformation characteristics of field-produced and cured asphalt-stabilized, cold-recycled mixtures. These properties were determined for cold-recycled materials sampled from field projects across the United States. Suggested Level 3 modulus inputs were developed by the research team for use in structural design and analysis programs. Finally, structural analyses were conducted with these inputs in Pavement ME Design that demonstrated the sensitivity of the test data to the different stabilizing agents used in the various field projects.

This report fully documents the research and includes one Appendix: Deviations from AASHTO TP 79-15.

CONTENTS

1 Summary

5 **Chapter 1** Introduction
5 1.1 Background
6 1.2 Study Objectives

8 **Chapter 2** Projects and Materials Investigated
8 2.1 Description of Projects
8 2.2 Description of Cores

13 **Chapter 3** Specimen Preparation and Testing Methods
13 3.1 Test Specimen Fabrication
16 3.2 Small-scale Test Specimen Geometry
18 3.3 Dynamic Modulus Testing
19 3.4 RLPD Testing

21 **Chapter 4** Dynamic Modulus Test Results
21 4.1 Outlier Analysis
22 4.2 Significance Testing of Dynamic Modulus Data at 10 Hz
25 4.3 Master Curve Analysis
30 4.4 Analysis of Fitting Parameters
32 4.5 Analysis of Phase Angle
37 4.6 Relationship between Stiffness and Mixture Properties

42 **Chapter 5** RLPD Test Results
42 5.1 RLPD Analysis
42 5.2 Outlier Analysis
45 5.3 RLPD Data Envelopes
48 5.4 Relationship between Rutting Susceptibility and Density

50 **Chapter 6** Performance Evaluation
50 6.1 The *Mechanistic-Empirical Pavement Design Guide*
51 6.2 Initial Comparisons
63 6.3 Rutting Performance Evaluation of All Cold-recycled Materials

69 **Chapter 7** Conclusions

72 References

74 Appendix

Note: Photographs, figures, and tables in this report may have been converted from color to grayscale for printing. The electronic version of the report (posted on the web at www.trb.org) retains the color versions.

SUMMARY

Material Properties of Cold In-Place Recycled and Full-Depth Reclamation Asphalt Concrete

Pavement recycling techniques, including cold in-place recycling (CIR), cold central-plant recycling (CCPR), and full-depth reclamation (FDR), are effective techniques for rehabilitating existing pavements or constructing new pavements while reducing construction costs, environmental impacts, and construction time. Emulsified asphalt or foamed asphalt can be used as a recycling agent for CIR and CCPR or as a stabilizing agent for FDR, but it is not clear if performance differences exist among the recycling techniques or recycling/stabilizing agents. In addition to using recycling/stabilizing agents, chemical additives such as hydraulic cement, lime, fly ash, or lime kiln dust may be added for some mixtures.

The lack of quantitative values for the engineering properties of CIR/CCPR/FDR materials that can be used with confidence in pavement structural design is a major impediment to more widespread use of these fast, cost-effective, and sustainable rehabilitation strategies. The *Mechanistic–Empirical Pavement Design Guide (MEPDG)* methodology developed under NCHRP Project 1-37A and implemented in the AASHTOWare Pavement ME Design software provides little guidance for using these processes. Accordingly, NCHRP Project 09-51 was undertaken to determine the relevant material properties for CIR/CCPR/FDR materials using bituminous stabilizing agents for mechanistic-empirical pavement design. Specifically, the determination of typical values of dynamic modulus (|E*|) and repeated load permanent deformation (RLPD) structural properties was the primary objective of this study, as these are the inputs required by the Pavement ME Design software. Although CIR/CCPR layers could be candidates for bottom-up fatigue cracking, very little in the literature suggests this as an important distress mode for the types of pavements considered in this study; thus, no fatigue characterization was performed for the cold-recycled materials.

An important complication is the effect of field curing on the properties of cold-recycled materials. Stiffness has been observed to increase substantially during field curing; it is assumed that permanent deformation resistance similarly increases during curing. Measurement of the structural properties of cold-recycled materials during design is problematic because of the difficulties of simulating field mixing, compaction, and curing conditions in the laboratory. Consequently, this study focused on the evaluation of typical structural properties (dynamic modulus, permanent deformation) of CIR/CCPR/FDR materials using bituminous stabilizing agents under field-mixed, field-compacted, and field-cured conditions via laboratory testing of field cores taken 12 or more months after placement.

Cores were obtained from 27 projects located throughout the United States and Canada. Projects were selected for coring if the recycled layer was approximately 12–24 months old at the time of sampling and a mix design was available for the recycled layer. The original intention was to find projects spanning a matrix of environmental conditions, recycling techniques, and recycling agents, but it was difficult to obtain cores from a sufficient number

of projects to meet all the desired criteria of the matrix. Within the timeframe of the study, cores were therefore sought from as many projects as possible that met the requirements of time since construction and availability of mix design. The final project mix included 15 CIR projects (three foamed and 12 emulsified asphalt), three CCPR projects (all emulsified asphalt), and six FDR projects (4 foamed and 2 emulsified asphalt). Project mixes also included a range of additives (cement, lime) and, in some cases, no additives.

The thin layers for most CIR/CCPR/FDR construction preclude testing of conventional full-size 100 mm diameter by 150 mm tall cylindrical specimens. Instead, small-scale cylindrical specimens were fabricated for testing. The small-scale cylindrical specimens enabled the same boundary conditions and specimen geometry for both dynamic modulus and RLPD testing. Cylindrical 50 mm diameter test specimens were extracted by sub-coring perpendicular to the long axis of a field core. Following the sub-coring procedure, the ends of the 50 mm diameter sub-cores were trimmed with a diamond wet saw to create a 110 mm tall specimen with flat ends. Tests conducted in this study and by others in previous studies found very good agreement between full-size (100 mm diameter, 150 mm length) and small-scale (50 mm diameter, 110 mm length) specimens for dynamic modulus testing.

Unconfined dynamic modulus testing of the cold-recycled materials was conducted on the small-scale cylindrical specimens extracted from field cores. The testing was performed generally in accordance with AASHTO TP 79. Modifications to the specification included a reduced set of temperatures (4.4°C, 21.1°C, and 37.8°C), the small-scale cylindrical specimens, and adjustments to the accepted test result variability.

RLPD testing of the cold-recycled materials also was conducted on small-scale cylindrical specimens extracted from field cores. A repeated deviator stress of 482.6 kPa was applied at a constant confining stress of 68.9 kPa. The testing was performed generally in accordance with AASHTO TP 79. Modifications to the test included a lower test temperature (45°C), the small-scale cylindrical specimen geometry, and adjustments to the accepted test result variability.

Predicted pavement performance was evaluated for all of the cold-recycled materials tested in this study. Two baseline pavement scenarios were considered: (1) a rehabilitated pavement having a cold-recycled inlay and (2) an asphalt surface wearing course and a rehabilitated pavement having a hot mix asphalt (HMA) recycled inlay and an asphalt surface wearing course. Three wearing course thicknesses with appropriate traffic levels and three climate scenarios were evaluated. All performance predictions were performed using Version 2.0 of the Pavement ME Design software with laboratory-measured (i.e., Level 1) dynamic modulus and RLPD property inputs for the cold-recycled inlay, the HMA inlay, and the asphalt surface wearing course. The investigation focused on rutting as the principal distress mode.

A significant result of this study is the development of an initial catalog of measured typical dynamic modulus and RLPD properties for bituminously stabilized CIR, CCPR, and FDR cold-recycled materials. Prior to this study, little was known regarding appropriate dynamic modulus and RLPD values for cold-recycled materials to use as inputs to mechanistic-empirical pavement design.

Another significant result of this study is the evaluation of differences in the measured dynamic modulus and RLPD properties of FDR, CIR, and CCPR mixtures using different recycling/stabilizing agents and chemical additives. These evaluations included statistical analyses (with a systematic procedure for eliminating outliers) and data envelopes. Data envelopes, bounded by the maximum and minimum average material property values, were developed to compare project and material types by visual observation. The data envelopes

are useful because the statistical analyses indicate only that a difference exists between project or material types, not the direction of the difference. The material properties for similar project or material types were grouped together. The groupings included recycling process, stabilizing/recycling agent, and presence or absence of chemical additives.

For dynamic modulus, the investigations included statistical analyses of |E*| data at 10 Hz and temperatures of 4.4°C, 21.1°C, and 37.8°C, as well as an evaluation of the data envelopes developed from the mixture master curves. The principal conclusions regarding stiffness derived from these investigations include the following:

- All three recycling processes had a similar range of dynamic modulus values at intermediate and high reduced frequencies. Many highway agencies specify lower structural values (whether layer coefficients or moduli) for FDR than for CIR and CCPR; these lower values may be too conservative.
- FDR showed less temperature dependency and higher stiffness at low reduced frequencies (or higher temperatures). The likely cause is that CIR and CCPR are composed mostly or entirely of RAP (reclaimed asphalt pavement) and the temperature dependency of stiffness is controlled by the existing RAP binder.
- The master curve data envelopes exhibited much overlap between emulsified asphalt versus foamed asphalt as stabilizing/recycling agents and no significant difference was shown by the statistical tests. Visual observations of the master curve data envelopes suggest that recycled mixtures using foamed asphalt as the stabilizing/recycling agent may be slightly stiffer at higher temperatures whereas recycled mixtures using emulsified asphalt as the stabilizing/recycling agent may be slightly stiffer at lower temperatures.
- The master curve data envelopes showed that the presence of a chemical additive generally increased the dynamic modulus values of the recycled mixtures as compared to mixtures with no chemical additive. When separating the recycling process, the recycling/stabilizing agent and, the use of chemical additives, significant differences were shown.
- No significant difference was found when comparing the use of hydraulic cement versus lime as a chemical additive at 21.1°C and 37.8°C; however, only the CIR process had projects that used both hydraulic cement and lime as a chemical additive.
- The master curve data envelopes showed that the presence of a chemical additive generally reduced the temperature dependency of stiffness for the cold-recycled materials. Although an increased temperature dependency was found for those mixtures having no chemical additive, no clear trend was shown by the statistical tests.
- The presence of chemical additives was found to be beneficial with respect to stiffness even though the materials used for testing were 12–24 months old. This finding suggests that the benefits of chemical additives last beyond the initial performance period.
- The acceptable coefficient of variation (COV) from AASHTO TP 79 does not adequately reflect the typical variation seen in recycled materials. The allowable variation needs further study for cold-recycled materials.

No strong correlations were found between mixture characteristics (e.g., volumetrics, gradation, density) and stiffness. This result likely is a consequence of the small number of mixtures given the large range of processing types, stabilizing agents, and chemical additives.

The slope and intercept properties of the RLPD data (in log-log space) were evaluated using the same techniques as for dynamic modulus. The principal conclusions regarding RLPD properties include the following:

- All three recycling processes had similar RLPD characteristics as defined by their data envelopes. CIR and CCPR were found to behave very similarly. FDR was found to exhibit

4 Material Properties of Cold In-Place Recycled and Full-Depth Reclamation Asphalt Concrete

lower permanent deformations than CCPR and CIR in some cases. This finding is consistent with the trends in the dynamic modulus envelopes.
- Emulsified asphalt and foamed asphalt stabilizers performed similarly in terms of RLPD. This result is consistent with the trends in the dynamic modulus envelopes.
- The data envelopes showed that the presence of chemical additives generally increased the resistance to permanent deformation. In particular, cement reduced the amount of permanent deformation exhibited by the recycled materials.
- The presence of chemical additives was found to be beneficial even though the materials used for testing were 12–24 months old. This finding suggests that the benefits of chemical additives last beyond the initial performance period.
- The acceptable COV from AASHTO TP 79 does not adequately reflect the typical variation seen in recycled materials. The allowable variation needs further study for cold-recycled materials.

No strong correlations were found between slope and intercept values and density. This result is most likely a consequence of the small number of mixtures given the large range of processing types, stabilizing agents, and chemical additives.

Predicted rutting performance was evaluated for all of the cold-recycled materials considered in this study and compared against predicted rutting for an equivalent conventional HMA rehabilitation scenario. Conclusions drawn from the rutting predictions for the cold-recycled mixtures considered in this study include the following:

- The predicted rutting performance of the cold-recycled sections generally fell within acceptable ranges. Thirty percent of the analysis cases exhibited poor rutting performance; most of these cases were sections with a thin HMA surface wearing course.
- Predicted rutting for the cold-recycled inlay scenarios decreased as HMA surface wearing course thickness increased. As the cold-recycled layer is pushed deeper into the pavement structure, rutting approaches that of the HMA inlay reference scenario.
- Cold-recycled materials that exhibited poor laboratory RLPD behavior (e.g., high traffic exponent k_3, high temperature susceptibility exponent k_2) also exhibited poor predicted rutting performance.
- The asphalt mixture performance tester (AMPT) used for laboratory testing in this study did not report the resilient strains during RLPD testing, so these were estimated based on the measured unconfined dynamic modulus modified to correct for the influence of confining stresses in the RLPD test. It is recommended that future testing use an AMPT that directly reports the resilient strains in the RLPD test. Alternatively, the dynamic modulus tests could be performed under confined rather than unconfined conditions so that the appropriate resilient strains can be estimated more accurately.

Rehabilitated pavement sections having good quality cold-recycled materials and a moderately thick HMA surface wearing course (e.g., 2 in. thick or greater) exhibited predicted pavement performance comparable to that of conventional HMA rehabilitated sections.

CHAPTER 1

Introduction

1.1 Background

Pavement recycling techniques, including cold in-place recycling (CIR), cold central-plant recycling (CCPR), and full-depth reclamation (FDR), are effective techniques for rehabilitating existing pavements or constructing new pavements while reducing the construction costs, environmental impacts, and construction time (Bemanian et al. 2006; Thenoux et al. 2007; Stroup-Gardiner 2011). The use of these techniques is not widespread, however, partially because of the lack of quantitative values for the engineering properties that can be used with confidence for pavement structural design. In addition, the measurement of relevant structural properties can be problematic given the lack of consensus and difficulties of simulating field mixing, compaction, and curing conditions in the laboratory.

Emulsified asphalt or foamed asphalt can be used as a recycling agent for CIR and CCPR or as a stabilizing agent for FDR, but it is not clear if performance differences exist among the recycling techniques or recycling/stabilizing agents. In addition to using recycling/stabilizing agents, chemical additives such as hydraulic cement, lime, fly ash, or lime kiln dust may be added for some mixtures. Chemical additives often are included in mixtures to improve early strength and improve resistance to the detrimental effects of moisture, as well as for other potential uses (Asphalt Academy 2009; ARRA 2014); however, it is not well established whether the chemical additives contribute positively to the long-term performance of recycled mixtures.

CIR often is used to rehabilitate existing asphalt pavements by recycling a portion of the existing bound layers to a depth of 2 in. to 5 in. (ARRA 2014). CIR may be completed using a single-unit train, wherein the milling and recycling agent addition processes (and blending of chemical additives, if used) are incorporated into a single machine. CIR also may be completed using a multi-unit train that includes a cold planer, a screening and crushing unit, and a pug mill unit. For either process, the resulting material may be picked up from a windrow into a conventional paver or deposited directly into a paver hopper.

CCPR is similar to CIR, but the recycling agent and secondary additives (if used) are added at a mobile plant located at or near the recycling project or RAP source stockpile. If the source material for the CCPR process comes directly from an existing pavement, the materials are milled, processed at the CCPR plant, and then placed using traditional asphalt mixture paving equipment. If the source material for the CCPR process is an existing RAP stockpile, the mobile plant can be centrally located, and processed material can be hauled to the construction project and placed using traditional asphalt mixture paving equipment. CCPR is advantageous because materials from an existing project can be removed and stockpiled, thus allowing access to stabilize or replace the underlying foundation, if needed. Additionally, the CCPR process can be used to (1) place multiple lifts for thicker applications of recycled materials and (2) produce a recycled base course for new construction projects, including lane widening, shoulder strengthening,

and other uses. Typical layer thicknesses for CCPR range from 2 in. to 6 in. (ARRA 2014), but multiple lifts may be used to increase the total thickness of the recycled material.

If deeper structural deficiencies are encountered, FDR can be used to reconstruct a pavement section by recycling a portion of the existing bound and unbound layers. FDR is used to stabilize a layer between 4 in. and 12 in. thick (ARRA 2014). The FDR process is completed using a reclaimer, motor grader, and compaction equipment. FDR can be advantageous because it provides a foundation layer that can aid in reducing the strain in the overlying pavement under load but at a lower cost than complete replacement with conventional base materials (Diefenderfer et al. 2016).

Despite the many advantages of incorporating pavement recycling techniques into pavement rehabilitation or new construction projects, for many reasons, highway agencies generally have not widely embraced these processes (Stroup-Gardiner 2011; Diefenderfer and Bowers 2015). These reasons include a lack of familiarity with the processes, hesitation to try processes still thought to be experimental, inconsistencies with specifications across agencies, limited long-term field performance data, and a lack of consensus about the fundamental engineering properties used for pavement design, among others.

Much published work related to determining the fundamental engineering properties of recycled materials has focused on measuring either the stiffness of an asphalt-like material (Kim et al. 2009; Diefenderfer and Link 2014) or the shear properties of a stabilized aggregate-like material (Jenkins et al. 2007). Given that ongoing work has shown that recycled materials can successfully be incorporated as a load-bearing layer within a heavily trafficked pavement (Diefenderfer, Bowers, and Diefenderfer 2015; Diefenderfer et al. 2017), a need exists to assess the permanent deformation properties using test procedures that can relate the two perspectives.

1.2 Study Objectives

The lack of quantitative values for the engineering properties of CIR/CCPR/FDR materials that can be used with confidence in pavement structural design is a major impediment to more widespread use of these fast, cost-effective, and sustainable rehabilitation strategies. The *Mechanistic–Empirical Pavement Design Guide (MEPDG)* methodology developed under NCHRP Project 1-37A and now available as the AASHTOWare Pavement ME Design software provides little guidance for using these processes (AASHTO 2015). This study was undertaken to determine the relevant material properties for CIR/CCPR/FDR materials using bituminous stabilizing agents for pavement structure design.

The determination of typical values of dynamic modulus (stiffness) and permanent deformation structural properties is the primary objective of this study, as these are the inputs required for mechanistic-empirical pavement structural design. Although CIR/CCPR layers could be candidates for bottom-up fatigue cracking, very little in the literature suggests this as an important distress mode for the types of pavements considered in this study. The exceptions cited in the literature are primarily from South Africa, where the pavements have high stress-to-strength ratios because of the thin surfacing over the CIR coupled with high traffic/load levels. In the United States, only very lightly trafficked roads are likely to have thin surfacing over the CIR/CCPR layer. Most other pavements—and specifically the types of higher traffic volume pavements that would be designed using the *MEPDG,* the focus of this study—will have moderately thick HMA surface/wearing courses that will suppress stress ratios below the threshold at which fatigue cracking develops. The stiffness of the recycled materials was quantified by conducting dynamic modulus tests. The rutting susceptibility was quantified by conducting RLPD tests.

A final and important complication is the effect of field curing on the properties of cold-recycled materials. Stiffness has been observed to increase substantially during field curing; it is assumed that permanent deformation resistance similarly increases during curing. Measurement of the structural properties of cold-recycled materials during design is problematic because of the difficulties of simulating field mixing, compaction, and curing conditions in the laboratory. Consequently, this study focuses on the evaluation of typical structural properties (dynamic modulus, permanent deformation) of CIR/CCPR/FDR materials using bituminous stabilizing agents under field-mixed, compacted, and cured conditions via laboratory testing of field cores taken 12 or more months after placement.

CHAPTER 2

Projects and Materials Investigated

2.1 Description of Projects

Cores were obtained from 27 projects located throughout the United States and Canada. Projects were selected for coring if the recycled layer was approximately 12–24 months old at the time of sampling and a mix design was available for the recycled layer. Originally, the project team sought projects that would fulfill a matrix of environmental conditions, recycling techniques, and recycling agents. During the course of the study, the project team found it difficult to obtain cores from a sufficient number of projects to meet all the desired criteria of the project matrix. Consequently, the project team sought cores from as many projects as possible within the time frame of the study; however, cores from projects were only included that met the requirements of time since construction and availability of mix design. Figure 1 shows the distribution of projects and the recycling techniques. Not all the cores from projects identified in Figure 1 were used, as some were damaged during coring or shipment, or were unsuitable for other reasons.

Table 1 provides a summary of the locations and types of recycled mixtures for each project. From the table it can be seen that 15 CIR, three CCPR, and six FDR projects were included. Among the CIR projects, three included foamed asphalt as a recycling agent while 12 included emulsified asphalt. Two of the CIR projects using foamed asphalt included no chemical additive, whereas one project included cement. Four of the CIR projects using emulsified asphalt included lime as a chemical additive, two projects included cement, and five projects included no chemical additive. All three CCPR projects used emulsified asphalt as the recycling agent. Of these, two projects included cement as a chemical additive and the third used no chemical additive. Of the six FDR projects, four projects used foamed asphalt as the stabilizing agent and two projects used emulsified asphalt. All four of the FDR projects using foamed asphalt and one of the two FDR projects using emulsified asphalt included cement as a chemical additive. The other FDR project using emulsified asphalt included no chemical additive.

2.2 Description of Cores

The project team sought cores from projects where a mix design was completed and where the volunteer agency had the ability to collect the cores. During the course of the study, between seven and ten 6-in. diameter cores were received from each of 26 projects. For all projects but one, the volunteer agency collected all cores and shipped them to the project team. The VTRC research team collected the cores from the CIR project in West Virginia. Most of the cores included all overlying surface layers, recycled layers, and underlying bound layers (if any existed).

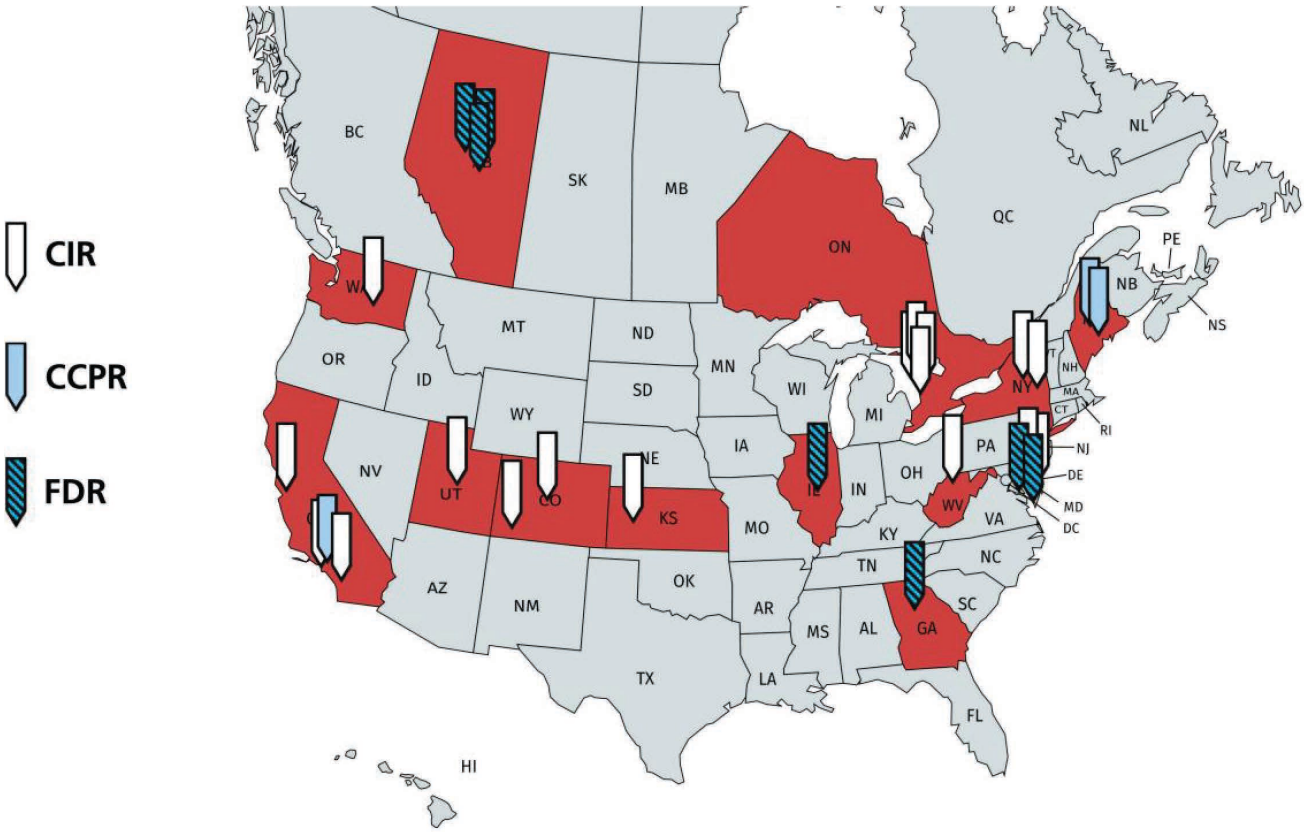

Figure 1. Approximate locations of recycling projects.

For shipping, the project team had suggested that each core be wrapped in plastic wrap, placed inside a 6-in. diameter concrete cylinder mold, cushioned in bubble wrap, and boxed. Most cores prepared in this way arrived undamaged from the shipping process and were suitable for testing. Figure 2 and Figure 3 show sample intact cores from two projects. Some cores from the projects in Illinois and New York (see Figure 1) were damaged during shipping and were not used for subsequent testing.

As seen in Figures 2 and 3, the recycled layer on most cores was received in good condition. In some cases, where the recycled layer was at the bottom of the core, the full thickness of the recycled layer was not always retrieved. Figure 4 shows a core in which a portion of the bottom of the FDR layer (seen at the top of the photo) was not retrieved during the coring process. It is not possible to determine if this issue was caused by insufficient curing of the recycled layer or was an artifact of the coring process. Despite some missing material, such cores could be used to obtain test specimens provided sufficient material remained elsewhere within the core.

Figure 5 shows an example of the surface layer separated from the recycled layer in a core from an FDR project from Edmonton, Alberta, Canada. It is not possible to tell if this separation was a construction defect or a result of the coring process, but if the core is representative of the entire project, the performance of this section certainly would be expected to be compromised. All eleven cores from this project had a debonded surface layer, suggesting that the issue was widespread. The debonded condition did not, however, affect the research team's ability to obtain a test specimen for this project.

10 Material Properties of Cold In-Place Recycled and Full-Depth Reclamation Asphalt Concrete

Table 1. Details of recycling projects.

Location	Constr. Year	Project ID	Project Description (Road, city, town, or county)	Type	Primary Recycling Agent	Chemical Additive
Kansas	2012	13-1093	Scott County	CIR	Emulsion	Lime
Ontario	2012	13-1111	Highway 10/89	CIR	Foam	--
Ontario	2012	13-1112	Highway 21 (Tiverton to Port Elgin)	CIR	Foam	--
Ontario	2012	13-1113	Highway 24	CIR	Emulsion	--
Ontario	2012	13-1114	Highway 21 (Amberley to Kincardine)	CCR	Emulsion	--
Alberta	2012	13-1115	Dovercourt, 141 Street (Edmonton)	FDR	Foam	Cement
Alberta	2012	13-1116	Windsor Park 1, 92 Avenue (Edmonton)	FDR	Foam	Cement
Alberta	2012	13-1117	Windsor Park 2, 117 Street (Edmonton)	FDR	Foam	Cement
California	2012	13-1124	Redmond Avenue (San Jose)	CIR	Foam	Cement
Colorado	2012	13-1127	State Highway 83	CIR	Emulsion	Lime
California	2012	14-1001	50th Street West (Los Angeles)	CCPR	Emulsion	--
California	2012	14-1002	Vasquez Canyon Road (Los Angeles)	CIR	Emulsion	Cement
California	2012	14-1003	Altadena Drive (Los Angeles)	CIR	Emulsion	--
West Virginia	2013	14-1011	Fort Martin Road	CIR	Emulsion	Cement
Delaware	2013	14-1025	Seashore Highway (Lewes to Georgetown)	CIR	Emulsion	--
Delaware	2013	14-1026	Gravel Hill Road	CIR	Emulsion	--
Delaware	2013	14-1027	Springfield Road	FDR	Emulsion	--
Delaware	2013	14-1028	Sussex Pine Road	FDR	Emulsion	Cement
Utah	2013	14-1055	State Route 32	CCR	Emulsion	Lime
Georgia	2012	14-1057	Kelly Mill Road	FDR	Foam	Cement
Washington State	2013	14-1058	State Route 14	CIR	Emulsion	Lime
Colorado	2013	14-1062	State Highway 160 (Cortez)	CCR	Emulsion	Lime
Maine	2013	15-1001	(Lyman)	CCPR	Emulsion	Cement
Maine	2013	15-1002	(Corinna, Exeter)	CCPR	Emulsion	Cement

Figure 2. Core obtained from FDR project in Delaware.

Figure 3. Core obtained from CIR project in West Virginia.

Figure 4. Core from FDR project in Delaware showing missing portion of recycled layer.

Figure 5. Core from FDR project in Edmonton showing a debonded surface layer.

CHAPTER 3

Specimen Preparation and Testing Methods

To focus on the desired structural properties of the recycled materials, the dynamic modulus and RLPD tests were performed to investigate the stiffness and rutting susceptibility, respectively, of each test specimen. Before testing, the project team had to decide if the testing and expected properties of the recycled materials best matched those of an asphalt mixture or of a loosely bound granular material. In reality, the field performance probably lies somewhere between the two extremes. For this study, the project team decided that testing the materials assuming asphalt mixture-like behavior was the proper path. This decision was based on previous experience with these materials and the following observations: (1) the stiffness values of the recycled materials often were very near those of asphalt mixtures (and were thus greatly underrepresented in previous versions of the *MEPDG*), and (2) the stiffness values were found to vary with respect to changes in temperature like an asphalt mixture and unlike a granular material.

3.1 Test Specimen Fabrication

After the cores were unboxed, allowed to dry in ambient laboratory conditions, and photographed, test specimens were fabricated. Following the procedures outlined in Bowers, Diefenderfer, and Diefenderfer (2015), small-scale cylindrical specimens were fabricated for testing. Small-scale cylindrical specimens were used based on the research team's desire to have the same boundary conditions and use the same specimen geometry for all laboratory tests. Cylindrical 50 mm diameter test specimens were extracted by sub-coring perpendicular to the long axis of a field core using a sample holder as shown in Figure 6. The field core was fastened horizontally beneath a hollow drill bit with a nominal 50 mm interior diameter. If the recycled layer was of sufficient thickness, multiple 50 mm diameter sub-cores were obtained. Figure 7 shows a series of specimens from which sub-cores were extracted. Before adopting the small-scale cylindrical test specimen geometry, a series of comparisons with full-size specimens was performed.

Following the sub-coring procedure, the ends of the 50 mm diameter sub-cores were trimmed with a diamond wet saw to create a 110 mm tall specimen with flat ends. The trimming process was performed so that an equal portion of each end was removed. The trimmed specimens were next placed in a forced-draft oven at 40°C for approximately 24 hours to remove any surface water added during the sub-coring and trimming steps. The specimens were then further dried in accordance with AASHTO PP 75, Standard Practice for Vacuum Drying Compacted Asphalt Specimens, to ensure that any internal water was removed without further aging the test specimens.

After the test specimens were dried, the diameter and length of each specimen was measured at four locations around its perimeter and at three locations along its length. The bulk density was then determined from these measurements and the mass of the test specimen.

Table 2 shows the average bulk density of the test specimens from each project location.

Figure 6. Core drill sample holder used to extract small-scale cylindrical specimens from a field core.

Next, the bulk specific gravity of each test specimen was determined in accordance with AASHTO T 331, Standard Method of Test for Bulk Specific Gravity (G_{mb}) and Density of Compacted Hot Mix Asphalt (HMA) Using Automated Vacuum Sealing Method. The average bulk specific gravity from each project location also is shown in Table 2.

Once the bulk specific gravity was determined, the test specimens were subdivided for dynamic modulus or RLPD testing. The test specimens were divided assuming that their parent cores were taken sequentially along the length of a project. Thus, the project team distributed the test specimens such that the tests would represent conditions from the entire length of the project.

Figure 7. Field cores from which test specimens were extracted.

Table 2. Average bulk density and bulk specific gravity of test specimens.

Location	Project ID	Average Bulk Density (lb./ft.^{3})	Coefficient of Variation (%)	Average Bulk Specific Gravity (g/cm^3)	Coefficient of Variation (%)
Kansas	13-1093	127.0	1.5	2.045	0.04
Ontario	13-1111	130.4	3.2	2.097	0.06
Ontario	13-1112	134.2	2.4	2.151	0.06
Ontario	13-1113	134.1	1.8	2.144	0.02
Ontario	13-1114	136.1	3.4	2.183	0.09
Alberta	13-1115	119.4	0.8	1.971	0.02
Alberta	13-1116	124.8	1.8	2.030	0.04
Alberta	13-1117	126.7	2.2	2.062	0.04
California (San Jose)	13-1124	130.7	4.8	2.155	0.06
Colorado	13-1127	127.6	1.9	2.053	0.04
California (Los Angeles)	14-1001	136.8	4.8	2.155	0.13
California (Los Angeles)	14-1002	118.6	0.9	1.927	0.03
California (Los Angeles)	14-1003	134.7	2.6	2.174	0.05
West Virginia	14-1011	123.3	4.0	1.967	0.09
Delaware	14-1025	138.6	2.7	2.242	0.06
Delaware	14-1026	138.4	2.7	2.256	0.07
Delaware	14-1027	136.5	2.7	2.220	0.05
Delaware	14-1028	127.3	3.4	2.063	0.07
Utah	14-1055	129.1	3.1	2.057	0.08
Georgia	14-1057	124.2	2.8	2.003	0.06
Washington State	14-1058	131.9	0.7	2.122	0.07
Colorado	14-1062	126.9	2.5	2.019	0.09
Maine (Lyman)	15-1001	128.4	4.8	2.085	0.06
Maine (Corinna, Exeter)	15-1002	130.5	1.6	2.095	0.04

3.2 Small-scale Test Specimen Geometry

The |E*| and RLPD tests frequently are performed using the AMPT. In accordance with AASHTO PP 60, the |E*| and RLPD test specimen geometry must be nominally 100 mm in diameter and 150 mm in height, and the specimens are cored from mixtures compacted using the Superpave Gyratory Compactor. Test specimens having this geometry can be produced using gyratory compacted samples, but it is much more difficult to attain the specified size from field cores because most pavement layers are placed at a lift thickness less than or equal to 150 mm. Given this limitation, many efforts have been made to evaluate alternate specimen geometries for calculating the dynamic modulus values of road cores such as prisms (Pellinen et al. 2006) or by testing in indirect tensile mode (Kim et al. 2004).

During the course of this project, a study by Li and Gibson (2013) investigated the use of small-scale cylindrical specimens for dynamic modulus testing and found a good correlation to full-size specimens. These specimens were 38 mm in diameter and 110 mm or 140 mm in height. The benefit of using cylindrical specimens is that the boundary conditions are generally the same as those in the full-size specimen; thus, the RLPD testing should be feasible using this geometry (whereas prismatic specimens or indirect tensile geometries would not allow the same specimen type to be used for dynamic modulus and RLPD testing). Bowers et al. (2015) and Diefenderfer and Bowers (2015) furthered the work of Li and Gibson (2013) and found strong agreement between full-size and small-scale (50 mm diameter, 110 mm length) specimens for dynamic modulus testing.

Dynamic modulus and RLPD testing for this study were performed in a commonly used AMPT. Because the research team was using small-scale specimens, some test fixture components had to be custom-machined to accommodate the reduced specimen size before testing. Specifically, custom arms for the linear variable displacement transducer (LVDT) stud gluing jig and reduced diameter testing platens for the AMPT were manufactured from aluminum (see Figure 8 and Figure 9, respectively).

Figure 8. LVDT stud gluing jig showing custom arms.

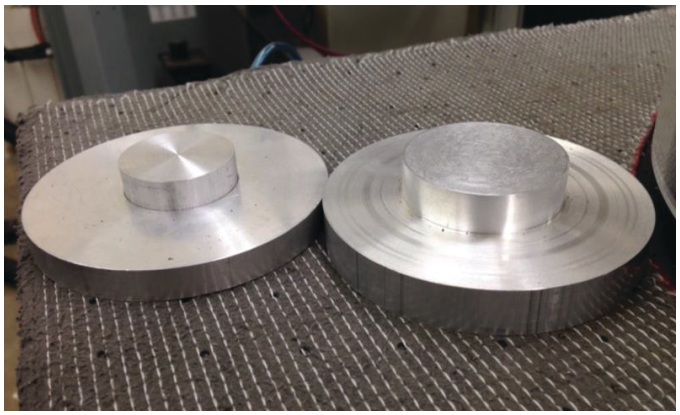

Figure 9. AMPT testing platens with removable pacer blocks for 38 mm and 50 mm diameter small-scale specimens.

A unique set of gluing jig arms was needed for the small-scale specimens because of their decreased diameter. The upper portion of each gluing jig arm had to be extended so that the arm could apply pressure to the LVDT stud as it was being glued to the specimen. For the 50 mm diameter specimens, the upper portions of the arms were extended by approximately 25 mm. All other dimensions for the custom arms were the same as for the stock gluing arms.

The custom testing platens for the AMPT were also machined to facilitate centering the specimen during testing. A unique set of platens was fabricated to match the diameter of the small-scale specimens. Removable spacer blocks, used as the lower support for the small-scale specimens, also were manufactured for the different specimen heights. Testing was conducted using standard LVDT gauges and studs; the LVDT stud spacing was 70 mm. Figure 10 shows an example of a CCPR specimen ready for testing.

Figure 10. Test specimen from Maine CCPR project ready for dynamic modulus testing.

18 Material Properties of Cold In-Place Recycled and Full-Depth Reclamation Asphalt Concrete

3.3 Dynamic Modulus Testing

The relationship between stress and strain under continuously applied sinusoidal loading for a linear viscoelastic material is defined as the *complex modulus* (E*) with the absolute value of this term defined as the *dynamic modulus* (|E*|). The dynamic modulus also may be defined as the maximum dynamic stress (σ_0) divided by the peak recoverable axial strain (ε_0). Given that asphalt mixtures are viscoelastic materials, the peak strain will lag behind the peak stress by an amount that depends on the properties of the materials, the test temperature, and the loading frequency. This relationship can be expressed as follows:

$$E^* = |E^*|\cos(\phi) + i|E^*|\sin(\phi) \quad (1)$$

For a purely elastic material, ϕ will equal zero and the complex modulus E* will equal the dynamic modulus |E*|; for a purely viscous material, ϕ will equal 90°. Additional information can be found in Witczak et al. (2002).

Unconfined dynamic modulus testing was conducted on the small-scale cylindrical specimens extracted from the field cores. The test was performed generally in accordance with AASHTO TP 79. Modifications to the specification included using a reduced set of temperatures (4.4°C, 21.1°C, and 37.8°C), using small-scale cylindrical specimens, and adjustments to the accepted test result variability. The specimen preparation and test procedures for the small-scale specimens are detailed in Bowers et al. (2015); this procedure incorporates a slight deviation from AASHTO TP 79-15, Appendix X3, by using 50 mm diameter specimens in lieu of smaller (38 mm diameter) specimens. An evaluation of the small-scale specimen geometry found that a larger diameter test specimen better correlated with full-size specimens when using larger particle sizes (Bowers, Diefenderfer, and Diefenderfer 2015). Testing was conducted at loading frequencies of 25 Hz, 10 Hz, 5 Hz, 1 Hz, 0.5 Hz, and 0.1 Hz at each of the three temperatures.

Approximately 80% of the dynamic modulus tests at 10 Hz had a within-batch COV of less than 20% for the tests at 4.4°C and 21.1°C. For approximately 5% of the tests at 10 Hz at 4.4°C and 21.1°C, the within-batch COV was higher than 50%. At the 37.8°C test temperature, approximately 45% of the tests had a within-batch COV less than 20%; however, the percentage of tests with a COV greater than 50% was similar to that at other test temperatures. Generally, larger COVs were found at the higher test temperatures and lower test frequencies.

AASHTO TP 79 defines an acceptable range of COV from 9% to 24% for a single operator testing asphalt mixtures having a 25 mm nominal maximum aggregate size (NMAS) over the range of stiffness values experienced in this study for recycled materials; however, this allowance in AASHTO TP 79 is based on asphalt mixtures and not on cold-recycled materials. The higher-than-allowable COV was expected, based on the authors' experiences and the literature (Cross and Jakatimath 2007; Schwartz and Khosravifar 2013; Diefenderfer and Link 2014), and it suggests that revisions to AASHTO TP 79 tolerances are needed when recycled materials are evaluated.

The measured dynamic moduli for replicate specimens were averaged with respect to temperature and frequency and were then shifted to construct a master curve using standard time-temperature superposition techniques as follows:

$$\log|E^*| = \delta + \frac{\alpha}{1 + e^{\beta + \gamma \log t_R}} \quad (2)$$

in which |E*| is the dynamic modulus, t_r is the reduced time at the reference temperature, δ is the minimum value of |E*| (lower shelf), $\delta + \alpha$ is the maximum value of |E*| (upper shelf), and

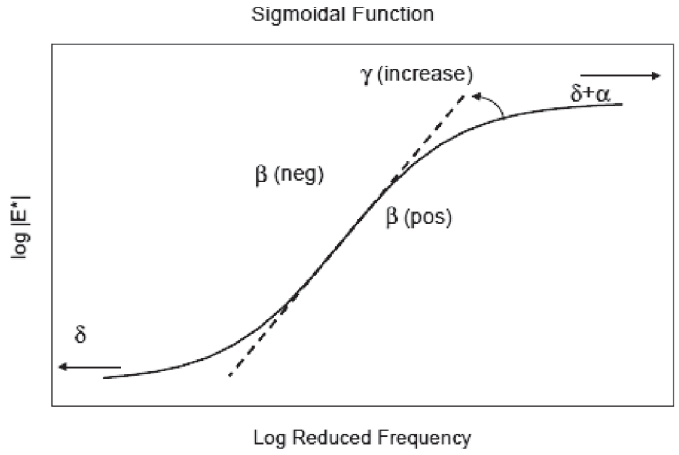

Figure 11. Sigmoidal master curve function (Pellinen et al. 2004).

β, γ are shape parameters. The temperature dependency of the modulus is incorporated in the reduced time parameter t_R:

$$t_R = \frac{t}{a(T)} \tag{3}$$

in which t is the actual loading time, $a(T)$ is the shift factor as a function of temperature, and T is temperature. A simple quadratic polynomial is used to fit the temperature shift factors:

$$\log a(T) = aT^2 + b^T + c \tag{4}$$

in which a, b, and c are the polynomial constants. Figure 11 shows an example of a master curve.

3.4 RLPD Testing

The rutting susceptibility of the recycled mixtures was assessed in accordance with AASHTO TP 79. Modifications to the test included using a lower test temperature (45°C) and the same small-scale cylindrical specimen geometry as used for the dynamic modulus testing. A repeated deviator stress of 482.6 kPa was applied at a constant confining stress of 68.9 kPa. The test temperature was determined following the procedure developed in NCHRP Project 9-30A (Von Quintus et al. 2012). As a check, LTPPBind software was used to predict the average high pavement temperatures for selected stations in the eastern United States (ranging from Tampa, Florida, to Caribou, Maine). These predicted temperatures were found to range from approximately 34°C to 56°C at depths of 100 mm and 150 mm. The depths of 100 mm and 150 mm were chosen as typical depths of the recycled layer for high volume pavement structures. Given the limited number of cores from each project and because the RLPD test specimens were not reusable, multiple test temperatures were not attempted.

The RLPD test results were analyzed following the procedures developed in NCHRP Project 9-30A (Von Quintus et al. 2012). A power-law function was used to characterize the secondary stage of the permanent deformation behavior as follows:

$$\varepsilon_p = AN^B \tag{5}$$

20 Material Properties of Cold In-Place Recycled and Full-Depth Reclamation Asphalt Concrete

in which ε_p is the permanent strain, N is the number of cycles applied, A is the regression constant representing the intercept in log-log space, and B is the regression constant representing the slope of the line in log-log space. This analysis methodology is particularly appropriate when testing mixtures in a confined state that tend not to reach tertiary flow.

The power-law equation was regressed starting at 2,000 cycles, as recommended by Khosravifar et al. (2015), and continued through 10,000 cycles with the exception of five specimens for which there was a plastic failure before 10,000 cycles. In the case of a plastic failure before 10,000 cycles, the range of regressed equation was limited to between 2,000 cycles and the point at which the plastic failure occurred. In all cases, the coefficient of determination (R^2) was above 0.99.

CHAPTER 4

Dynamic Modulus Test Results

Dynamic modulus testing was conducted on small-scale cylindrical specimens while unconfined with axially applied loading using an AMPT in general accordance with AASHTO TP 79. Modifications to the specification included using a reduced set of temperatures (4.4°C, 21.1°C, and 37.8°C) and using small-scale cylindrical specimens. At each temperature, testing was conducted at loading frequencies of 25 Hz, 10 Hz, 5 Hz, 1 Hz, 0.5 Hz, and 0.1 Hz. To minimize the potential for damage, each specimen was reused throughout the testing regime and tested in an increasing order of temperature and a decreasing order of frequency at each temperature.

4.1 Outlier Analysis

The results of dynamic modulus testing of the recycled materials were examined for outliers by visually inspecting the modulus values at a test frequency of 10 Hz at the three test temperatures (4.4°C, 21.1°C, and 37.8°C). Figure 12 shows an example of the data at 10 Hz and 21.1°C, grouped by project type.

Figure 12 marks the dynamic modulus result from one test specimen. Visual observation of the dynamic modulus test results identified several data points that appeared to vary significantly from the results of similar project types. It is difficult to determine if these cases of data variability were caused by inherent variability in the construction processes or by a low quality test or specimen. Previous research has shown that dynamic modulus test results for recycled mixtures can be more variable than the results typically seen for asphalt mixtures (Diefenderfer and Link 2014). Also, the AASHTO TP 79 specification data quality indicators were developed for asphalt mixtures, and it is not yet clear if they are appropriate for recycled mixtures.

The authors considered several methods by which to eliminate potentially abnormal data. First, the data were compared with the dynamic modulus data quality indicators suggested in AASHTO TP 79. This analysis showed that the deformation uniformity was the most commonly violated quality indicator; however, many of the results fell within the recommended ranges. The deformation uniformity parameter describes the variation in deformation between the multiple LVDTs mounted on the specimen (Bonaquist et al. 2003; Von Quintus et al. 2012). Bonaquist (2008) suggested that deformation uniformity values beyond the recommended ranges may be influenced by non-uniformity of the specimen. However, it was found that some data points that had very low deformation uniformity values (e.g., less than 10%) also appeared to be outside the expected ranges. In addition, some data points had large deformation uniformity values (e.g., greater than 75%), but the dynamic modulus COV of specimens from the same project was quite low (e.g., also less than 10%). Because of these issues, using data quality indicators to identify potentially abnormal values was not pursued further. The specimen bulk density also was investigated to see if it played a role in the variability of the dynamic modulus test results. As

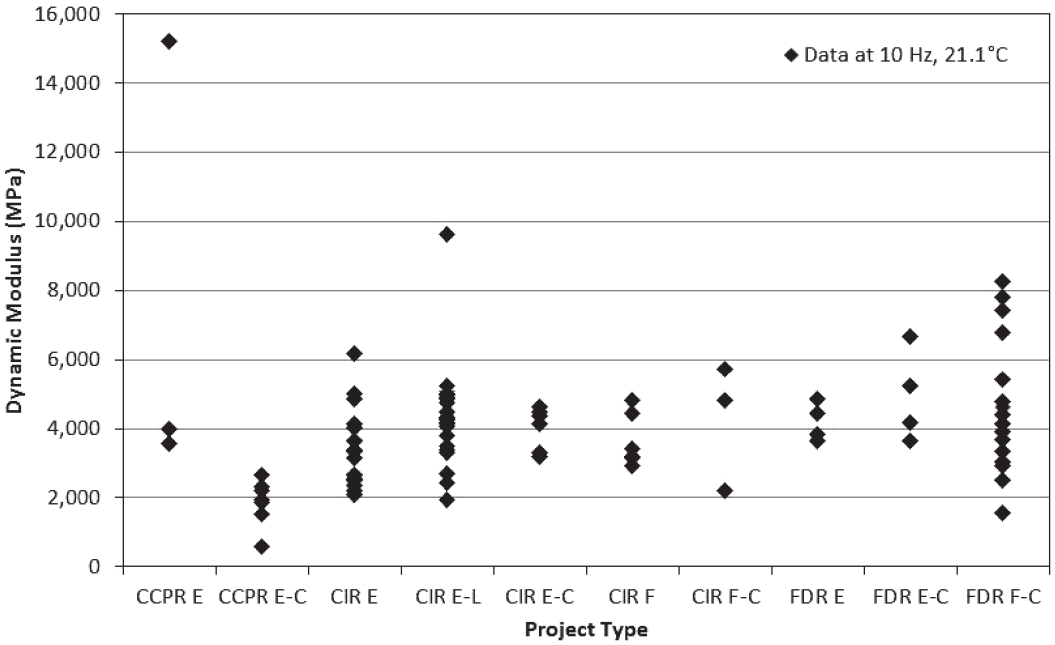

E = emulsified asphalt, F = foamed asphalt, C = hydraulic cement, and L = lime.

Figure 12. Dynamic modulus results at 10 Hz and 21.1°C.

with the data quality indicators, no consistent trend was apparent with respect to bulk density and dynamic modulus.

Next, an outlier procedure was performed using a quartile analysis. For each stabilizing/recycling agent and chemical additive type, the difference between the calculated third and first quartile was determined and identified as the interquartile range (IQR). The IQR was added to the third quartile value and subtracted from the first quartile value to calculate an upper and lower fence from which to consider outliers. This process identified most of the same outliers as were identified by visual observation. The quartile analysis was conducted independently for the 10 Hz data at the three test temperatures; the resulting data were termed *trimmed data*. Figure 13 shows an example of the trimmed data at 10 Hz and 21.1°C.

4.2 Significance Testing of Dynamic Modulus Data at 10 Hz

Using the trimmed data, a two-tailed, two-sample Student's t-test assuming unequal variance was used to determine if differences in the mean dynamic modulus with respect to recycling processes, stabilizing/recycling agents, and chemical additive combinations were statistically significant. The t-test for each comparison was performed separately at each test temperature using data from a test frequency of 10 Hz and considered a significance level (α) of 0.05.

Table 3 and Table 4 show the results of significance testing for recycling processes and stabilizing/recycling agent combinations, respectively. From Table 3, it can be seen that the differences in the mean dynamic modulus values of the different recycling processes are not significant at 4.4°C. At 21.1°C and 37.8°C, however, the difference in the value of the mean dynamic modulus for CCPR versus FDR is significant at both temperatures. Considering CCPR versus CIR, the difference in the mean dynamic modulus values was found to be significant only at 21.1°C; and the difference in the mean dynamic modulus considering CIR versus FDR was found to be significant only at 37.8°C. Generally, the differences become more significant with increasing temperature.

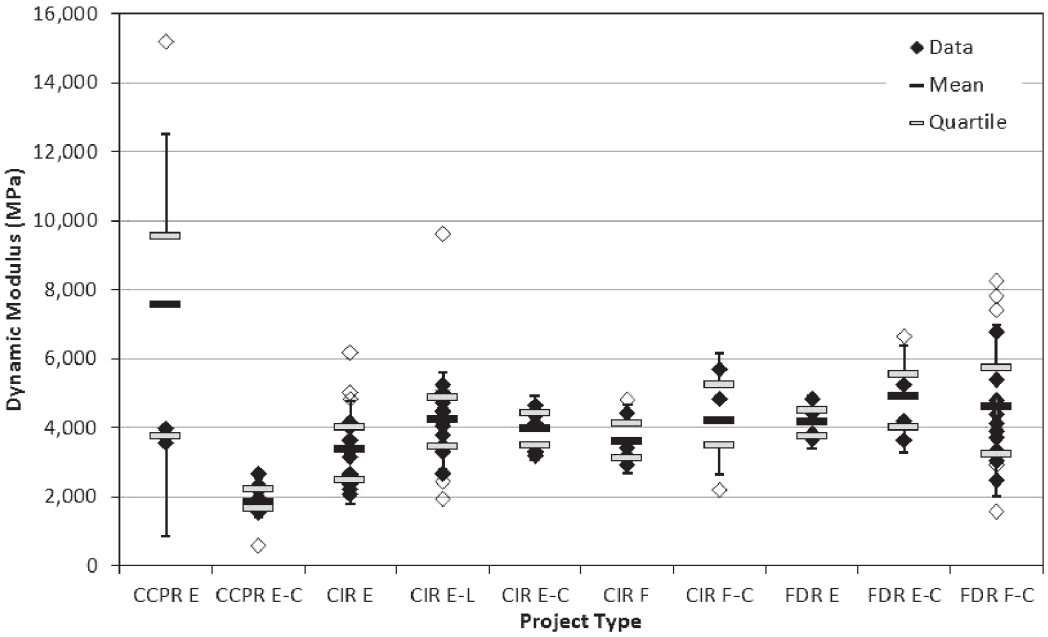

Data points identified as outside the IQR are shown with no shading.
E = emulsified asphalt, F = foamed asphalt, C = hydraulic cement, and L = lime.

Figure 13. Trimmed dynamic modulus data at 10 Hz and 21.1°C.

Table 4 shows that the difference in the mean dynamic modulus considering emulsified asphalt versus foamed asphalt was not significant except for the mixtures at 4.4°C temperature using FDR. When considering the presence of cement in addition to the bituminous stabilizing/recycling agents, three of the nine comparisons using emulsified asphalt (three processes at three temperatures) and none of the three comparisons using foamed asphalt (CIR at three temperatures) showed a significant difference in the dynamic modulus. The difference in dynamic modulus values for mixtures using cement as a chemical additive in mixtures stabilized/recycled with emulsified asphalt were found to be significant only for CIR at 21.1°C and 37.8°C and for CCPR at 21.1°C. When considering the presence of lime in addition to emulsified asphalt for CIR, the difference in the mean dynamic modulus was found to be statistically significant for the 21.1°C and 37.8°C temperatures.

Table 4 shows that the difference in the mean dynamic modulus when comparing the combination of emulsified asphalt plus cement versus foamed asphalt plus cement was significant only for one of the six comparisons (FDR and CIR at three temperatures): FDR at a temperature

Table 3. Recycling process statistical comparisons at (a) 4.4°C, (b) 21.1°C, and (c) 37.8°C.

a)	**4.4°C**	**CIR**	**FDR**
	CCPR	0.8764	0.8659
	CIR		0.2085
b)	**21.1°C**	**CIR**	**FDR**
	CCPR	0.0075	0.0018
	CIR		0.1989
c)	**37.8°C**	**CIR**	**FDR**
	CCPR	0.0929	0.0000
	CIR		0.0000

Shading highlights significant differences.

24 Material Properties of Cold In-Place Recycled and Full-Depth Reclamation Asphalt Concrete

Table 4. Stabilizing/recycling agent statistical combinations comparisons at (a) 4.4°C, (b) 21.1°C, and (c) 37.8°C.

a) 4.4°C	Emulsion vs. Foam	Emulsion vs. Emulsion + Cement	Emulsion vs. Emulsion + Lime	Emulsion + Cement vs. Foam + Cement	Foam vs. Foam + Cement	Cement vs. No Cement	Cement vs. Lime
CCPR	-	0.2873	-	-	-	0.2873	-
CIR	0.7285	0.1862	0.2422	0.7151	0.8320	0.2055	0.0042
FDR	0.0016	0.4958	-	0.0016	-	0.0422	-

b) 21.1°C	Emulsion vs. Foam	Emulsion vs. Emulsion + Cement	Emulsion vs. Emulsion + Lime	Emulsion + Cement vs. Foam + Cement	Foam vs. Foam + Cement	Cement vs. No Cement	Cement vs. Lime
CCPR	-	0.0203	-	-	-	0.0203	-
CIR	0.7356	0.0108	0.0000	0.1496	0.0804	0.0039	0.1970
FDR	0.7105	0.7840	-	0.7105	-	0.9558	-

c) 37.8°C	Emulsion vs. Foam	Emulsion vs. Emulsion + Cement	Emulsion vs. Emulsion + Lime	Emulsion + Cement vs. Foam + Cement	Foam vs. Foam + Cement	Cement vs. No Cement	Cement vs. Lime
CCPR	-	0.0513	-	-	-	0.0513	-
CIR	0.0641	0.0049	0.0068	0.2183	0.3671	0.0036	0.0582
FDR	0.9938	0.1466	-	0.9938	-	0.0095	-

Shading highlights significant differences.

of 4.4°C. The difference in the mean dynamic modulus for foamed asphalt CIR versus foamed asphalt CIR plus cement was found not to be statistically significant at any of the three temperatures considered.

Table 4 shows that the difference in the mean dynamic modulus for all stabilizing/recycling agents without cement versus with cement was statistically significant for five of the nine comparisons: CCPR at 21.1°C, CIR at 21.1°C and 37.8°C, and FDR at 4.4°C and 37.8°C. For the three CIR comparisons considering all stabilizing/recycling agents with cement versus all stabilizing/recycling agents with lime, the differences in the mean dynamic modulus values were found to be statistically significant only at 4.4°C.

In summary, the main systematic and significant difference in dynamic modulus values identified was between mixtures that used a stabilizing/recycling agent with a chemical additive versus mixtures without a chemical additive. This difference was more apparent at higher temperatures. No discernible trends were identified between the use of emulsified asphalt or foamed asphalt as stabilizing/recycling agents; the only statistically significant difference in dynamic modulus values was found at the 4.4°C test temperature for FDR. Also, no discernible trend was identified between the use of hydraulic cement or lime as the chemical additive; the only statistically

significant difference in dynamic modulus values was found at the 4.4°C test temperature (only the CIR process had projects using both hydraulic cement and lime as chemical additives).

4.3 Master Curve Analysis

To study the influence of the recycling process and the stabilizing/recycling agent and chemical additive combinations on the dynamic modulus over the complete temperature/frequency spectrum, the measured dynamic modulus data for each specimen (after applying the outlier analysis) were averaged for each project. These averages were used to create a master curve at a reference temperature of 21.1°C. Figure 14 shows an example of a dynamic modulus master curve created from the average measured dynamic modulus data at three test temperatures (4.4°C, 21.1°C, and 37.8°C) from a CIR project using foamed asphalt from San Jose, California. Generally, the master curves of the cold-recycled materials followed a sinusoidal shape as is seen for typical HMA mixtures.

From the master curves, data envelopes (bounded by the maximum and minimum average dynamic modulus data) were developed to compare project and material types by visual observation. The data envelopes were developed because the statistical analysis only indicates the existence of a difference between project or material types, not the direction of the difference. The master curves for similar project or material types were grouped together. The groupings included recycling process, stabilizing/recycling agent, and presence of chemical additive.

Figure 15 and Figure 16 show the dynamic modulus data envelopes for the CIR, CCPR, and FDR processes without discriminating between the presence of a chemical additive or the type of stabilizing/recycling agent (foamed or emulsified asphalt). Figure 15 shows the data using a log-linear plot that emphasizes the data at higher reduced frequencies (corresponding to lower test temperatures). Figure 16 shows the data using a log-log plot that emphasizes the data at lower reduced frequencies (corresponding to higher test temperatures).

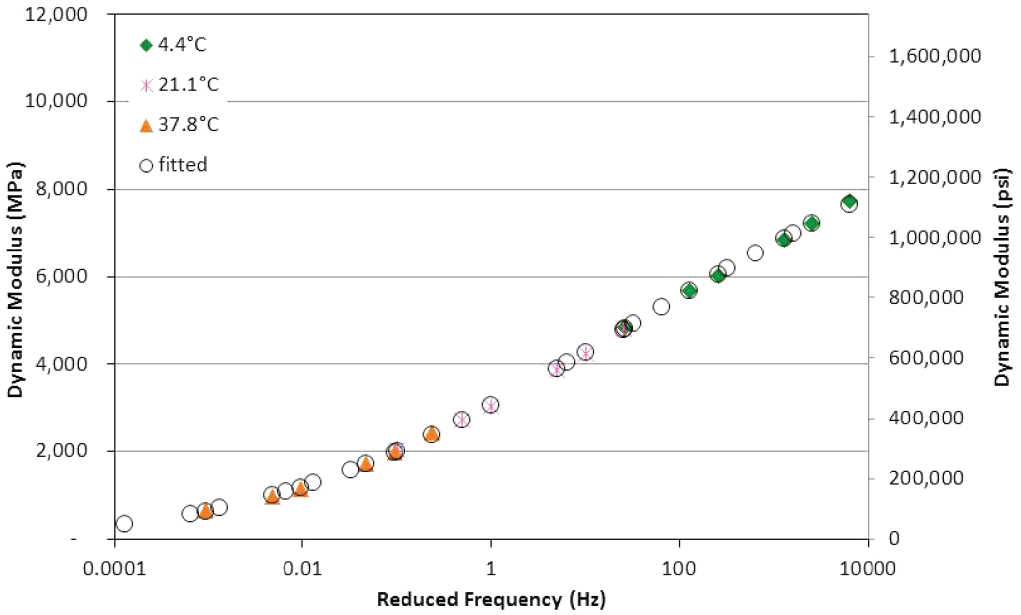

Master curve reflects averages of measurements from three specimens.

Figure 14. Dynamic modulus master curve from CIR project using foamed asphalt (San Jose, California, Project 13-1124).

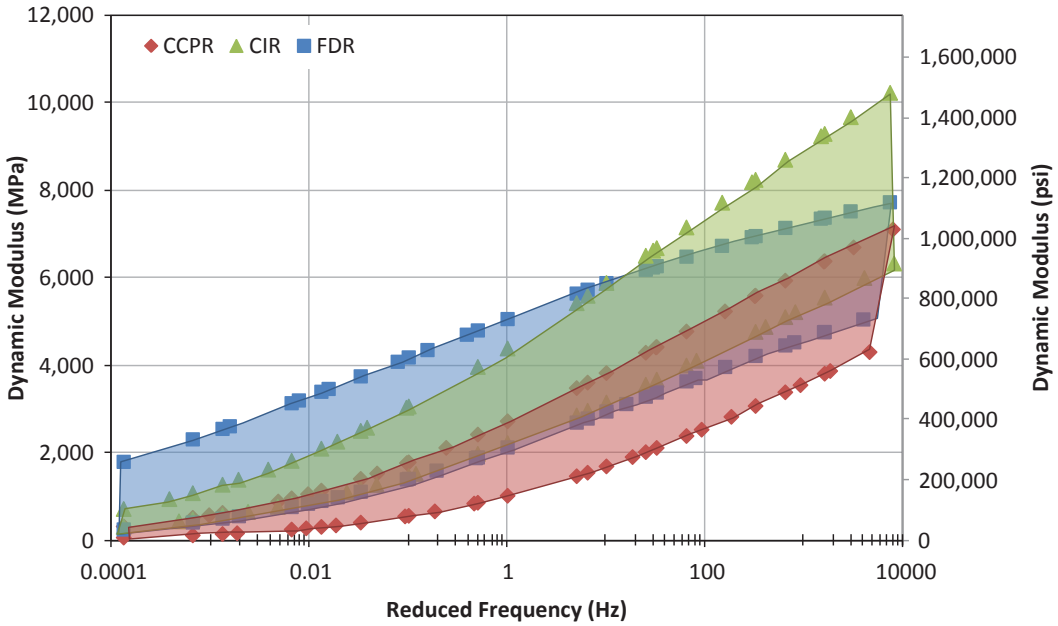

Figure 15. Dynamic modulus master curve data envelopes for mixtures produced by FDR, CIR, and CCPR using log-linear scale.

From Figure 15 and Figure 16 it can be seen that the FDR mixtures had a greater stiffness than the CIR and CCPR mixtures at lower reduced frequencies (less than approximately 10 Hz), which corresponds to higher test temperatures. The stiffness of the CIR mixtures overlaps the lower portion of the FDR envelope at frequencies less than approximately 10 Hz but then exceeds the stiffness of the FDR mixtures at higher reduced frequencies (greater than approximately 10 Hz), which correspond to lower test temperatures. The stiffness of the CCPR mixtures also overlaps the FDR envelope throughout the range of reduced frequencies; however, the CCPR mixtures

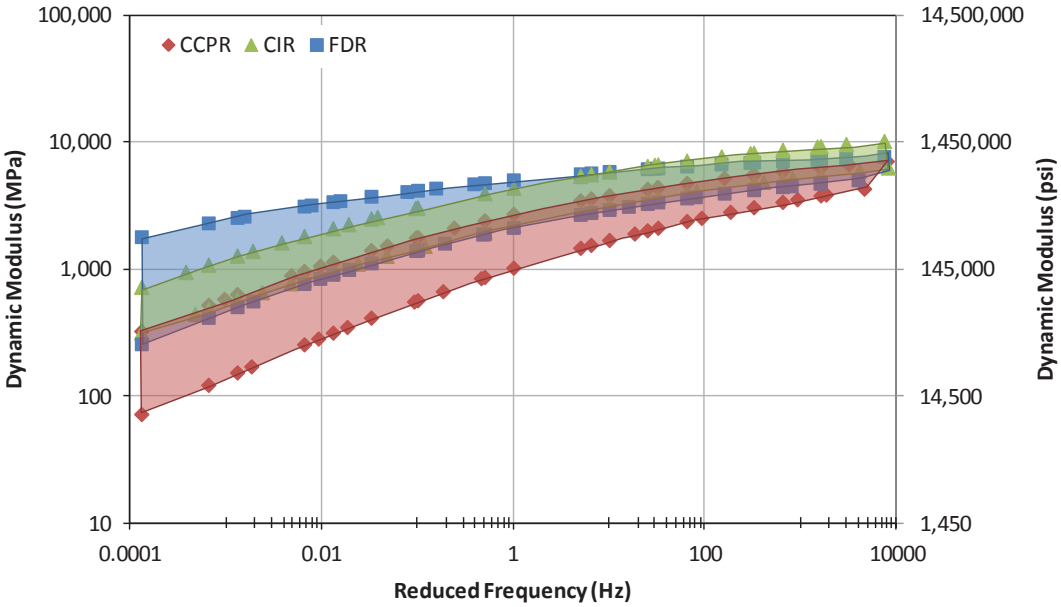

Figure 16. Dynamic modulus master curve data envelopes for mixtures produced by FDR, CIR, and CCPR using log-log scale.

data envelope minimum values are less than the minimum values of the other recycling process types throughout the range of reduced frequencies.

Most highway agencies and design procedures typically assign a lesser layer coefficient (or less modulus) to FDR; therefore, it may be surprising that the FDR data envelopes show a greater stiffness than either CIR or CCPR.

In an effort to compare the performance of in-place recycled mixes to traditional asphalt base mixes, cores from three in-service base mix projects from Virginia were collected. The base mixes had a NMAS of 25.0 mm and were tested under the same conditions of the in-place recycled mixes. Figure 17 again shows the dynamic modulus envelopes of the various in-place recycled mixes but adds the envelope for the three base mixtures. At low frequencies (analogous to higher temperatures) the base mix has similar modulus values to those of mixtures produced by CIR and CCPR, whereas at lower-middle frequencies the base mix is more comparable to the FDR mixture. However, at high frequencies (analogous to lower temperatures) the base mix exhibits higher moduli than any of the recycled mixes.

Figure 18 and Figure 19 show the dynamic modulus data envelopes for the recycled mixtures with respect to stabilizing/recycling agents without discriminating between the recycling process or the presence of a chemical additive. It can be seen that there is much overlap in the data for the two stabilizing/recycling agent types. Mixtures using foamed asphalt were found to be stiffer at lower reduced frequencies (less than approximately 20 Hz), corresponding to higher test temperatures, whereas mixtures using emulsified asphalt were found to be stiffer at higher reduced frequencies (greater than approximately 20 Hz), corresponding to higher test temperatures.

Figure 20 and Figure 21 show the dynamic modulus data envelopes for the recycled mixtures with respect to the presence of a chemical additive; the data envelopes are grouped by mixtures containing no chemical additive, lime, or cement regardless of stabilizing/recycling agent or recycling process. (Only the CIR process recycled with emulsified asphalt contained lime as a chemical additive.) The dynamic modulus data envelope for the mixtures that included cement overlaps the envelopes for the mixtures containing lime and no chemical additive at low and intermediate reduced frequencies (less than approximately 10 Hz and 100 Hz, respectively). At these same

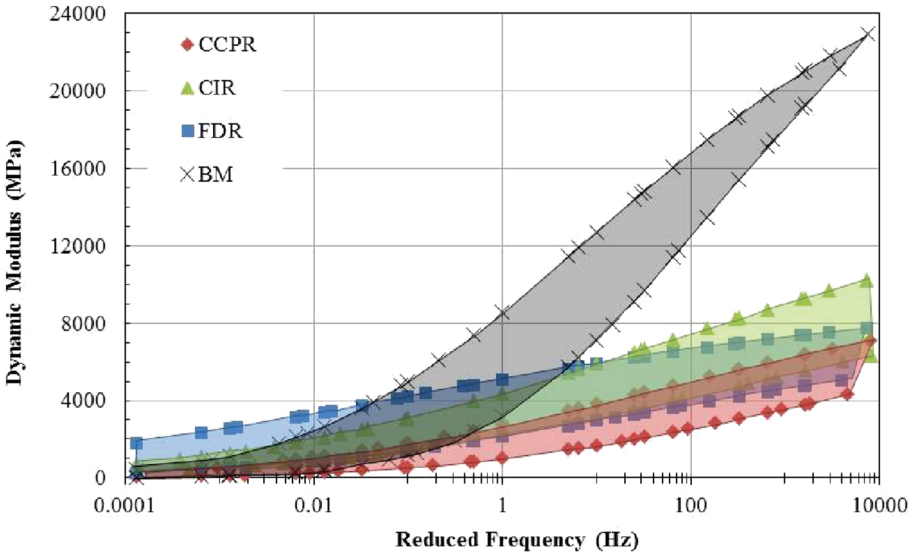

Figure 17. Dynamic modulus master curve data envelopes for mixtures produced by FDR, CIR, and CCPR, as well as asphalt base mixes, using log-log scale.

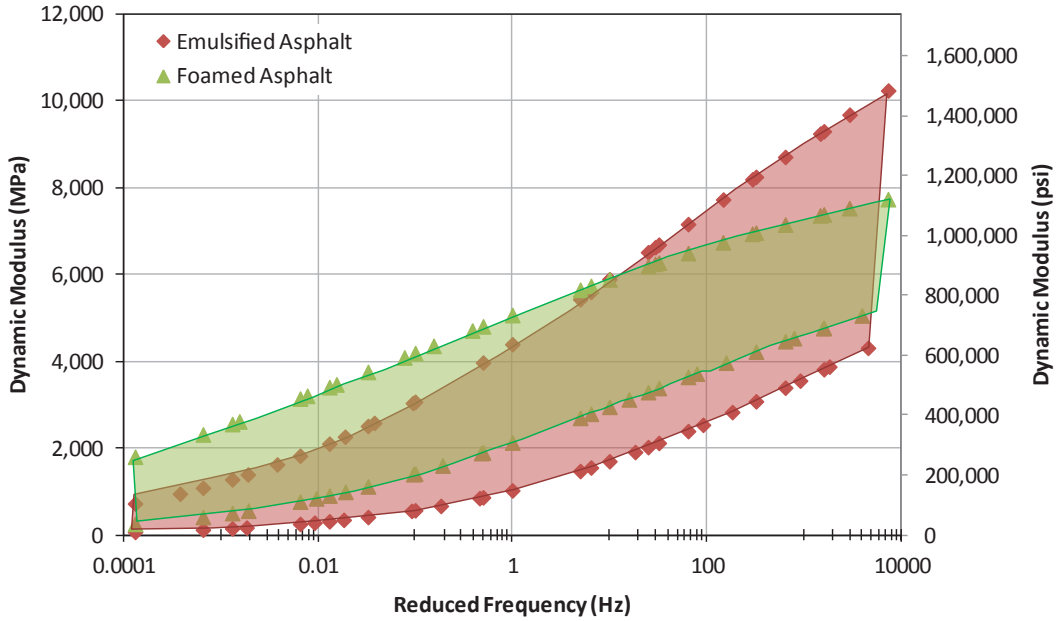

Figure 18. Dynamic modulus master curve data envelopes for mixtures using emulsified asphalt and foamed asphalt as stabilizing/recycling agents using log-linear scale.

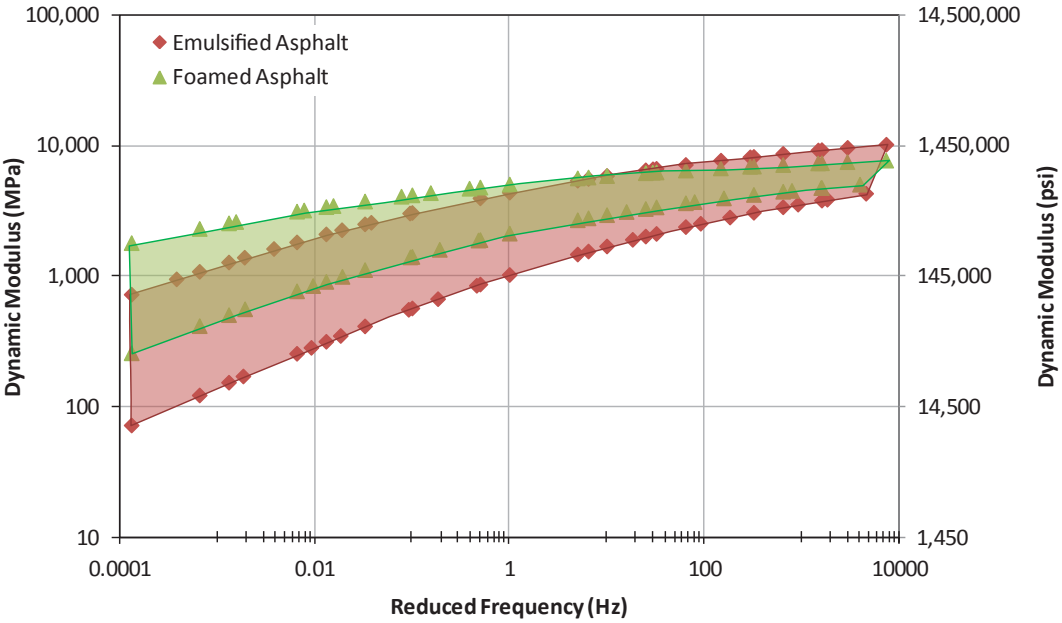

Figure 19. Dynamic modulus master curve data envelopes for mixtures using emulsified asphalt and foamed asphalt as stabilizing/recycling agents using log-log scale.

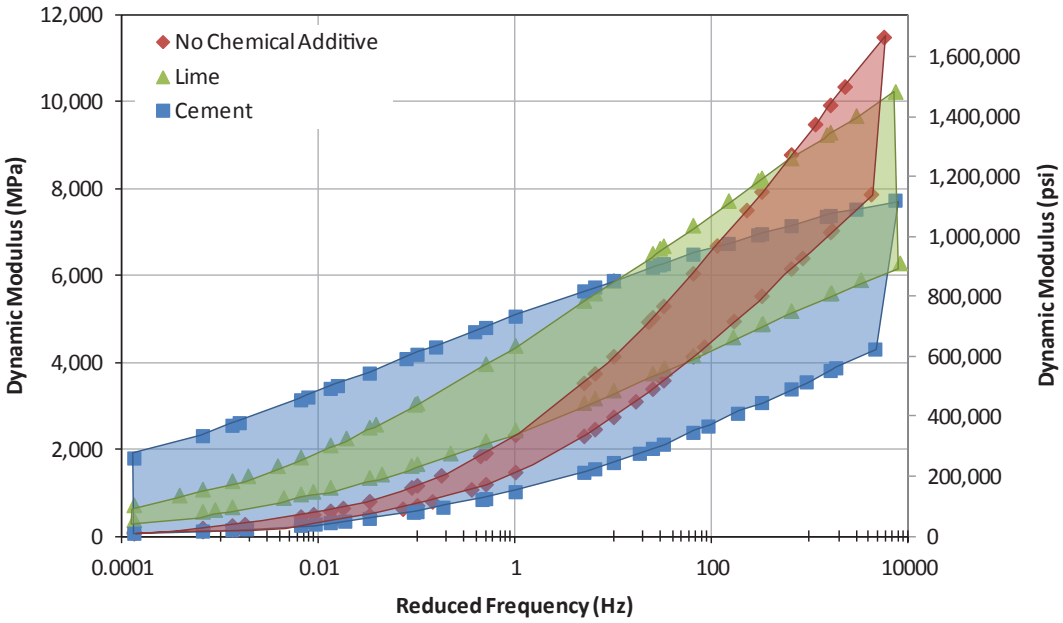

Figure 20. Dynamic modulus master curve data envelopes for mixtures with no chemical additive, with lime, and with cement, using log-linear scale.

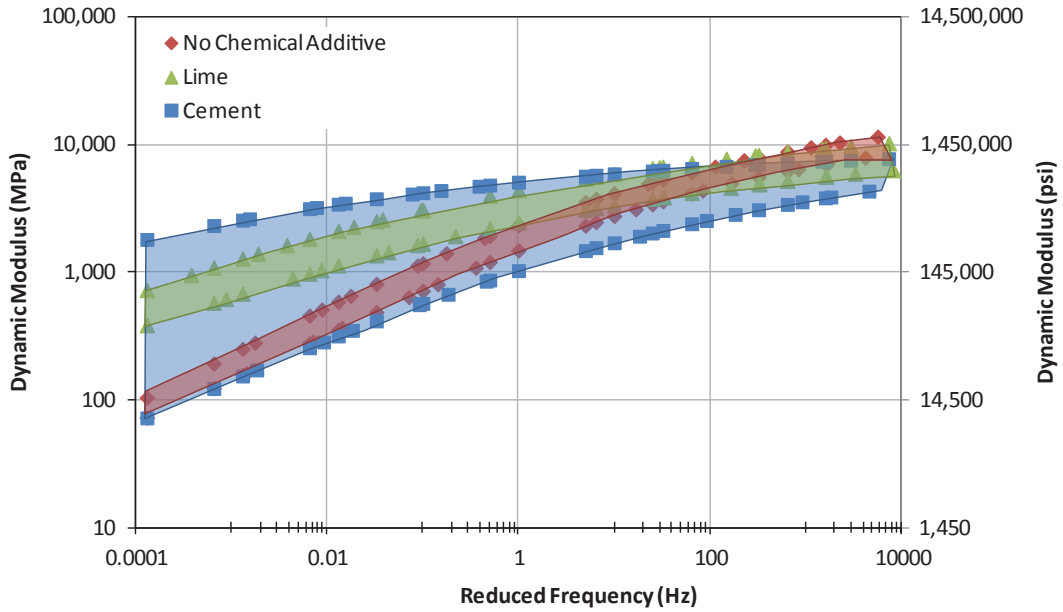

Figure 21. Dynamic modulus master curve data envelopes for mixtures with no chemical additive, with lime, and with cement using log-log scale.

30 Material Properties of Cold In-Place Recycled and Full-Depth Reclamation Asphalt Concrete

reduced frequency ranges, mixtures containing lime were found to be stiffer than mixtures having no chemical additive. At higher reduced frequencies (greater than approximately 100 Hz), however, the stiffness of the mixtures with no chemical additive overlapped with the stiffness of those mixtures containing lime and also were generally found to be stiffer than the mixtures containing cement.

Mixtures containing cement may be stiffer at lower reduced frequencies (higher test temperatures) because the cement has hydrated and produced bonds that are stiffer than the asphalt binder at higher temperatures. As the binder in the mixture from the RAP and/or the stabilizing agent softens, the presence of a stiff hydration product would be noticeable. Like those containing cement, mixtures containing lime also seem to stiffen at lower temperatures as compared to mixtures that contain no chemical additive. The effect is less pronounced with lime than it is with cement.

The master curve envelopes also show that mixtures containing a chemical additive are generally less temperature dependent than those containing no chemical additive. The lower temperature dependency for mixtures containing a chemical additive may be caused by the presence of a non-viscoelastic material as part of the stabilizing mechanism. It is also worth noting that a wider range of stiffness values occurs for the recycled materials that contain cement as an additive. This result could reflect the inclusion of all project types and recycling processes in the stiffness comparison.

The increased stiffness at lower reduced frequencies for mixtures containing cement is also noteworthy in that many design procedures report that the chemical additives are available for recycling agent dispersion or improved strength at early ages. Given that these materials were tested at 12–24 months after construction, it is clear that this strength increase continues beyond the initial age of the recycled layer.

4.4 Analysis of Fitting Parameters

The four fitting parameters from Equation 2 (α, β, δ, and γ) can be used to reconstruct any master curve. Table 5 shows the fitting parameters describing the average master curve for each project site. A statistical analysis of the fitting parameters was performed to quantify any observed trends from within the data. A two-tailed, two-sample Student's t-test assuming unequal variance was used to determine if differences in the fitting parameters with respect to recycling processes, stabilizing/recycling agents, and chemical additive combinations were statistically significant at a significance level (α) of 0.05.

Table 6 shows the results of the statistical testing of the master curve shape parameters for the three recycling processes considered. In Table 6, the effects of the different stabilizing/recycling agents and recycling agent/chemical additive combinations are included with averaging for each process. From the comparison, the difference in the fitting parameters for any of the recycling processes was not found to be statistically significant.

Table 7 shows the results of statistical testing of the master curve shape parameters for the different stabilizing/recycling agents and recycling agent/chemical additive combinations. Not all combinations were considered because in some instances an insufficient number of projects were available for a particular condition, and thus the t-test could not be performed. The results in Table 7 show that the differences in the beta (β) and delta (δ) parameters for CIR projects including emulsion versus those containing emulsion plus cement were statistically significant. The β parameter indicates that the difference in horizontal position of the turning point shown in Figure 11 is statistically significant. Also, the δ parameter indicates that the difference in minimum modulus value is statistically significant.

Table 5. Dynamic modulus master curve fitting parameters.

Location	Project ID	Alpha (α)	Beta (β)	Delta (δ)	Gamma (γ)
Kansas	13-1093	4.3194	-1.5444	1.9507	-0.2626
Ontario	13-1111	4.3670	-1.4334	1.9662	-0.3523
Ontario	13-1112	4.7391	-1.4374	1.6832	-0.3480
Ontario	13-1113	4.3712	-1.3721	1.9571	-0.3465
Ontario	13-1114	3.5732	-0.9951	2.7638	-0.4074
Alberta	13-1115	0.6706	1.5158	4.9562	-1.9025
Alberta	13-1116	4.2084	-1.8426	1.8577	-0.3202
Alberta	13-1117	4.1272	-1.6234	1.7471	-0.3104
California (San Jose)	13-1124	4.2913	-1.8334	1.9469	-0.3212
Colorado	13-1127	4.2620	-1.9634	1.9202	-0.3105
California (Los Angeles)	14-1001	4.3253	-1.7761	1.8988	-0.3072
California (Los Angeles)	14-1002	4.1005	-2.0384	1.7765	-0.3895
California (Los Angeles)	14-1003	4.3227	-1.7923	1.9877	-0.3247
West Virginia	14-1011	4.2673	-1.9638	1.9110	-0.2650
Delaware	14-1025	3.5213	-0.8741	2.8475	-0.4030
Delaware	14-1026	4.3564	-1.1814	2.1968	-0.3505
Delaware	14-1027	3.4839	-0.9139	2.9062	-0.4087
Delaware	14-1028	4.5154	-1.2669	2.0818	-0.2449
Utah	14-1055	4.4060	-1.4641	2.0232	-0.3092
Georgia	14-1057	4.3148	-2.1788	1.9247	-0.2066
Washington State	14-1058	4.3487	-1.8578	2.0427	-0.2781
Colorado	14-1062	4.2884	-1.6808	1.9354	-0.2670
Maine (Lyman)	15-1001	4.3257	-1.1786	1.8657	-0.3054
Maine (Corinna, Exeter)	15-1002	4.3500	-1.2693	1.9350	-0.2535

32 Material Properties of Cold In-Place Recycled and Full-Depth Reclamation Asphalt Concrete

Table 6. Dynamic modulus master curve fitting parameters statistical comparisons by process.

Process Comparison	Fitting Parameter			
	Alpha (α)	Beta (β)	Delta (δ)	Gamma (γ)
CIR vs. CCPR	0.2411	0.5104	0.0805	0.1289
CIR vs. FDR	0.4414	0.8379	0.5104	0.4791
CCPR vs. FDR	0.3629	0.9763	0.3498	0.4039

Table 7 also shows that, for CIR mixtures using emulsion versus emulsion plus lime, the difference in the γ parameter, representing the rate of change between the minimum and maximum modulus values, was statistically significant. Like the analysis of the dynamic modulus values, the analysis of the fitting parameters shows that differences in foamed asphalt versus emulsified asphalt were not statistically significant. Also, the differences in the fitting parameters for CIR projects using lime versus cement as a chemical additive were not statistically significant.

4.5 Analysis of Phase Angle

Black Space diagrams are useful in showing the relationship between stiffness and phase angle as measured during the dynamic modulus test. The phase angle represents the lag between the applied stress and the resultant strain in the specimen during the dynamic modulus test. A phase angle of zero degrees implies a purely elastic material and a phase angle of 90° corresponds to a purely viscous material. Figure 22 shows a Black Space diagram for three base asphalt

Table 7. Dynamic modulus master curve fitting parameters statistical comparisons by stabilizing/recycling agents and recycling agent/chemical additive combinations.

Process	Stabilizing/Recycling Agents and Recycling Agent/Chemical Additive Combinations	Fitting Parameter			
		Alpha (α)	Beta (β)	Delta (δ)	Gamma (γ)
CIR	Emulsion vs. Foam	0.1574	0.9676	0.1089	0.4491
	Emulsion vs. Emulsion + Cement	0.9641	0.0031	0.0610	0.9890
	Emulsion vs. Emulsion + Lime	0.1332	0.3517	0.2066	0.0448
	Cement vs. Lime	0.2134	0.0713	0.1942	0.3854
FDR	Emulsion vs. Foam	0.3481	0.7052	0.4708	0.3903

Shading highlights significant differences.

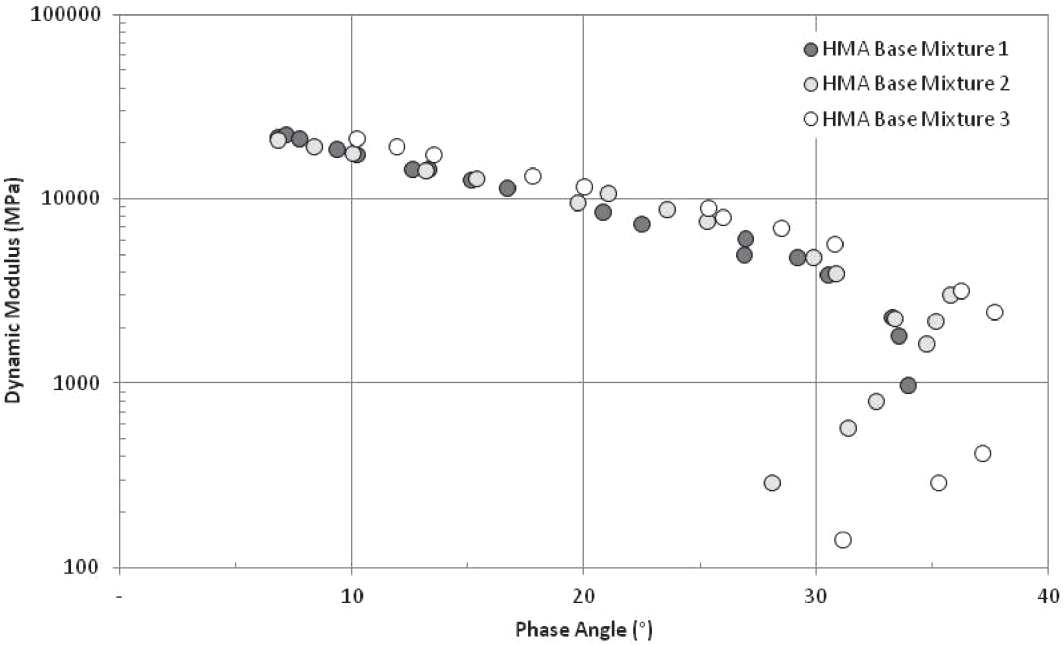

Figure 22. Black Space diagram for three asphalt base mixtures produced in Virginia.

mixtures produced in Virginia. The results show that the phase angle peaks at lower stiffness values and reaches a maximum value and then decreases. If labels for the test temperatures also appeared in Figure 22, it would be seen that the phase angle increases (and the modulus decreases) as the test temperature increases. The phase angles reach their maximum values at higher test temperatures because the asphalt mixtures exhibit more viscous behavior. At the highest test temperatures, the aggregate structure begins to play a larger role in the material behavior and the phase angle peaks and begins to decrease.

The relationship between phase angle and stiffness for the various pavement recycling techniques and additives was investigated visually using a Black Space diagram. The Black Space diagram for a typical asphalt mixture shows a peak phase angle value (see the right side of Figure 22) that is caused by the behavioral influence of the aggregate structure at higher temperatures. At lower temperatures, the mixture volumetrics and binder stiffness control the behavior (Biligiri et al. 2010). The highest values of phase angles in this plot are associated with the inflection points in the master curve. It can be seen in Figure 22 that these occur around a stiffness of 1,000–1,200 MPa.

Figure 23 shows the Black Space diagram for all recycled mixtures after removing outlier dynamic modulus values. While there is much overlap between the recycling types, it appears that the phase angle is generally the least for FDR and greatest for CIR; the phase angle for CCPR is between the other two recycling process types. This pattern indicates that the FDR mixtures tested generally had the most elastic response. This result was expected because the FDR mixtures contained a lower proportion of asphalt binder and they used a combination of RAP and unbound materials. Given the differences shown in Figure 23 between the recycling processes, further investigation was performed with respect to recycling agents and chemical additives.

Figure 24 shows the Black Space diagram for emulsified asphalt and foamed asphalt CIR mixtures. These mixtures contained no chemical additives. In Figure 24 it can be seen that the phase angle versus stiffness data overlap for the two recycling agents shown. This pattern suggests that CIR mixtures using emulsified asphalt or foamed asphalt should have similar viscoelastic behavior.

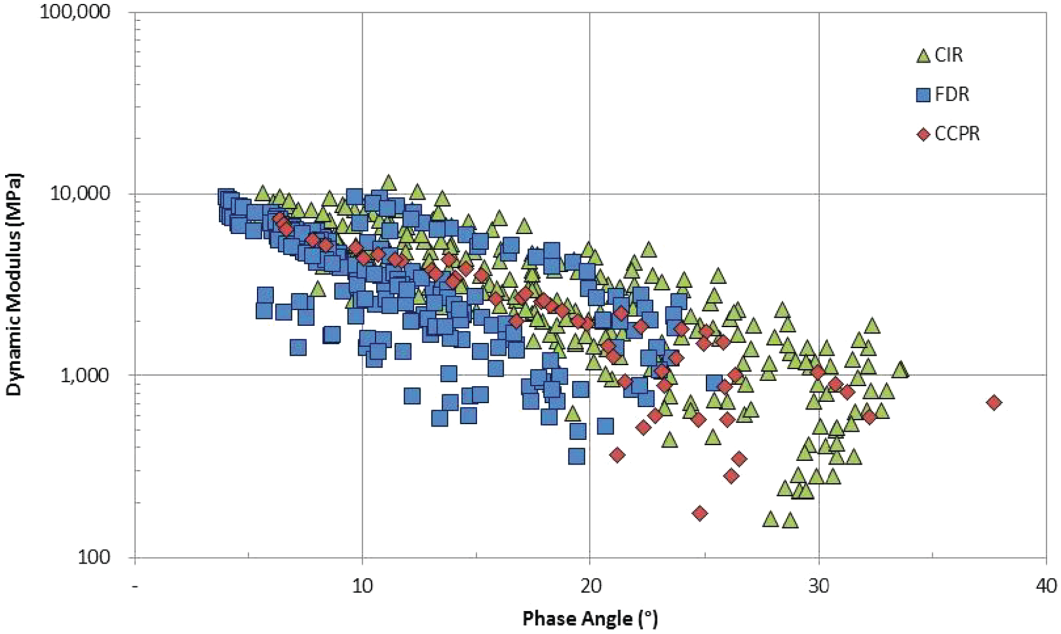

Figure 23. Black Space diagram for mixtures produced by FDR, CCPR, and CIR.

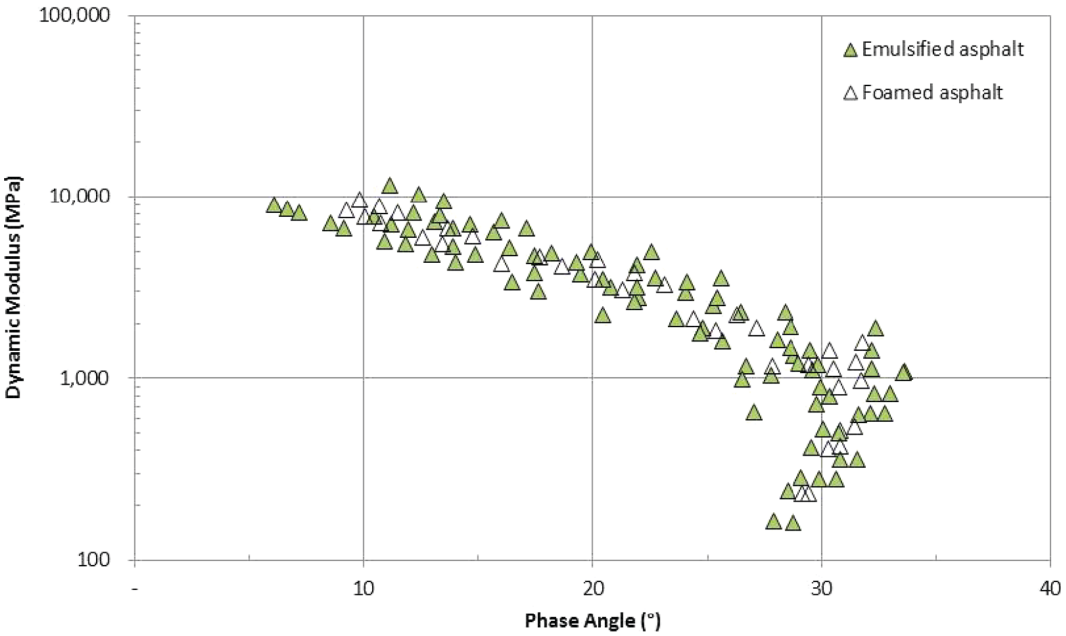

Figure 24. Black Space diagram for emulsified asphalt and foamed asphalt CIR mixtures having no chemical additive.

Figure 25 shows the Black Space diagram for emulsified asphalt CIR mixtures having lime, cement, or no chemical additive. Mixtures including a chemical additive generally have a more elastic response in that their phase angles are smaller than those mixtures with no chemical additive. Figure 25 also shows that those mixtures using cement as a chemical additive generally had a smaller phase angle than the mixtures using lime. This observation was expected because cement exhibits little viscoelastic behavior. Of particular interest in this figure is the lack of an inflection point in the mixtures containing a chemical additive. The inflection point is indicative of the transition point at which the aggregate begins to control the stiffness (i.e., the point at which the binder's viscosity no longer controls the mixture's stiffness). The lack of an inflection point in Figure 25 likely reflects the limited temperatures in the test procedure. If higher temperatures were evaluated, it is probable that an inflection point would also appear for the mixtures containing chemical additives. It is not clear if the lack of an inflection point in Figure 25 indicates that the recycled mixtures maintain a predominately elastic response at higher temperatures.

Figure 26 shows the Black Space diagram for foamed asphalt CIR mixtures having cement or no chemical additive. (No foamed asphalt CIR mixtures having lime as a chemical additive were sampled.) The presence of cement reduces the phase angle in a manner similar to that shown for emulsified asphalt CIR mixtures and suggests a more elastic response.

Figure 27 shows the Black Space diagram for emulsified and foamed asphalt FDR mixtures with cement as a chemical additive. It can be seen that the one emulsified asphalt FDR mixture with cement had slightly greater phase angle values than the foamed asphalt FDR mixtures with cement. This result may have been caused by the differences in stabilization mechanisms for emulsified mixtures versus foamed mixtures. Asphalt Academy (2009) states that emulsified mixtures are held together in a coating process whereas foamed mixtures utilize a spot-welding process to hold the recycled particles together. If this is true, the emulsified asphalt mixture may be expected to have a more viscous response if the interparticle bonding is more dependent on the coating process. Furthermore, this would create an increased surface area throughout the mixture in which a softer binder is present. If blending between the emulsified asphalt and the RAP binder occurs, a composite binder layer would form that is stiffer than the base binder

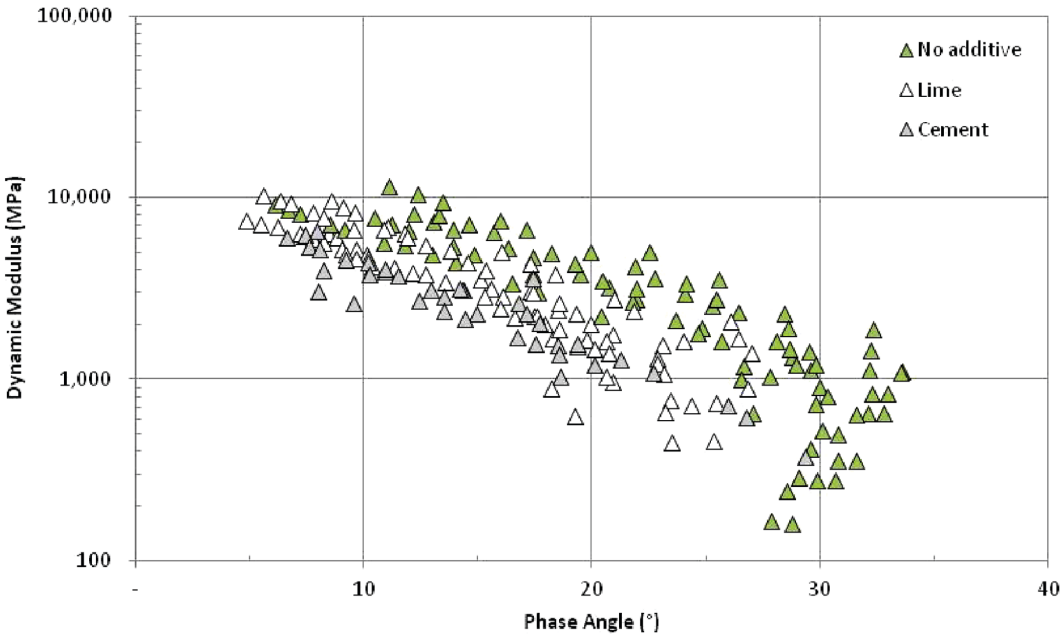

Figure 25. Black Space diagram for emulsified asphalt CIR mixtures.

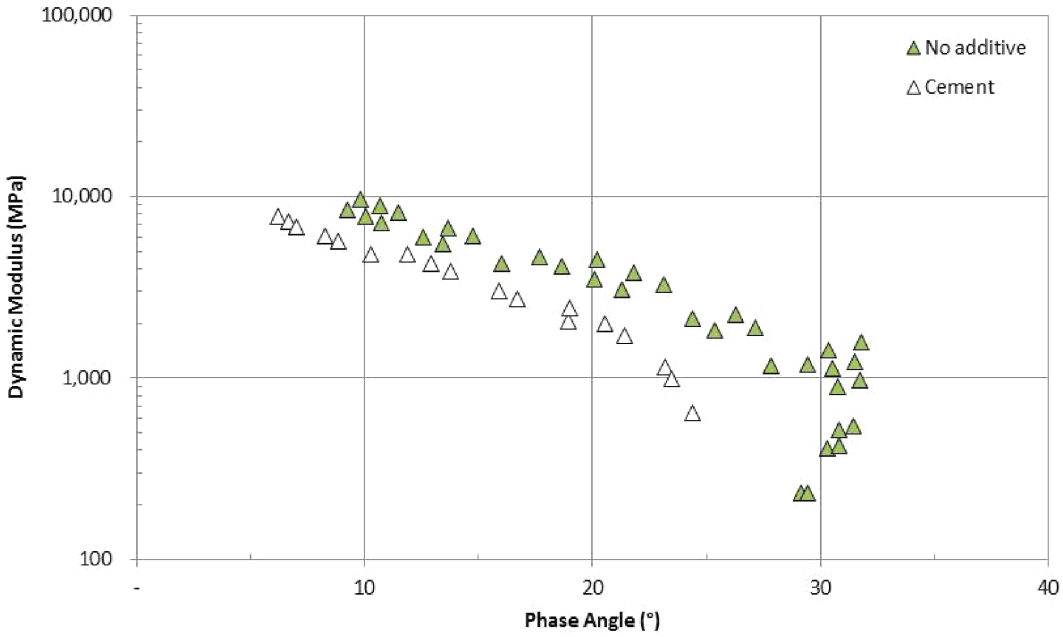

Figure 26. Black Space diagram for foamed asphalt CIR mixtures having cement or no chemical additive.

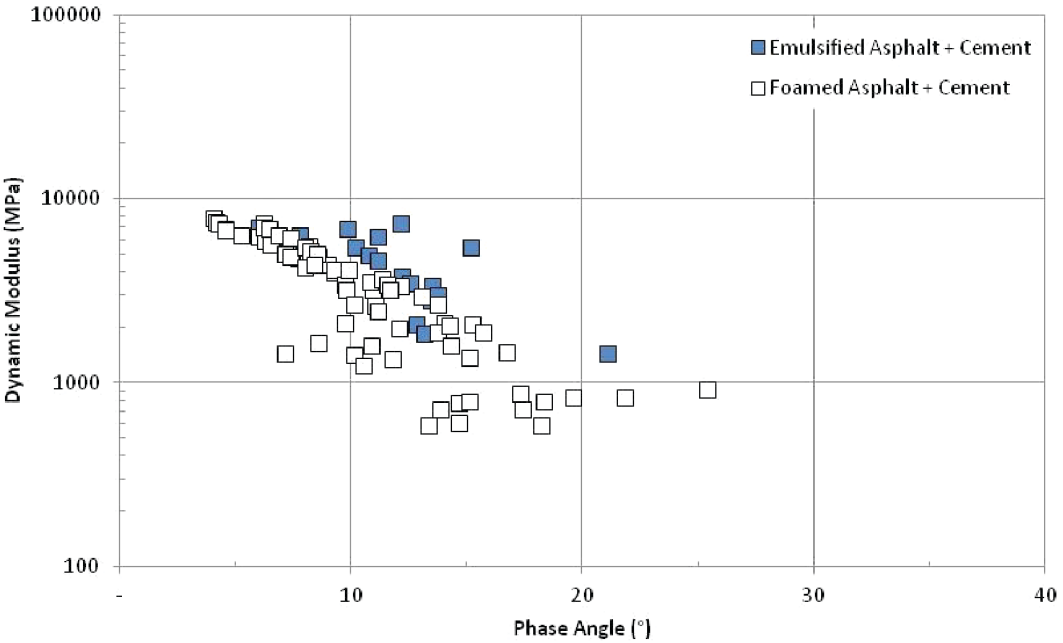

Figure 27. Black Space diagram for emulsified and foamed asphalt FDR mixtures with cement.

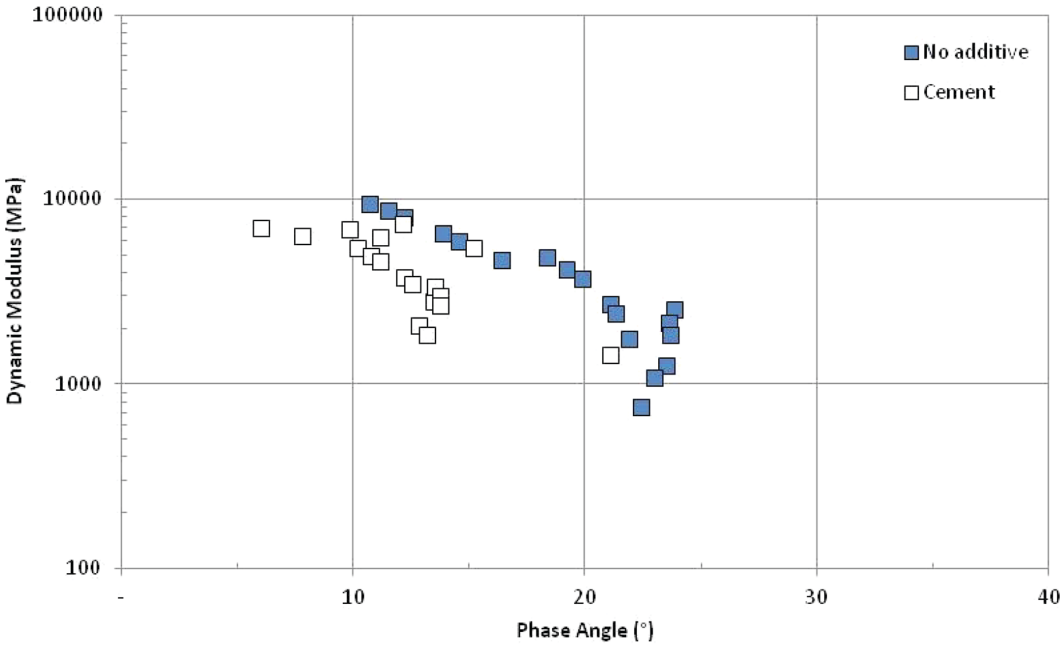

Figure 28. Black Space diagram for emulsified asphalt FDR mixtures having no chemical additive and no cement.

used in the emulsion and softer than the RAP binder. In the foaming process, the spot-welding effect allows the RAP binder stiffness to control the mixture performance, hence the more elastic response. In the described emulsion-composite case, the composite layer would control, resulting in a less stiff material. If a composite is not formed initially (i.e., if the RAP binder is simply coated with the softer emulsified binder), the molecular dynamics of binder blending over time would lead to a composite layer that might result in a stiffer mix overall. Unfortunately, the data set is not representative of the same mix tested over time, so this theory cannot be validated. Some interaction with the cement chemical additive also is likely. This variable could not be eliminated because all foamed asphalt FDR mixtures included cement as a chemical additive.

Figure 28 shows the Black Space diagram for the two emulsified asphalt FDR mixtures in the study. One mixture has no chemical additive and the other includes cement. The presence of cement is noticeable in that the phase angle for the FDR mixture with cement is smaller than that of the mixture having no chemical additive, suggesting a more elastic behavior.

4.6 Relationship between Stiffness and Mixture Properties

The density of a cold-recycled material is a commonly cited property that is included as a quality measure in many agency specifications (Stroup-Gardiner 2011). It is not known, however, whether density is always a good predictor of future performance or if it is just an easily measured surrogate property. Table 8 shows the coefficient of correlation (R^2) between the bulk density of the dynamic modulus specimen and the dynamic modulus result at 10 Hz for the three test temperatures. The results are grouped to show the correlation for all projects of a particular recycling process and also separated by recycling/stabilizing agent and chemical additive combination. In Table 8, cells that contain a dash indicate that too few results were available for comparison after outliers were removed. Table 8 shows that (1) in some cases, density and stiffness are highly correlated and (2) in general, the correlation improves with decreasing temperature.

Table 8. Coefficient of correlation (R^2) between bulk density and dynamic modulus at 10 Hz.

Process	Recycling/ Stabilizing Agent	Chemical Additive	Test Temperature		
			4.4°C	21.1°C	37.8°C
CIR	All		0.48	0.04	0.04
	Emulsion	None	0.46	0.31	0.10
	Emulsion	Lime	0.55	0.47	0.33
	Emulsion	Cement	0.66	0.71	0.09
	Foam	None	0.87	0.69	0.84
	Foam	Cement	0.73	--	--
CCPR	All		0.11	0.09	0.26
	Emulsion	None	--	--	--
	Emulsion	Cement	0.13	0.09	0.01
FDR	All		0.30	0.01	0.01
	Emulsion	None	0.10	0.36	--
	Emulsion	Cement	0.37	0.19	0.42
	Foam	Cement	0.34	0.01	0.10

Dashes indicate too few data were available for comparison after outliers removed.

The R^2 value was greater than 0.5 in only 7 of the 33 comparisons, however, indicating that the density describes more than 50% of the variability in the measured stiffness in only 21% of the comparisons. Figure 29 shows the relationship between density and stiffness with respect to recycling process.

Table 9 shows the coefficient of correlation (R^2) between the percentage of mix design density of the dynamic modulus specimen and the dynamic modulus result at 10 Hz for the three test temperatures. As with Table 8, cells that contain dashes indicate that too few results were available for comparison after outliers were removed. Table 9 also shows that the percentage of mix design density and stiffness is highly correlated in certain cases and that the correlation generally increases with decreasing temperature. The R^2 value was greater than 0.5 in only 9 of the 30 comparisons, indicating that the percentage of mix design density describes more than 50% of the variability in the measured stiffness in only 30% of the comparisons. Figure 30 shows the relationship between percentage mix design density and stiffness with respect to recycling process.

A correlation analysis was performed between design properties and performance properties for the cold-recycled materials. Design properties include the mixture design characteristics and information collected at time of construction (e.g., construction equipment, weather conditions, compaction). A limited number of these properties were known across all of the cold-recycled material types. Performance properties are the dynamic modulus master curve parameters and dynamic modulus values at specific temperature and loading rate combinations.

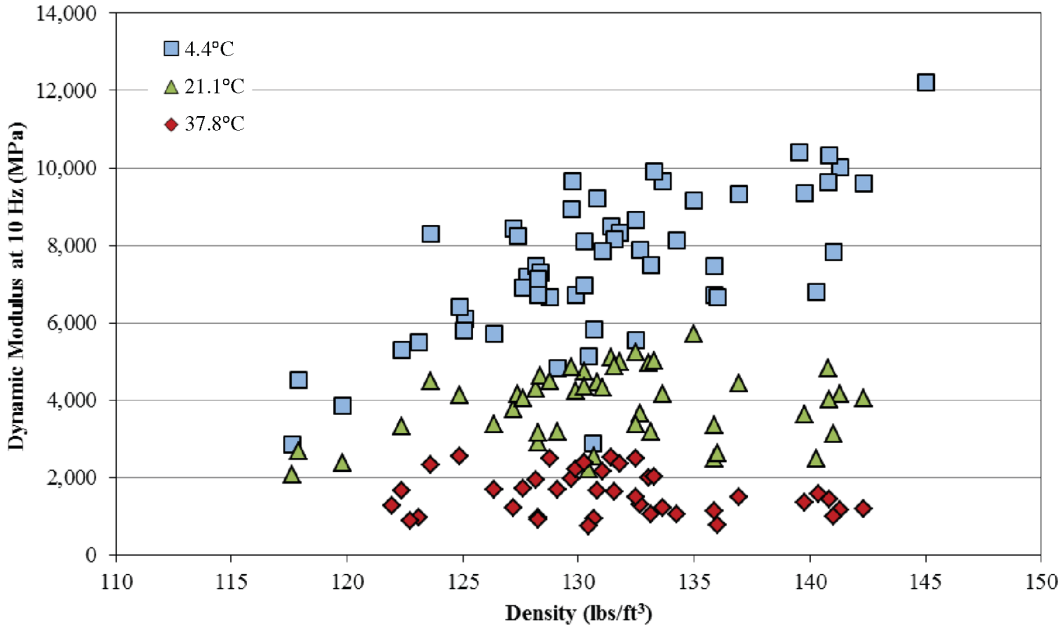

Figure 29. Relationship between specimen bulk density and stiffness.

Table 9. Coefficients of correlation (R^2) between percentage maximum density and dynamic modulus at 10 Hz.

Process	Recycling/ Stabilizing Agent	Chemical Additive	R^2 at Test Temperature		
			4.4°C	21.1°C	37.8°C
CIR	All		0.51	0.12	0.03
	Emulsion	None	0.36	0.21	0.04
	Emulsion	Lime	0.49	0.06	0.02
	Emulsion	Cement	0.66	0.64	0.09
	Foam	None	0.96	0.88	0.94
	Foam	Cement	0.04	--	--
CCPR	All		0.07	0.66	0.10
	Emulsion	None	--	--	--
	Emulsion	Cement	0.14	0.66	0.80
FDR	All		0.25	< 0.01	< 0.01
	Emulsion	None	0.10	0.36	--
	Emulsion	Cement	0.37	0.19	0.42
	Foam	Cement	0.19	< 0.01	0.08

Dashes indicate too few data were available for comparison after outliers removed.

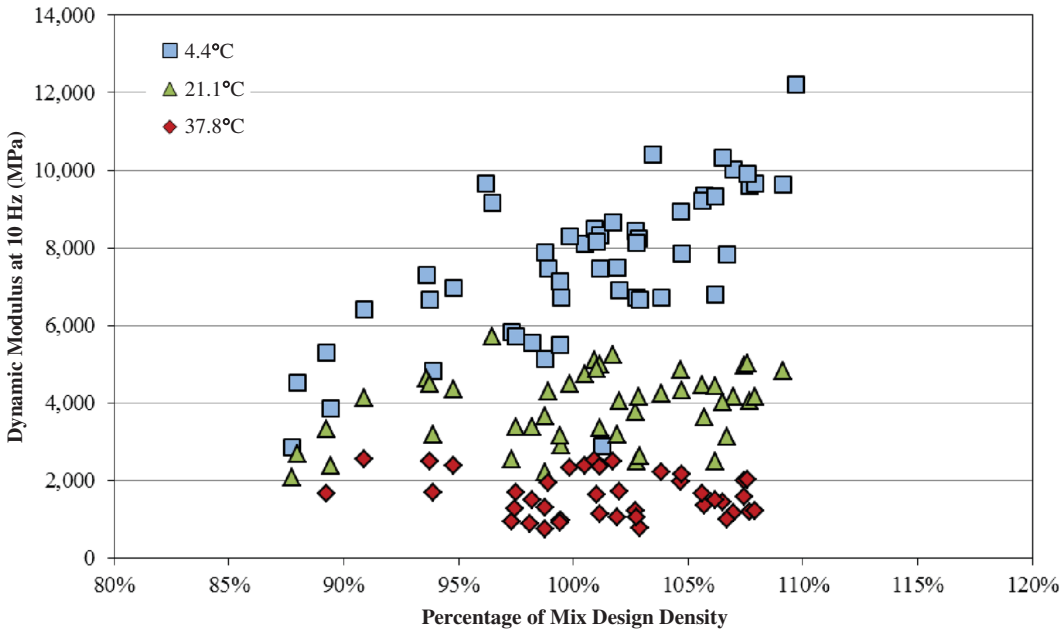

Figure 30. Relationship between percentage mix design density and stiffness.

A bivariate correlation was performed between the design and performance properties. Correlation coefficients between these two groups are summarized in Table 10. Very few strong correlations were observed; nearly all of the correlation coefficients were less than 0.3 in absolute value terms. At 4°C, 25 Hz and 20°C, 10 Hz, the modulus values were more strongly correlated with bulk density. A modestly strong correlation also was observed between lower shelf and dry additive.

The intercorrelations within each category of properties are presented in Table 11 and Table 12. As expected, modulus values had higher intercorrelations among themselves (E* @ 4°C, 25 Hz versus E* @ 20°C, 10 Hz versus E* @ 40°C, 1 Hz), as shown in Table 11. Gradation parameters (P200, Cu, Cz) also had higher intercorrelations, as shown in Table 12.

Overall, the limited set of cold-recycled materials at the end of this study prevented any stronger statistical conclusions between mixture and construction parameters and expected material behavior.

Table 10. Correlation coefficients of design versus performance parameters.

	Stabilizer Content	P200	Cu	Cz	OL Thickness	Curing Time	Dry Additive	Depth of Recycling	Bulk Density
Max. E*	0.09	0.037	0.06	0.135	0.061	0.023	-0.029	0.044	-0.091
Min. E*	-0.043	0.218	0.004	0.212	0.089	0.035	0.32	0.225	-0.074
Beta (β)	0.092	0.073	0.128	0.205	-0.071	0.116	0.142	0.072	0.061
Gamma (γ)	0.016	-0.211	-0.156	-0.069	-0.18	0.084	-0.056	-0.174	0.254
EA	-0.141	-0.144	-0.247	0.013	-0.084	0.011	0.107	-0.123	0.169
E* @ 4.4°C, 25 Hz	-0.022	-0.239	-0.276	-0.17	-0.268	-0.064	-0.165	-0.141	0.766
E* @ 21.1°C, 10 Hz	-0.055	-0.059	-0.208	0.113	0.123	-0.092	0.097	0.159	0.382
E* @ 37.8°C, 1 Hz	-0.033	-0.129	-0.129	0.459	0.391	-0.027	0.428	0.536	-0.112

Table 11. Intercorrelation of performance parameters.

	Max. E*	Min. E*	Beta (β)	Gamma (γ)	EA	E* @ 4°C, 25 Hz	E* @ 20°C, 10 Hz	E* @ 40°C, 1 Hz
Max. E*	1	0.085	0.518	-0.016	-0.688	-0.178	-0.152	-0.031
Min. E*		1	0.243	-0.488	0.052	0.017	0.221	0.298
Beta (β)			1	-0.162	-0.318	-0.159	-0.265	-0.117
Gamma (γ)				1	0.37	0.309	0.123	0.052
EA					1	0.413	0.344	0.152
E* @ 4.4°C, 25 Hz						1	0.811	0.286
E* @ 21.1°C, 10 Hz							1	0.717
E* @ 37.8°C, 1 Hz								1

Table 12. Intercorrelation of design parameters.

	Bulk Density	Stabilizer Content	P200	Cu	Cz	OL Thickness	Curing Time	Dry Additive	Depth of Recycling
Bulk density	1	0.069	-0.181	-0.151	-0.412	-0.49	0.013	-0.391	-0.478
Stabilizer content		1	0.455	0.681	0.463	-0.221	0.595	-0.083	-0.495
P200			1	0.479	0.248	-0.225	0.165	0.287	0.139
Cu				1	0.237	0.097	0.004	0.055	0.067
Cz					1	0.359	0.386	0.638	0.617
OL thickness						1	-0.288	0.51	0.381
Curing time							1	0114	-0.335
Dry additive								1	0.721
Depth of recycling									1

CHAPTER 5

RLPD Test Results

RLPD testing was conducted on cylindrical specimens with axially applied loading using an AMPT in general accordance with AASHTO TP 79. Modifications to the test included using a lower test temperature (45°C) and the same small-scale cylindrical specimen geometry as used for the dynamic modulus testing. A repeated deviator stress of 482.6 kPa was applied at a constant confining stress of 68.9 kPa.

5.1 RLPD Analysis

Two methods of analysis, one qualitative and one quantitative, were considered for evaluating the RLPD data. The quantitative analysis regressed a power-law function fit to the RLPD curve between 2,000 and 10,000 cycles with the exception of one mixture and a few individual specimens that experienced premature termination. The slope and intercept values were calculated in a spreadsheet from the regressed power-law function for the outlier analysis used in the qualitative investigation. An example of this fit is shown in Figure 31. Upon removing outliers, RLPD envelopes were developed to qualitatively examine the effects of recycling type, recycling agent, and chemical additives on the different in-place recycling mixes. A MATLAB code was used to extract slope and intercept values that were then used in the AASHTOWare Pavement ME Design® software for performance prediction. The performance prediction using RLPD values is discussed further in Chapter 6.

5.2 Outlier Analysis

The slope values calculated in the spreadsheet are shown in Figure 32, and the intercept values are shown in Figure 33. Each mixture type was grouped with its primary stabilizing additive and with its chemical additive if one was used. The outlier identification approach is similar to that described for determining dynamic modulus outlier values (see the section on outlier analysis in Chapter 4). Specimens were arranged by each mix type/stabilizing agent/chemical agent combination and the IQR was calculated for each grouping. If the dynamic modulus of a specimen was greater than the third quartile plus the IQR or less than the first quartile minus the IQR, that specimen was deemed an outlier. All specimens that fell between the outer limits were considered for further analysis.

Of the 24 mixes used for analysis, one mix was removed before outlier analysis due to early catastrophic failure. Deficiencies in specimens, believed to be due to sampling and/or preparation issues, led to the removal of five additional specimens (from three unique mixes), each of which never reached 2,000 cycles. The outlier analysis led to the removal of eight specimens over six mixes. Table 13 summarizes the number of mixes evaluated, specimens considered, and specimens remaining after outlier analysis.

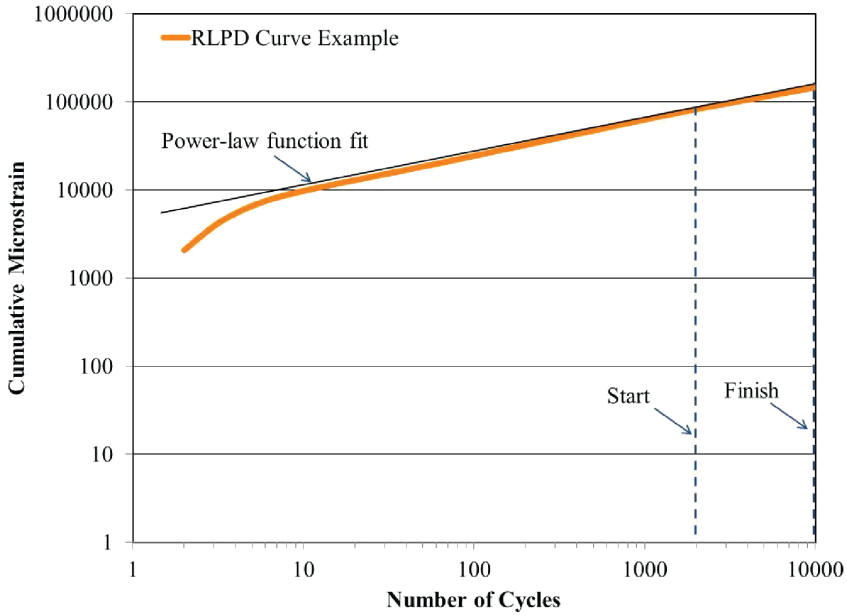

Figure 31. Example RLPD curve and power-law function fit with start and finish points indicated.

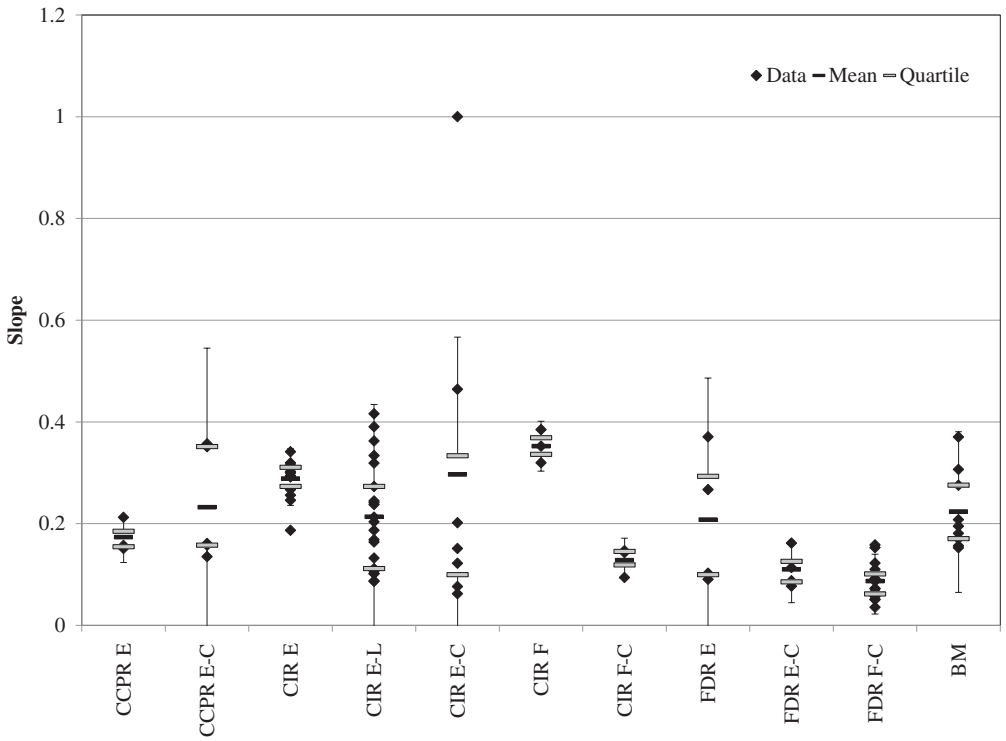

BM = HMA base mixture, E = emulsified asphalt, F = foamed asphalt, C = hydraulic cement, and L = lime.

Figure 32. Slope of the secondary stage of the RLPD data and potential outliers.

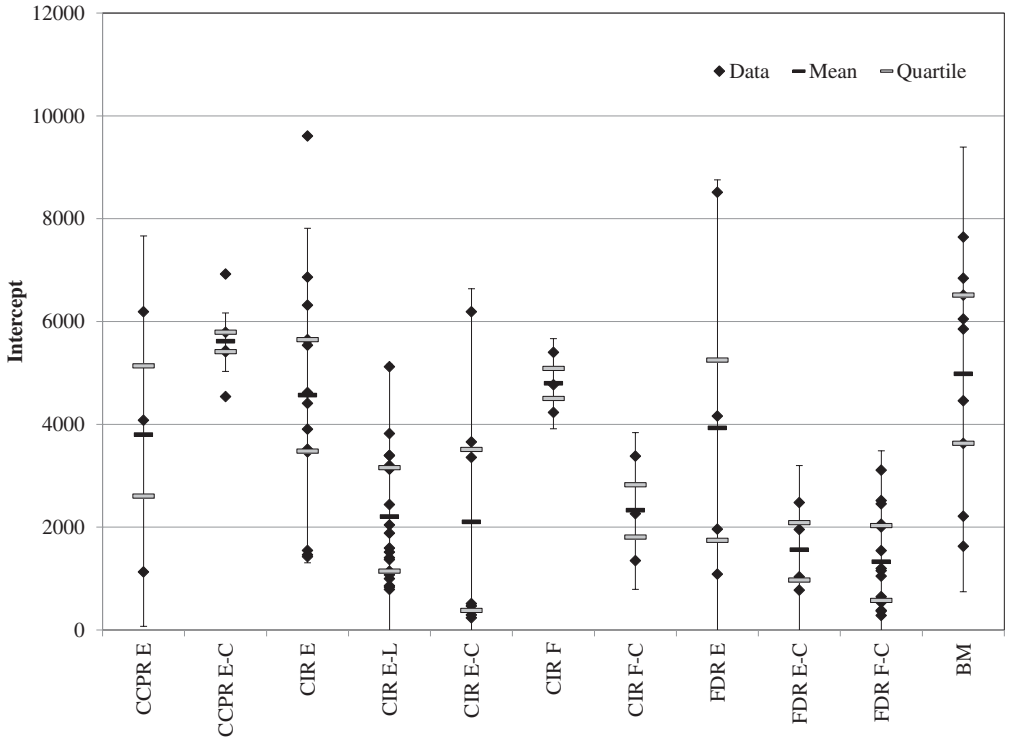

BM = HMA base mixture, E = emulsified asphalt, F = foamed asphalt, C = hydraulic cement, and L = lime.

Figure 33. Intercept of the secondary stage of the RLPD data and potential outliers.

Table 13. Test specimen summary.

Mixture Type	No. Mixtures	No. Specimens	Samples after Outlier Removal
CCPR E	1	3	3
CCPR E-C	2	6	4
CIR E	5	14	12
CIR E-L	5	21	21
CIR E-C	2	7	6
CIR F	1	3	3
CIR F-C	1	3	3
FDR E	1	4	4
FDR E-C	1	4	4
FDR F-C	4	15	12
Asphalt Base Mixture	3	9	9
TOTAL	26	89	81

E = emulsified asphalt, F = foamed asphalt, C = hydraulic cement, and L = lime.

5.3 RLPD Data Envelopes

After removing all outliers, a qualitative measure was taken to compare the permanent deformation performance of each mix type, primary stabilizing agent, and chemical additive. RLPD envelopes were defined by the greatest and least deformation curves for each mix combination. Figure 34 shows the RLPD envelopes for CIR, CCPR, and FDR mixtures. Each of these combinations contains some mixes that are stabilized with foamed or emulsified asphalt and may contain a chemical additive. CCPR and CIR have a higher upper limit than FDR, meaning that they are subject to higher deformation. The CIR and CCPR have good agreement, with the lower limit of the CIR being below that of the CCPR. This would indicate that some of the CIR mixtures tested have better deformation properties. Only three CCPR mixtures are represented in this data set, however, whereas 14 CIR mixtures are represented. It is possible that with more CCPR mixtures even more agreement would occur between CIR and CCPR mixtures. The FDR envelope shows the least deformation, meaning that it has the least deformation.

When comparing these results to the dynamic modulus data trends represented in Figure 15 and Figure 16, similar relationships can be found at the lower frequencies. The FDR mixtures had the highest dynamic modulus values, a result that corresponds well with the lowest permanent deformation characteristics from the RLPD testing. Similarly, the CCPR mixtures had slightly lower dynamic modulus values than did the CIR mixtures, which corresponds to the slightly higher rate of permanent deformation in the RLPD data. When compared to that of the CCPR mixtures, the dynamic modulus envelope of the CIR mixtures had a greater upper bound. This result similarly corresponds to a lower bound deformation found in the RLPD envelope.

Figure 35 shows the same data seen in Figure 34 but adds the RLPD results of three asphalt base mixtures for comparison. Figure 35 shows that the base asphalt mixture envelope overlaps

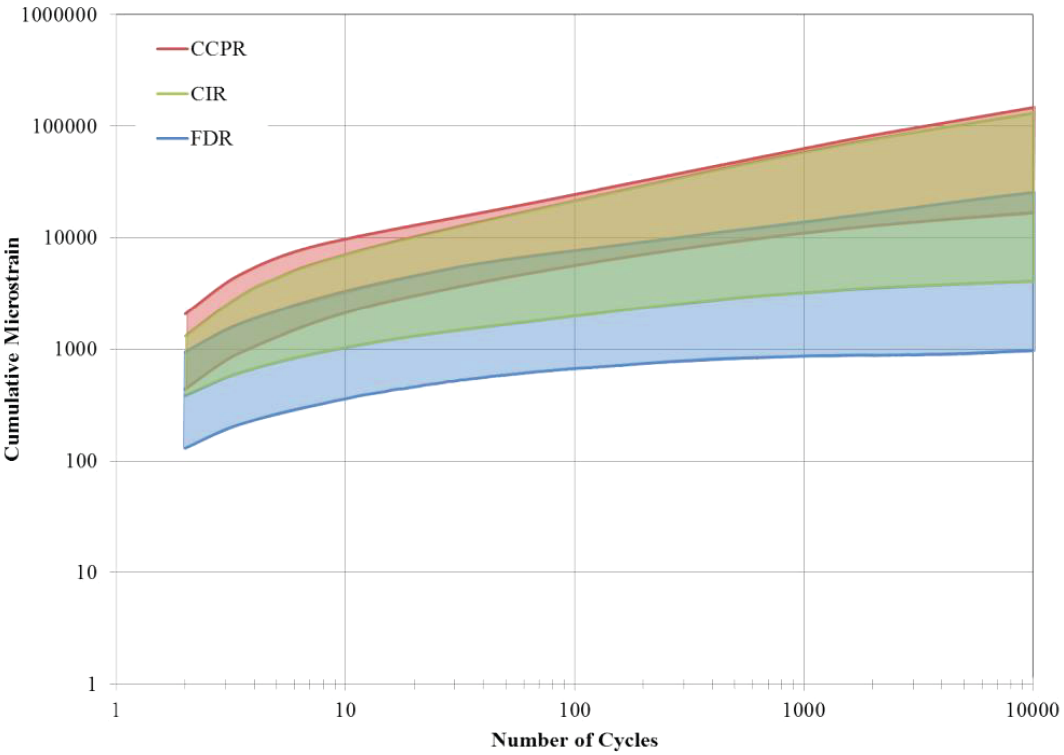

Figure 34. RLPD envelopes for mixtures produced by FDR, CIR, and CCPR.

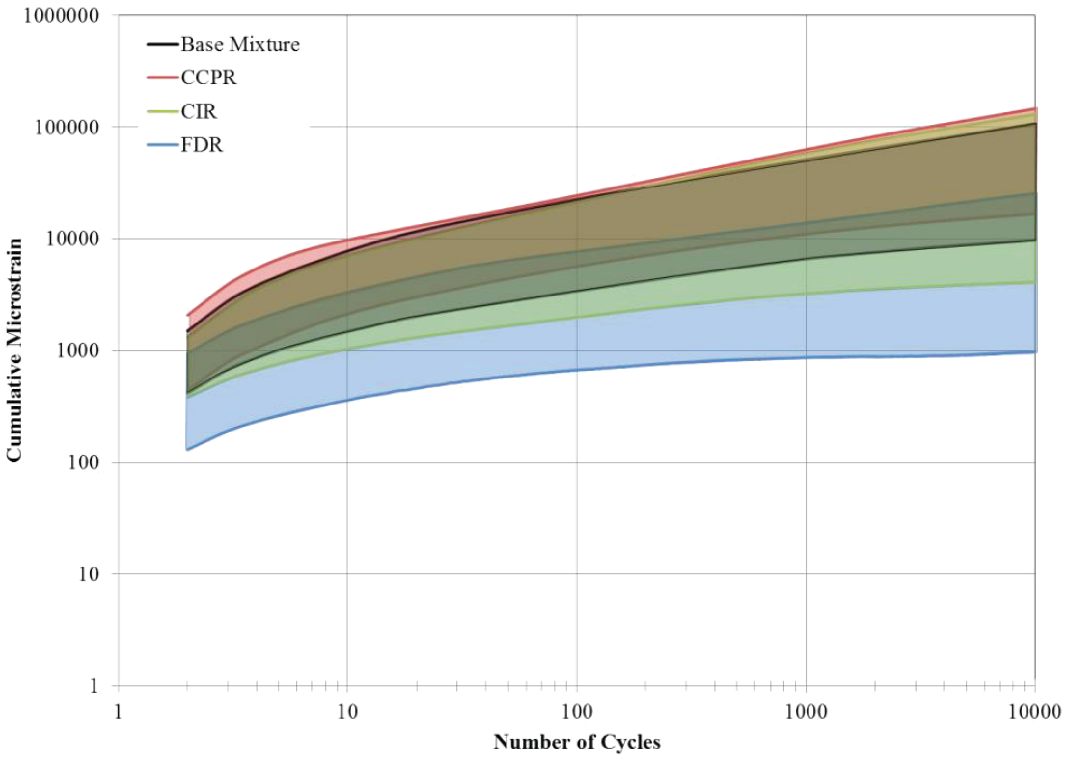

Figure 35. RLPD envelopes for mixtures produced by FDR, CIR, and CCPR, as well as an HMA base mixture.

with much of the area covered by the CCPR and CIR envelopes. This overlap indicates that the permanent deformation characteristics of CCPR and CIR mixtures may be similar to those of traditional base asphalt mixtures, whereas FDR mixtures—whose RLPD envelope was lower than those of the other mixtures—may have better performance. This finding complements ongoing studies that show good rutting performance of recycled mixtures, similar back-calculated stiffness values from falling weight deflectometer (FWD) data when compared to base asphalt mixtures, and similar dynamic modulus test results (Jenkins et al. 2007, Diefenderfer et al. 2016).

The RLPD envelopes comparing emulsified asphalt to foamed asphalt are shown in Figure 36. As with the dynamic modulus data, no clear distinction is seen between the recycling agent types. The emulsified asphalt has a slightly higher upper limit than does the foamed asphalt, but the lower limit of the foamed asphalt is much lower than that of the emulsified asphalt. Figure 36 represents 17 emulsified mixes and six foamed mixes. When comparing the dynamic modulus envelopes to those presented in Figure 18 and Figure 19, a similar trend in stiffness can be found. Generally, the mixtures containing foamed asphalt exhibited a higher stiffness value at the lower frequencies. The lower limit of the dynamic modulus values for the mixtures containing emulsified asphalt was slightly lower than that for the foamed asphalt, which corresponds well with the slightly higher deformation characteristics of emulsified asphalt seen in Figure 36.

The data envelopes showing the results of chemical additives are shown in Figure 37. The presence of cement yielded both the highest and the lowest permanent deformation envelope limits. This same trend was found in the dynamic modulus data shown in Figure 20 and Figure 21. The lower envelope limit of the recycled mixtures with no chemical additive was the highest,

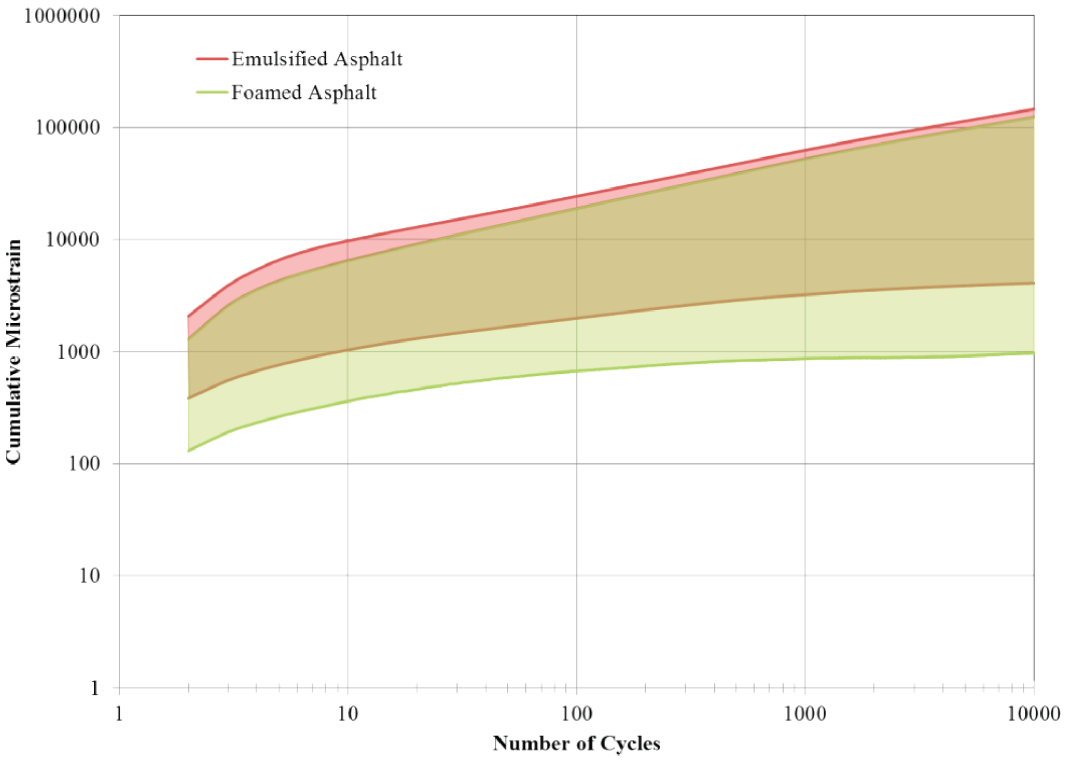

Figure 36. RLPD envelopes for mixtures produced using emulsified asphalt and foamed asphalt as stabilizing/recycling agents.

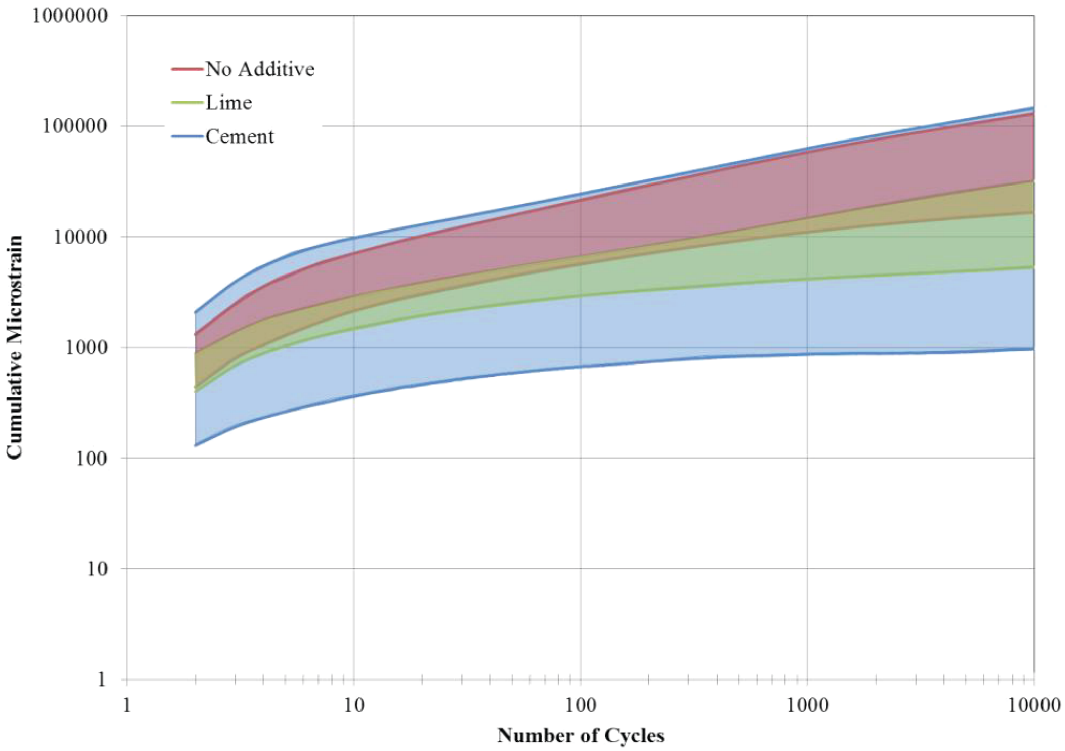

Figure 37. RLPD envelopes for mixtures produced with lime, with cement, or with no additive.

indicating that these mixtures consistently experienced more permanent deformation. The mixtures containing lime performed better than the mixtures with no chemical additive, with some overlap of the data envelopes near the lower limit of the mixtures with no chemical additive. The addition of cement was found to greatly decrease the permanent deformation characteristics in the RLPD test. Similarly, the dynamic modulus data showed an increased modulus for mixtures containing cement.

5.4 Relationship between Rutting Susceptibility and Density

To investigate the relationship between rutting performance and density, the measured bulk density versus slope and intercept values were plotted for each specimen tested. For all in-place recycling processes after outliers were removed, Figure 38 shows the slope versus density and Figure 39 shows the intercept versus density. No clear trend could be established between the slope or the intercept in relation to density. This relationship was further investigated by primary stabilizing agent and by the presence of a chemical additive. In both cases, no clear relationship was found between density and RLPD output.

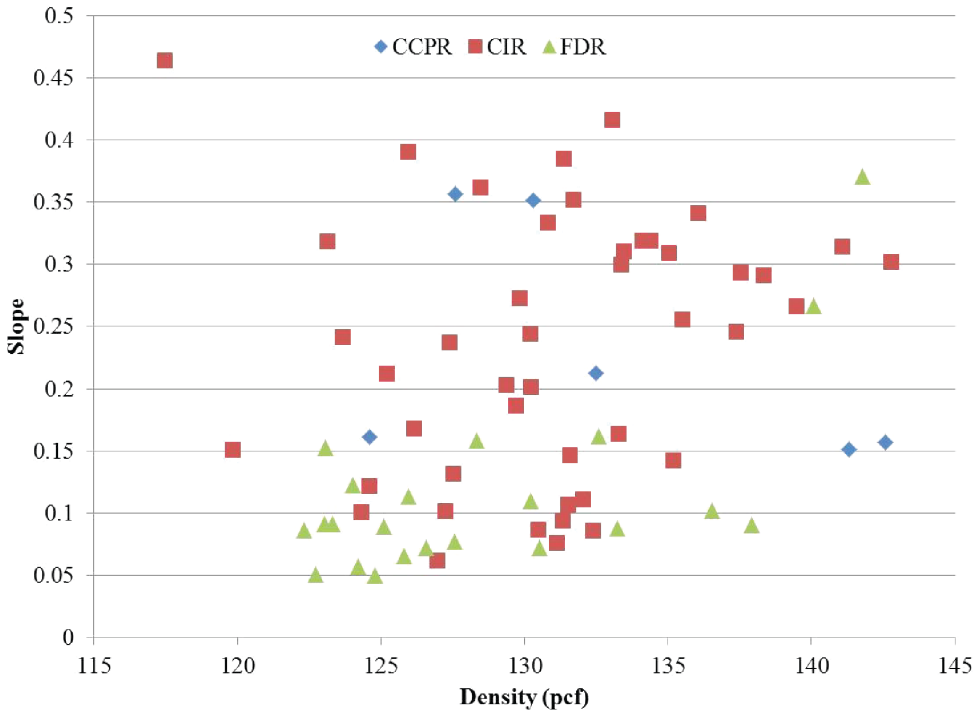

Figure 38. Relationship between bulk density and RLPD slope for CIR, CCPR, and FDR mixtures.

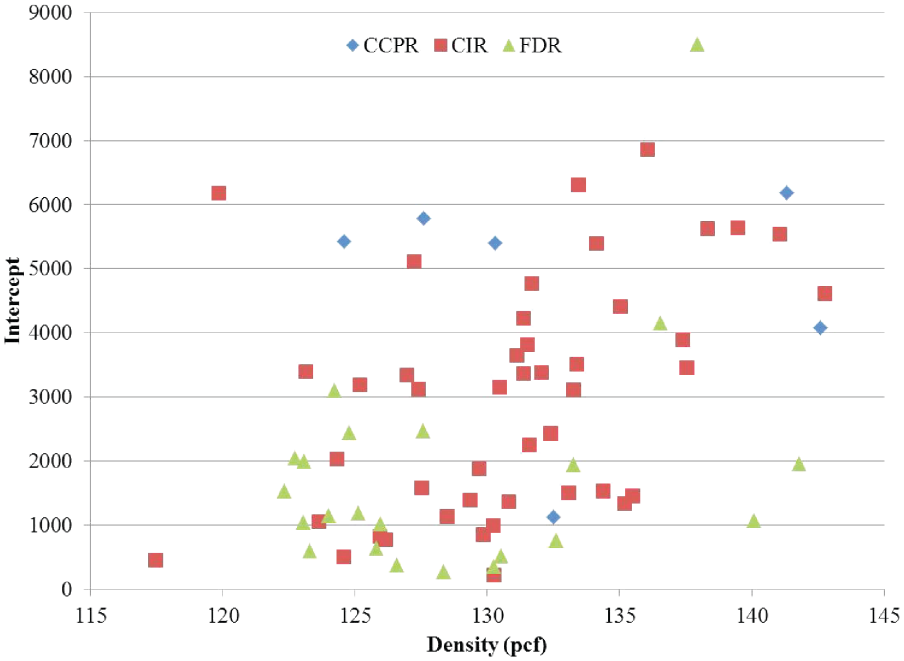

Figure 39. Relationship between bulk density and RLPD intercept for CIR, CCPR, and FDR mixtures.

CHAPTER 6

Performance Evaluation

6.1 The *Mechanistic-Empirical Pavement Design Guide*

The *MEPDG* (AASHTO 2015) is the current recommended method for the structural design of heavily trafficked pavements in the United States. The *MEPDG* methodology is implemented in the AASHTOWare Pavement ME Design software. This software predicts distresses and ride quality in various types of pavements (flexible, rigid, semi-rigid/composite) as functions of traffic, climate, material properties, and other design inputs. It evaluates flexible pavement performance based on rutting, fatigue cracking, thermal cracking, and the International Roughness Index (IRI).

Three levels of inputs are in the Pavement ME Design software, corresponding to different levels of accuracy. Level 1 data, which provide the highest level of accuracy, typically are project-specific values measured in the field or in the lab. Level 2 data typically are based on correlations and require less measured data from the field or lab. Level 3 data, the least accurate level, provide typical default values for inputs.

Material properties for flexible pavements are categorized into three groups: asphalt materials, chemically stabilized materials, and unbound materials. The principal material characteristics are the thickness and stiffness of each layer. Asphalt material stiffness is defined by the dynamic modulus, which takes into account the time-temperature sensitivity of the material. Stabilized and unbound material stiffness levels are specified by the materials' elastic and resilient moduli, respectively.

Additional inputs for rehabilitation designs include the pavement condition at the time of rehabilitation. Rutting in each layer, percentage of fatigue cracking, and milled thickness are the principal inputs. The damaged modulus as measured from nondestructive testing (NDT) also can be input.

The principal outputs from the Pavement ME Design software are the predicted distresses, which are then compared to the design criteria. The primary pavement distress considered for the cold-recycled pavement rehabilitation scenarios is asphalt rutting. Although CIR/CCPR layers could be candidates for bottom-up fatigue cracking, little in the literature suggests this as an important distress mode for the types of pavements considered in this study. The exceptions cited in the literature are primarily from South Africa, where the pavements have high stress-to-strength ratios because of the thin surfacing over the CIR coupled with high traffic/load levels. In the United States, only very lightly trafficked roads are likely to have thin surfacing over the CIR/CCPR layer. Most other pavements—and specifically the types of higher traffic volume pavements that would be designed using the *MEPDG,* the focus of this study—will have moderately thick HMA surface/wearing courses that will suppress stress ratios below the threshold at which fatigue cracking develops.

6.2 Initial Comparisons

6.2.1 Analysis Scenarios

Two rehabilitation scenarios having equivalent structural capacity were designed to evaluate HMA versus cold-recycled material performance. The two pavement structures are shown in Figure 40. The first structure is a recycled pavement with a cold-recycled inlay (RP-CIR). It consists of, from bottom to top, an A-7-5 subgrade with an input resilient modulus of 5,000 psi, 12 in. of A-1-a granular base with an input resilient modulus of 25,000 psi, 2 in. of existing HMA, 5.5 in. of cold-recycled material, and an HMA wearing course of variable thickness (1.5 in., 2 in., 3 in., and 4 in.). The second structure is an HMA pavement (RP-HMA), but the 5.5 in. cold-recycled layer in the first section is replaced with a 4-in. HMA layer. This difference in overlay thickness is consistent with the typical ratios of structural layer coefficients for these materials in AASHTO's 1993 *Guide for Design of Pavement Structures* (i.e., 0.32 for cold-recycled versus 0.40 for a base HMA [Khosravifar, Schwartz, and Goulias 2015]). The RP-HMA structure is the standard against which the cold-recycled inlay in the RP-CIR structure is compared. Level 1 dynamic modulus (|E*|) and RLPD characteristics developed in the 2015 study by Khosravifar, Schwartz, and Goulias were used for the cold-recycled inlay; similar properties for the HMA wearing course and intermediate layers were taken from previous studies. Typical Level 3 properties were used for the existing asphalt. Varying annual average daily traffic (AADT) values consistent with typical traffic volumes were applied.

6.2.2 Analysis Inputs

6.2.2.1 Dynamic Modulus

Each pavement section had three different asphaltic material layers: the HMA wearing course, the HMA or CIR inlay, and the existing underlying HMA layer. Level 1 dynamic modulus data for the wearing course and inlay in both sections were used as inputs in the

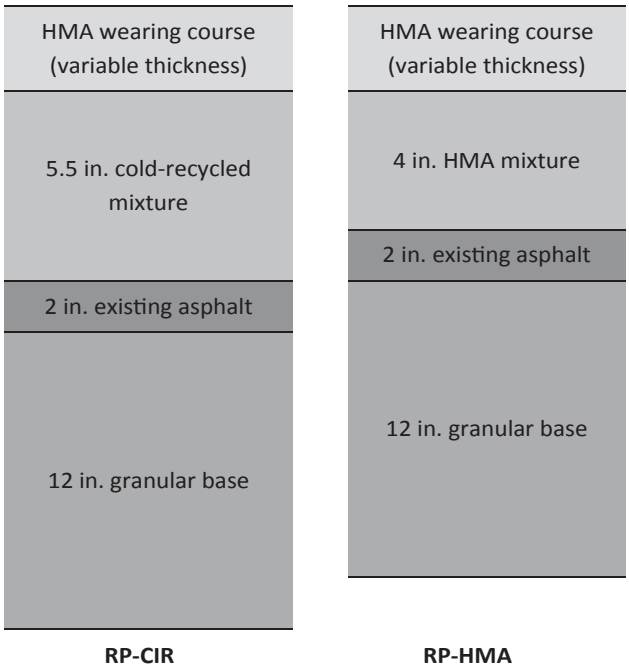

Figure 40. Pavement sections: RP-CIR and RP-HMA.

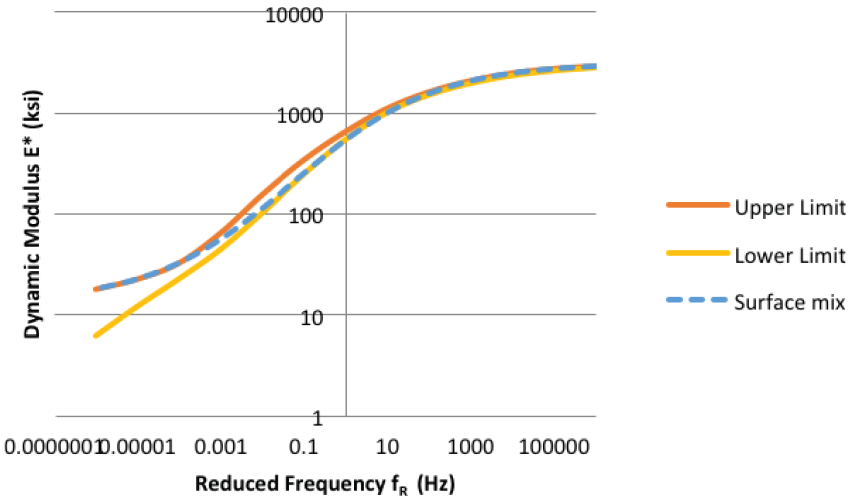

Upper and lower bounds for typical Maryland SHA 9.5 mm and 12.5 mm NMAS mixtures also shown.

Figure 41. Master curve for 9.5 mm NMAS HMA surface wearing course mixture.

Pavement ME Design software (Version 2.0). The HMA wearing surface properties for both sections were taken from a typical Maryland State Highway Administration (Maryland SHA) 9.5 mm NMAS surface mix. Several 9.5 mm NMAS mixes were tested in the lab with a fairly narrow range of dynamic modulus master curves, as shown in Figure 41. The HMA inlay properties for the RP-HMA structure correspond to a typical Maryland SHA 19 mm NMAS mix designated H151B19. The dynamic modulus master curves for this mix and for a range of other 19 mm mixtures are illustrated in Figure 42.

For the RP-CR layer, Level 1 dynamic modulus properties from recycled projects within this study were used. The recycled materials had a wider range of dynamic modulus values when compared to the HMA mixtures tested, as shown in Figure 43. The three cold-recycled inlay materials selected for evaluation in this comparison were from Delaware, Maine, and San Jose, California. The Delaware project (14-1025), a CIR material using emulsified asphalt as the recycling agent,

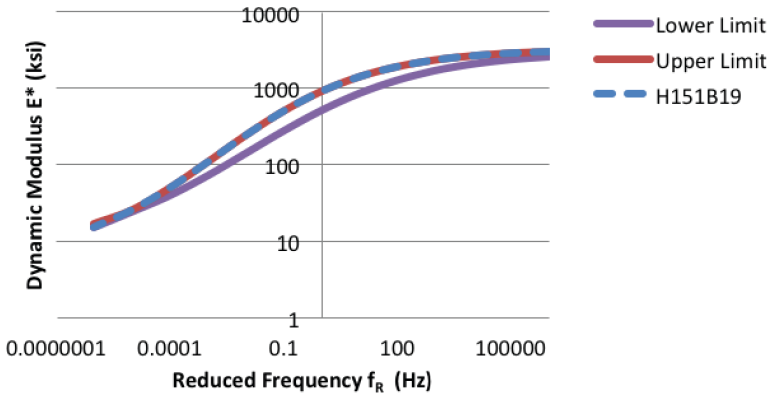

Upper and lower bounds for typical Maryland SHA 19 mm NMAS mixtures also shown.

Figure 42. Master curve for 19 mm NMAS HMA mid-layer mixture (H151B19).

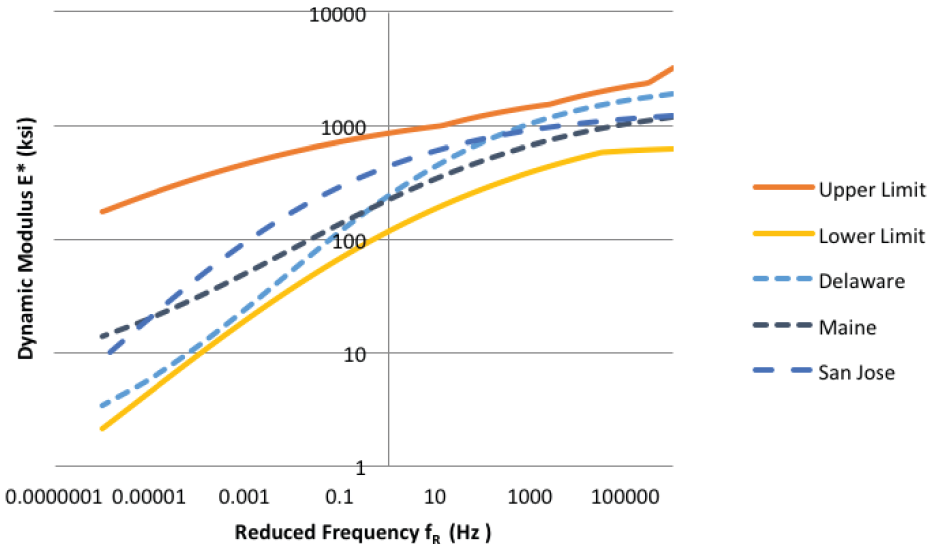

Upper and lower bounds for the cold-recycled materials in this study also shown.

Figure 43. Master curves for cold-recycled overlay materials (Delaware/CIR, Maine/CCPR, San Jose/CIR).

exhibited higher laboratory-measured permanent strains in comparison to the other materials. The Maine project (15-1003), a CCPR material also using emulsified asphalt as the recycling agent, had moderate measured permanent strains. The San Jose project (13-1124), a CIR material using foamed asphalt as the recycling agent, had the smallest measured permanent strains.

The temperatures and loading rates specified for dynamic modulus testing in AASHTO TP 79 do not conform to the temperatures and loading rates required for input to the Pavement ME Design software. This introduces an intermediate step as a minor complexity. A master curve must be developed externally from the measured dynamic modulus values collected using AASHTO TP 79. Then, the dynamic modulus values at temperatures and loading rates required by Pavement ME Design must be computed for input. The master curve optimization/fitting algorithm embedded in Pavement ME Design then regenerates a new master curve for internal use within the program. However, the Pavement ME Design master curve optimization algorithm did not converge for some of the cold-recycled materials.

Ranges of suggested dynamic modulus values for input into Pavement ME Design are included in Tables 14 through 19.

For Level 1 mixture |E*| inputs, the Pavement ME Design software also requires a measured binder G* master curve. This is used only by the global aging model when Level 1 mixture |E*| data have been entered. Past studies have shown that the Pavement ME Design distress predictions are insensitive to the binder G* master curve when Level 1 mixture |E*| data have been input. It is sufficient to have a binder G* master curve that is reasonably close to the actual effective binder behavior for the cold-recycled material.

6.2.2.2 RLPD Input

Rutting was the main distress measure evaluated in these comparisons. Therefore, the Level 1 rutting coefficient inputs were required for the Pavement ME Design software. The capability of specifying layer-specific rutting coefficients was a new feature added to Version 2.0 of the Pavement ME Design software. These coefficients are not input directly as layer properties, but rather as layer-specific calibration values.

54 Material Properties of Cold In-Place Recycled and Full-Depth Reclamation Asphalt Concrete

Table 14. Suggested dynamic modulus values for CIR projects—upper range.

Temperature	Dynamic Modulus (psi)					
	25 Hz	10 Hz	5 Hz	1 Hz	0.5 Hz	0.1 Hz
14°F	811,952	753,611	709,019	605,319	561,177	461,749
40°F	912,834	856,773	813,384	710,483	665,744	562,612
70°F	545,097	488,271	446,547	355,300	318,943	242,589
100°F	278,091	236,651	207,977	150,492	129,610	89,589
130°F	196,731	163,746	141,519	98,585	83,582	55,849

Table 15. Suggested dynamic modulus values for CIR projects—lower range.

Temperature	Dynamic Modulus (psi)					
	25 Hz	10 Hz	5 Hz	1 Hz	0.5 Hz	0.1 Hz
14°F	1,440,057	1,274,516	1,151,136	878,230	769,393	544,112
40°F	1,666,833	1,501,676	1,376,078	1,089,337	970,929	716,479
70°F	731,008	601,272	512,384	339,123	278,911	170,307
100°F	268,680	203,720	163,365	94,584	73,819	40,654
130°F	117,325	85,120	66,253	36,334	27,913	15,119

Table 16. Suggested dynamic modulus values for CCPR Projects—upper range.

Temperature	Dynamic Modulus (psi)					
	25 Hz	10 Hz	5 Hz	1 Hz	0.5 Hz	0.1 Hz
14°F	926,778	862,526	812,585	693,861	642,325	524,408
40°F	1,032,195	972,539	925,525	811,263	760,450	640,975
70°F	623,417	556,082	506,190	396,141	352,112	259,894
100°F	308,060	257,624	222,928	154,384	130,026	84,692
130°F	205,122	166,312	140,578	92,298	76,050	47,279

Table 17. Suggested dynamic modulus values for CCPR projects—lower range.

Temperature	Dynamic Modulus (psi)					
	25 Hz	10 Hz	5 Hz	1 Hz	0.5 Hz	0.1 Hz
14°F	553,849	492,244	446,812	347,297	307,773	225,594
40°F	625,372	562,692	515,819	410,920	368,278	277,420
70°F	293,825	246,546	213,915	149,123	125,967	82,624
100°F	123,317	97,360	80,712	50,844	41,242	24,887
130°F	60,230	45,910	37,140	22,304	17,805	10,483

56 Material Properties of Cold In-Place Recycled and Full-Depth Reclamation Asphalt Concrete

Table 18. Suggested dynamic modulus values for FDR projects—upper range.

Temperature	Dynamic Modulus (psi)					
	25 Hz	10 Hz	5 Hz	1 Hz	0.5 Hz	0.1 Hz
14°F	1,071,198	1,037,336	1,010,164	941,923	910,367	832,404
40°F	1,122,287	1,092,240	1,067,996	1,006,561	977,875	906,204
70°F	898,442	854,246	819,495	735,019	697,311	607,839
100°F	683,188	632,276	593,431	503,380	465,194	379,587
130°F	545,072	494,033	455,994	370,944	336,258	261,676

Table 19. Suggested dynamic modulus values for FDR projects—lower range.

Temperature	Dynamic Modulus (psi)					
	25 Hz	10 Hz	5 Hz	1 Hz	0.5 Hz	0.1 Hz
14°F	692,192	647,721	612,802	528,551	491,434	405,248
40°F	733,752	691,449	657,969	576,150	539,595	453,347
70°F	477,733	428,573	391,774	309,450	276,058	205,246
100°F	273,960	232,529	203,434	144,313	122,701	81,466
130°F	162,615	132,148	111,827	73,463	60,490	37,474

To derive the rutting calibration coefficients, the *MEPDG* rutting model was fit to the measured laboratory RLPD test results. The *MEPDG* rutting model is as follows:

$$\frac{\varepsilon_p}{\varepsilon_r} = k_z \beta_{r1} 10^{k_1} T^{k_2 \beta_{r2}} N^{k_3 \beta_{r3}} \tag{6}$$

in which

ε_p = the measured permanent strain,
ε_r = the resilient strain,
T = temperature (°F),
N = number of load repetitions,
k_1, k_2, and k_3 = RLPD properties for the secondary portion of the response, and
β_{r1}, β_{r2}, and β_{r3} = field calibration coefficients.

The k_z term is a depth correction function given as

$$k_z = (C_1 + C_2 z)(0.328196^z) \tag{7}$$

with

$$C_1 = -0.1030 H_a^2 + 2.4828 H_a - 17.342 \tag{8a}$$

$$C_2 = 0.0172 H_a^2 - 0.7331 H_a - 27.428 \tag{8b}$$

in which

z = depth from the surface, and
H_a = total thickness of the asphalt layers.

The depth function k_z was set to 1, as it is not relevant for interpreting laboratory test data having homogeneous stress conditions. The β_{r1}, β_{r2}, and β_{r3} field calibration coefficients also were set to 1. The resilient strain ε_p required for the strain ratio dependent variable $\varepsilon_p/\varepsilon_r$ is not measured or recorded by the AMPT used in this study and thus was estimated using the deviator stress and measured unconfined dynamic modulus |E*| at the RLPD test temperature and frequency (10 Hz). Best estimates for the k_1, k_2, and k_3 material coefficients were determined through least squares multivariate linear regression analysis in a transformed log-log coordinate space.

It has been assumed here that the HMA rutting model in the *MEPDG* also applies to bituminously stabilized cold-recycled materials. Given that the laboratory RLPD behavior of cold-recycled materials is similar to that of HMA (i.e., both materials follow the standard power-law relationship between permanent strains and number of load cycles), this assumption seems reasonable. It could be disproved if there were large discrepancies between predicted and measured rutting of cold-recycled pavements under in-service conditions, but these data do not exist at present. Although not evaluated for this research, it is also assumed that the IRI prediction models apply to cold-recycled materials. This assumption also seems reasonable, as the IRI prediction models are a function of total rutting only and do not distinguish among the layer sources.

One problem in the analysis is that the RLPD tests on the cold-recycled materials were performed at a single temperature. The *MEPDG* rutting model (Equation 6) is dependent on temperature, so plastic strain data for at least two other temperatures are needed. The technique developed by Khosravifar et al. (2015) was used to predict plastic deformations at other temperatures. The process is similar to fitting a master curve; after a reference temperature is picked, the temperature shift function determined from the dynamic modulus testing is used to shift the permanent strain data to the desired temperature, as show conceptually in Figure 44.

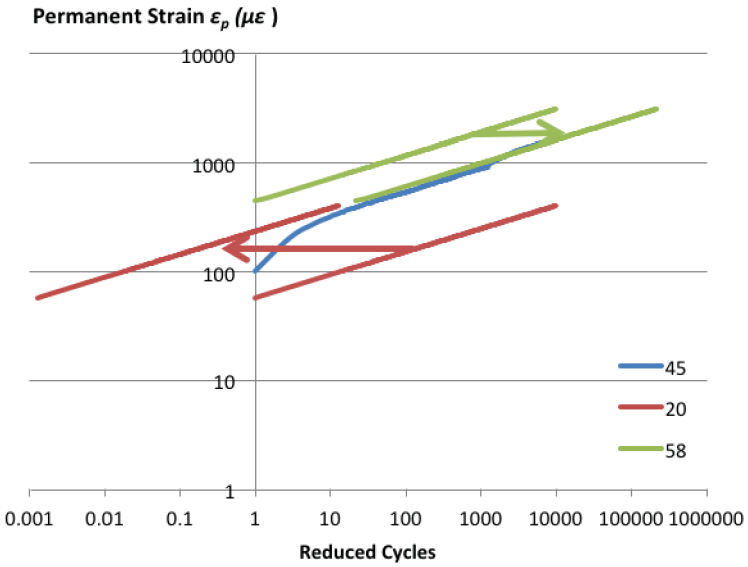

Figure 44. Time-temperature shift factor to form a RLPD master curve using method from Khosravifar et al. (2015).

The process uses the concept of reduced load cycles and reduced intercept, similar to the way dynamic modulus testing uses the concept of reduced frequencies:

$$\log(N_R) = \log(N) - \log[a(T)] \tag{9a}$$

$$\log(A') = \log(A) + B\log[a(T)] \tag{9b}$$

in which

N = number of load cycles,
N_R = reduced number of load cycles,
A = intercept of the secondary zone of the RLPD response,
A' = reduced intercept value, and
B = slope of the secondary zone of the RLPD response.

A typical fitted RLPD model for a cold-recycled material is shown in Figure 45.

The HMA materials were tested at three temperatures, so there was no need to predict the permanent deformations at other temperatures for these materials.

During the fitting procedure for some mixes, negative values were obtained for the temperature coefficient, which suggests that resilient strains are more sensitive to temperature than are permanent strains. Figure 46 shows the rates of change for the resilient strains and the plastic strains at the 10,000th cycle as a function of temperature. Each strain type is normalized by its respective strain at 20°C. For the Delaware CIR material, the plastic and resilient strains vary nearly identically with temperature, implying that their strain ratio (ε/ε at 20°C) is insensitive to temperature (i.e., that k_2 is nearly zero). On the other hand, the San Jose, California CIR material shows resilient strains increasing faster than plastic strains with temperature, implying that the ratio of plastic to resilient strains decreases with temperature (i.e., that k_2 is negative). These negative coefficients were hypothesized to be the consequence of using unconfined dynamic modulus values to estimate the resilient strains. Dynamic modulus is sensitive to confinement at high temperatures.

Because resilient strains were not measured in the AMPT, they were estimated from the applied stresses and the dynamic modulus of the material. However, the RLPD test is performed

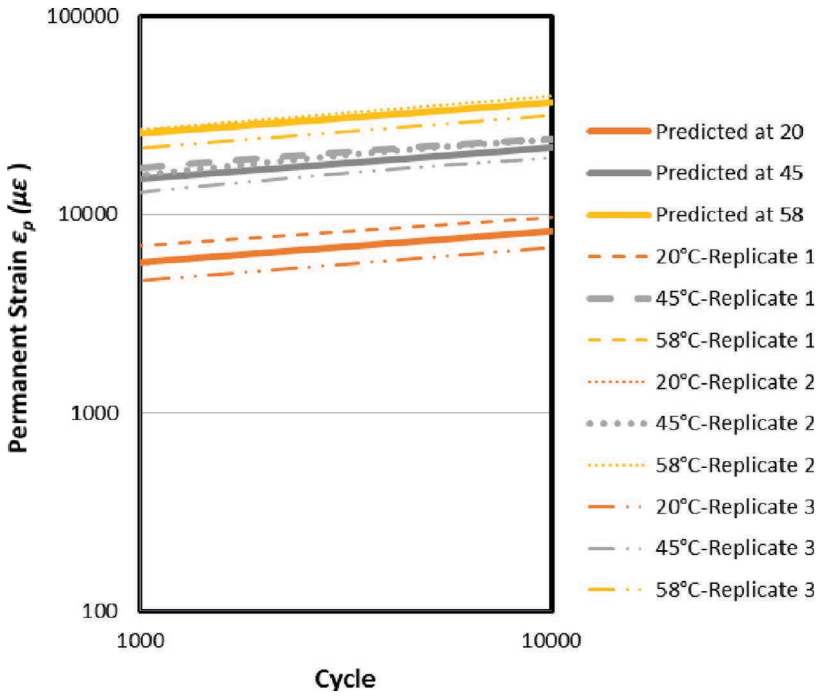

Figure 45. Typical RLPD fitted model for cold-recycled mixture 15-1003.

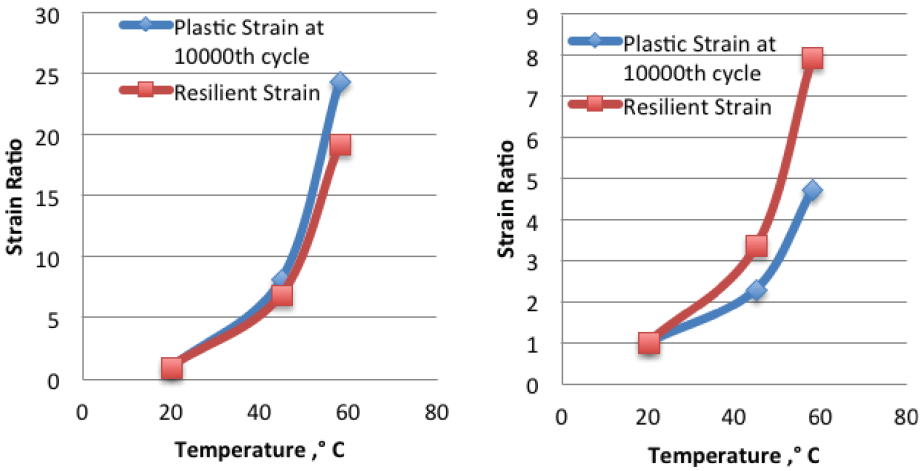

Delaware CIR Mixture
(Positive temperature coefficient k_{r2})

San Jose, California CIR Mixture
(Negative temperature coefficient)

$$\text{Strain ratio} = \frac{\varepsilon}{\varepsilon \text{ at } 20°C}.$$

Figure 46. Strain ratios for two mixes, one with a positive temperature coefficient and one with a negative temperature coefficient.

60 Material Properties of Cold In-Place Recycled and Full-Depth Reclamation Asphalt Concrete

Table 20. Calibration coefficients for confined master curve.

C3	C4	C5	C6
1.632	0.421	4.031	3.259

under confined conditions while the dynamic modulus test is performed under unconfined conditions. Previous researchers have shown that there can be significant differences between confined and unconfined dynamic modulus values, especially at the high temperatures of the RLPD test (Seo et al. 2007; Yun et al. 2010; Zhao et al. 2013).

Confined dynamic modulus values are required to estimate more realistically the resilient strains in the RLPD test. Zhao et al. (2013) proposed a model to derive confined dynamic modulus values at different confining pressures:

$$\ln(|E^*|) = \delta + \frac{\alpha}{1 + e^{\beta+\gamma \ln(\omega_r)}} + \frac{C_5\left(e^{-C_6 P_0} - e^{-C_6 P}\right)}{1 + e^{C_3 + C_4 \ln(\omega_r)}} \quad (10)$$

in which

P_0 = test confining pressure,
P = desired confining pressure,
ω_r = reduced loading frequency,
$\delta, \alpha, \gamma, \beta$ = master curve fitting parameters (similar to Equation 2, which is discussed in the section on "Dynamic Modulus Testing" in Chapter 3), and
C_3, C_4, C_5, C_6 = fitting parameters.

The model must be calibrated with confined dynamic modulus data. Zhao et al. (2013) performed the calibration for 19 mm and 25 mm NMAS Superpave HMA mixtures. Zhao et al.'s calibrated coefficients for the 19 mm NMAS mixture were assumed to be representative for the cold-recycled materials tested in this study. The coefficients are summarized in Table 20.

These calibrated coefficients were therefore used to estimate the confined modulus values for the HMA and cold-recycled materials in this study at the 10 psi confining pressure in the RLPD test, and thus to estimate the resilient strains for the confined conditions. Figure 47 shows

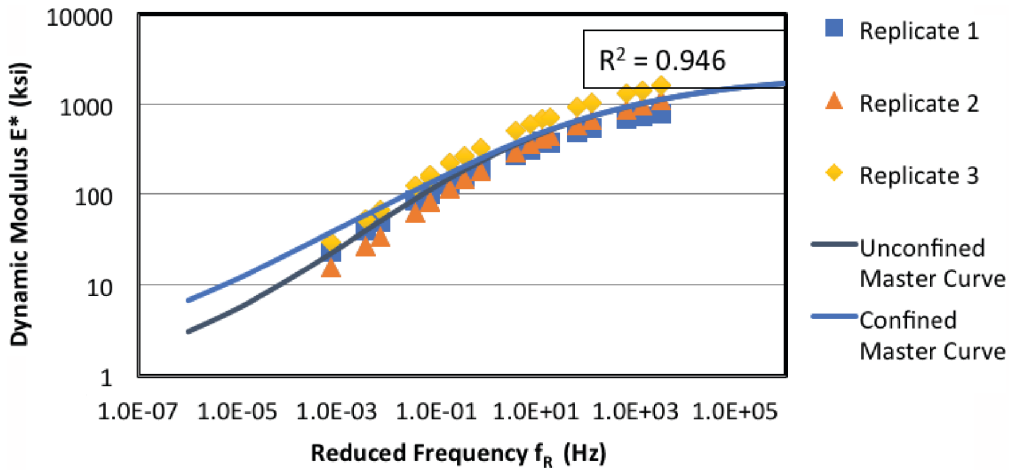

Figure 47. Confined versus unconfined dynamic modulus master curves for Project 13-1114.

typical confined versus unconfined dynamic modulus master curves for a cold-recycled material as determined using this procedure. A recommendation for future research is to either measure confined dynamic modulus directly for the cold-recycled materials or have resilient strain reported directly during RLPD testing using the AMPT.

Summaries of the *MEPDG* RLPD material coefficients attained from applying these procedures to the HMA and cold-recycled materials are provided in Table 21 and Table 22, respectively. For completeness, all HMA and cold-recycled materials evaluated in this study are included in the tables.

6.2.2.3 Traffic Input

Differing traffic loads were applied for the various HMA wearing course thicknesses. Appropriate AADT values were determined based on the 1993 AASHTO flexible pavement design standard. The 1993 AASHTO procedure predicted 10 million, 15 million, 27 million, and 46 million equivalent single axle loads (ESALs) over a 20-year design life for pavement structures having HMA wearing courses with thicknesses of 1.5 in., 2 in., 3 in., and 4 in., respectively. For inputs to the Pavement ME Design software, the vehicle mix was set as a 100% distribution of Class 5 vehicles. Class 5 vehicles include 2-axle vehicles with dual rear tires (e.g., single-unit trucks, mini school buses, and camping vehicles). To simplify the traffic loading, the load for all rear axles was set at 18 kips (i.e., one ESAL), and the load for all front axles was set at zero. The traffic distribution was assumed to be constant over all months with zero growth rate.

6.2.2.4 Climate Input

All analyses were conducted for temperate climates. The Baltimore, Maryland, weather station data were used as input to the *MEDPG*.

6.2.3 Comparisons of Predicted Performance

The predicted asphalt rutting results for the three HMA surface course thicknesses are shown in Figure 48. The predicted rut depths include the contributions from all bituminous materials—the HMA surface course, the HMA/cold-recycled structural inlay, and any additional rutting in

Table 21. *MEPDG* RLPD material coefficients for HMA mixtures.

Mixture	k_1	k_2	k_3
H160A09	1.55E-01	0.821	0.163
H151B19	6.64E-01	0.407	0.228
H135A19	6.45E+00	0.101	0.117
H077A09	5.22E-01	0.610	0.130
H083A12	6.06E-02	1.018	0.138
H127A12	5.09E+00	0.100	0.144
H135A12	1.66E-01	0.787	0.124
H168A09	8.25E+00	0.0002	0.116

62 Material Properties of Cold In-Place Recycled and Full-Depth Reclamation Asphalt Concrete

Table 22. *MEPDG* RLPD material coefficients for cold-recycled mixtures.

Project (Mixture)	k_1	k_2	k_3
13-1093	3.72E-07	3.3054	0.340
13-1111	1.61E-09	4.5055	0.530
13-1112	4.47E-03	1.5668	0.366
13-1113	5.62E-02	0.9332	0.304
13-1114	1.88E-01	0.7226	0.314
13-1115	1.59E+01	0.0687	0.027
13-1116	2.97E+00	0.2029	0.071
13-1117	6.06E-03	1.4279	0.126
13-1124	3.15E+00	0.1545	0.149
13-1127	2.11E+00	0.0968	0.155
14-1001	3.01E-04	2.1380	0.362
14-1002	1.73E-16	7.3551	0.705
14-1003	3.87E-03	1.5091	0.279
14-1011	2.92E-03	1.3187	0.183
14-1025	2.73E-02	1.1658	0.346
14-1026	3.03E-04	2.1724	0.413
14-1027	1.06E+00	0.5540	0.181
14-1028	3.17E-01	0.6648	0.118
14-1055	1.99E-08	4.0716	0.470
14-1057	2.39E-02	1.2063	0.140
14-1058	3.88E+00	0.2544	0.156
14-1062	5.58E-01	0.5587	0.168
15-1002	7.48E-05	2.3050	0.383
15-1003	4.47E+00	0.1373	0.159

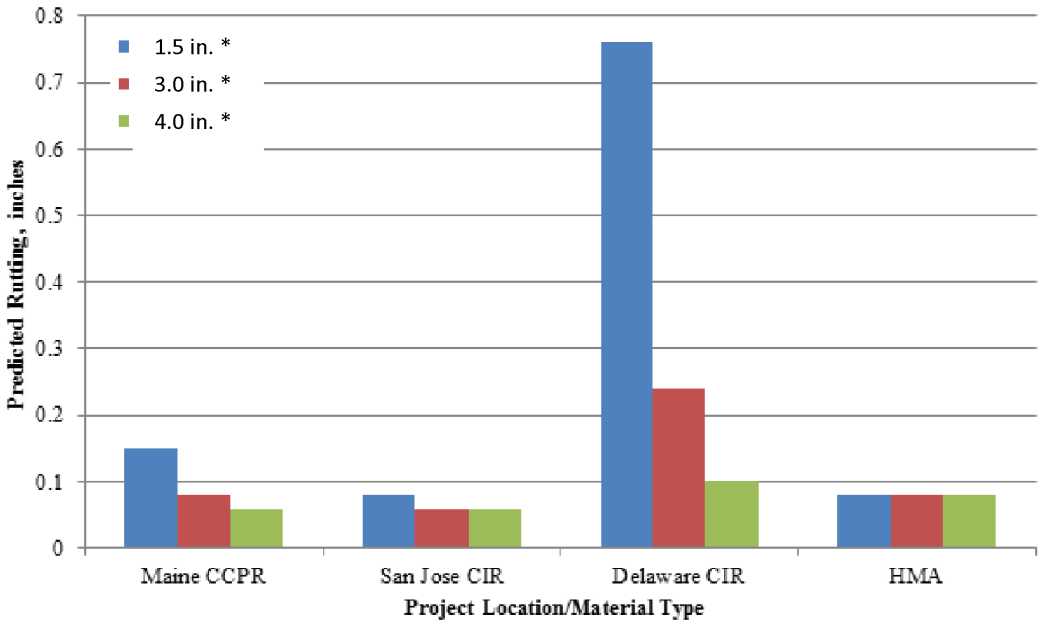

* HMA surface wearing course thickness.

Figure 48. Asphalt rutting for selected cold-recycled inlays in comparison to HMA inlay.

the underlying existing HMA material. From Figure 48, the predicted rutting performance for the CCPR materials from Maine and the CIR materials from San Jose, California, were similar or better to that predicted for the HMA inlay scenario. However, the predicted rutting performance for the CIR materials from Delaware was much worse than that predicted for the HMA inlay at HMA wearing course thicknesses of 1.5 in. and 3 in. The predicted rutting for the Delaware CIR with a 4-in. HMA wearing course was similar to that predicted for the HMA inlay condition with a 4-in. HMA wearing course. The two recycled materials that showed similar or better predicted rutting performance than HMA also included cement as a chemical additive. The recycled material that showed worse predicted rutting performance than HMA did not include any chemical additive.

The higher rutting susceptibility of the Delaware CIR material can be observed in the laboratory RLPD curves where the Delaware CIR material is at upper range of plastic strains at all temperatures. In the future, the interactions between pavement structure and cold-recycled material properties could be examined more comprehensively to develop guidelines for the appropriate inlay and surface wearing course thicknesses.

6.3 Rutting Performance Evaluation of All Cold-recycled Materials

In addition to the initial three projects selected to represent the range of material quality, all recycled projects assessed in this study were similarly analyzed for rutting performance. Different climatic conditions were also added to the study to observe the effect of temperature on rutting performance. Three locations having different climatic characteristics were selected: Maryland (temperate), Arizona (hot), and Minnesota (cold).

The pavement sections considered were the same as those used in prior analyses (see Figure 40). Four structural sections were analyzed (1.5-in., 2-in., 3-in., and 4-in. HMA surface wearing course thicknesses). For comparison purposes, approximated FDR "inlays" were included in the analyses along with CIR and CCPR inlays. (The pavement sections do not accurately represent how FDR

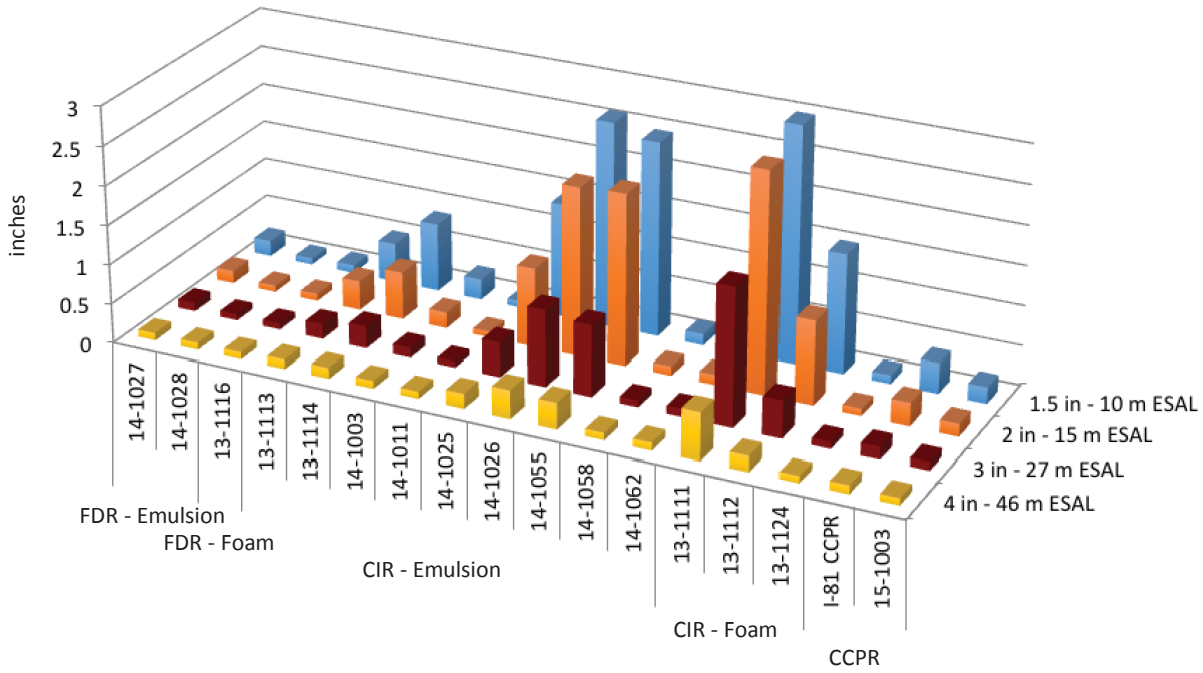

Figure 49. Predicted rutting performance for all cold-recycled projects: Arizona weather (hot).

materials would be used in a real pavement structure, but the approximation permits a better comparison of the FDR performance to the other cold-recycled materials.)

The predicted asphalt rutting results are summarized in Figures 49 through 51; the asphalt rutting includes the contributions from all of the bituminous layers—surface HMA, cold-recycled/HMA overlay, and additional rutting from underlying existing HMA layer. Projects 13-1093, 13-1115, 13-1117, 13-1127, 14-1001, 14-1002, 14-1057, and 15-1002 are not included in

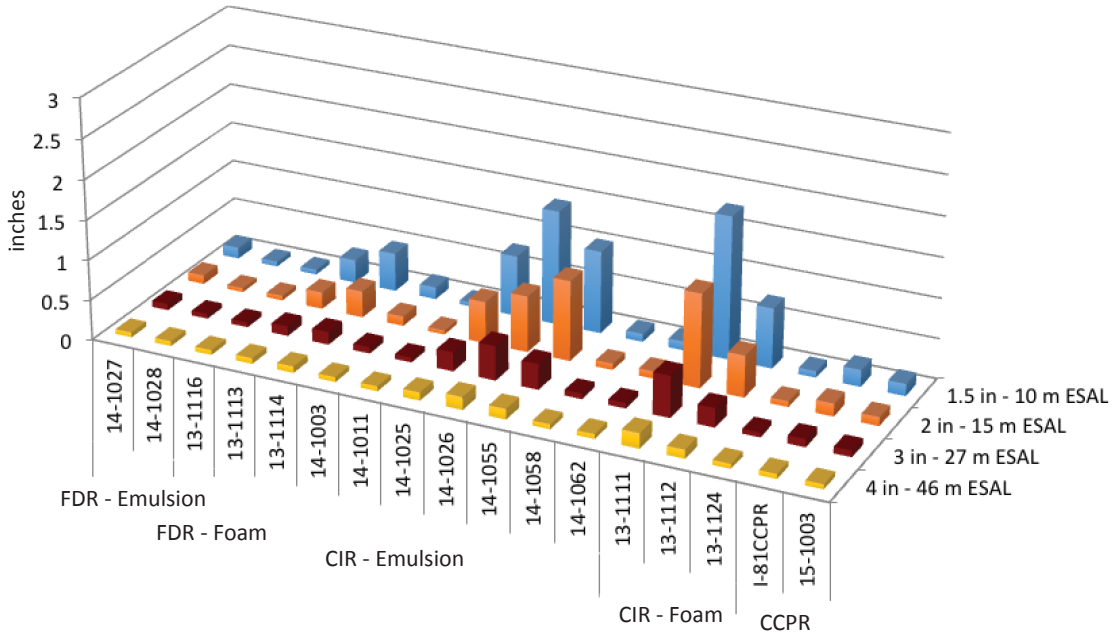

Figure 50. Predicted rutting performances for all cold-recycled projects: Maryland weather (temperate).

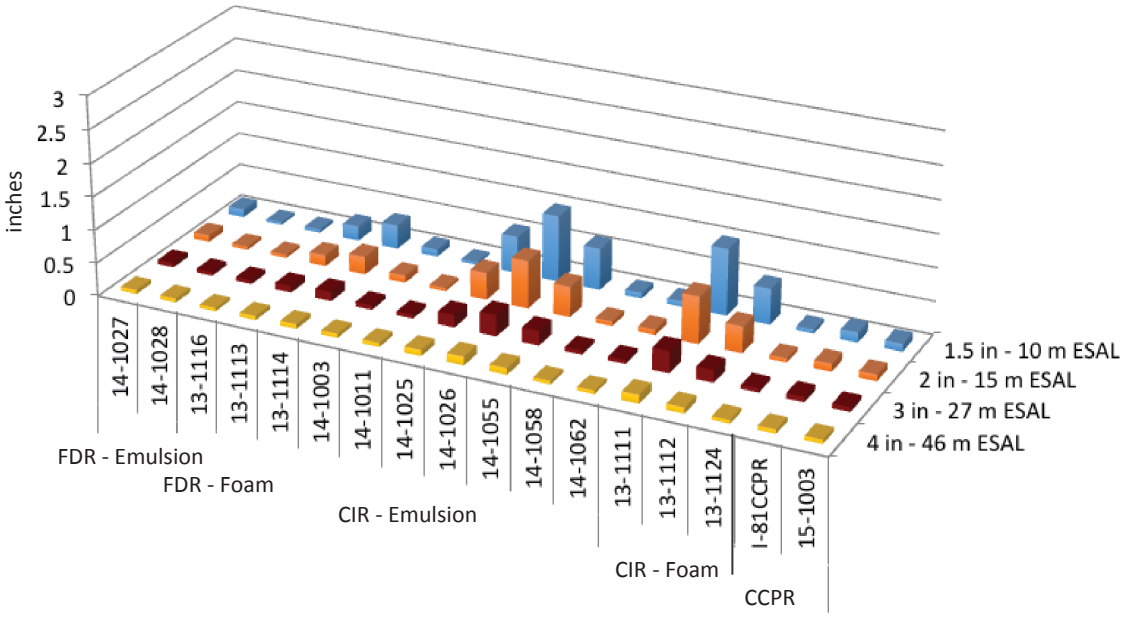

Figure 51. Predicted rutting performance for all cold-recycled projects: Minnesota weather (cold).

Figures 49 through 51. The program algorithms of the Pavement ME Design software were unable to fit master curves to the input laboratory-measured dynamic modulus data for these projects; consequently, these projects could not be analyzed. A more robust dynamic modulus master curve algorithm may be warranted for the Pavement ME Design software. In addition, rutting could not be predicted for the I-81 cold in-place recycling lane because no RLPD testing was performed for the CIR material.

As can be observed in Figures 49 through 51, five of the 17 analyzed projects had very high rutting values. These large rutting values are a consequence of the input RLPD material coefficients. The coefficients on temperature and traffic load strongly influence predicted rutting. The five projects with the highest predicted rutting (13-1111, 13-1112, 14-1025, 14-1026, and 14-1055) also exhibited high permanent strains in the laboratory RLPD tests as compared to the other cold-recycled materials.

The ranges of predicted rutting for all of the cold-recycled projects analyzed as compared with the predicted rutting of conventional HMA inlays are summarized in Figures 52 through 54. In these box-and-whisker plots, the vertical lines delineate the minimum and maximum limits of the data, the boxes delineate the first and third quartile values, and the horizontal lines in the middle of each box represent the median of the data. Each dot represents a single project, and project types (CIR/FDR/CCPR) are differentiated by color. The blue lines in the graphs represent the predicted rutting for the HMA inlay sections at each wearing course thickness.

The CIR projects exhibited a greater range of values in part because there were more of them. The Pavement ME Design software could be used to analyze only two CCPR and three FDR projects.

The trends seen in Figures 52 through 54 clearly show that wearing course thickness is an important factor for predicted rutting. The cold-recycled inlay sections having 3 in. and 4 in. wearing courses had predicted rutting values in a narrow range with a mean value very close to their HMA inlay counterparts for all weather conditions. Rutting decreased as the wearing course thickness increased despite increases in input traffic volume (noted as ESAL) with increased

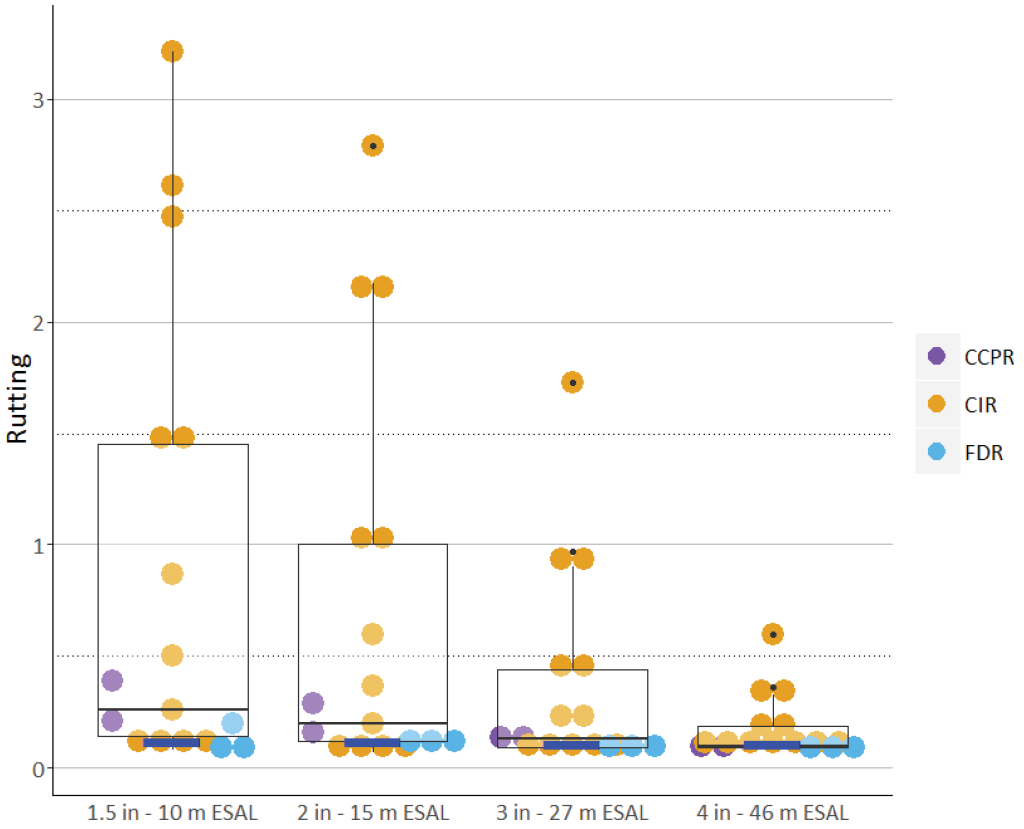

Figure 52. Predicted rutting: Arizona weather.

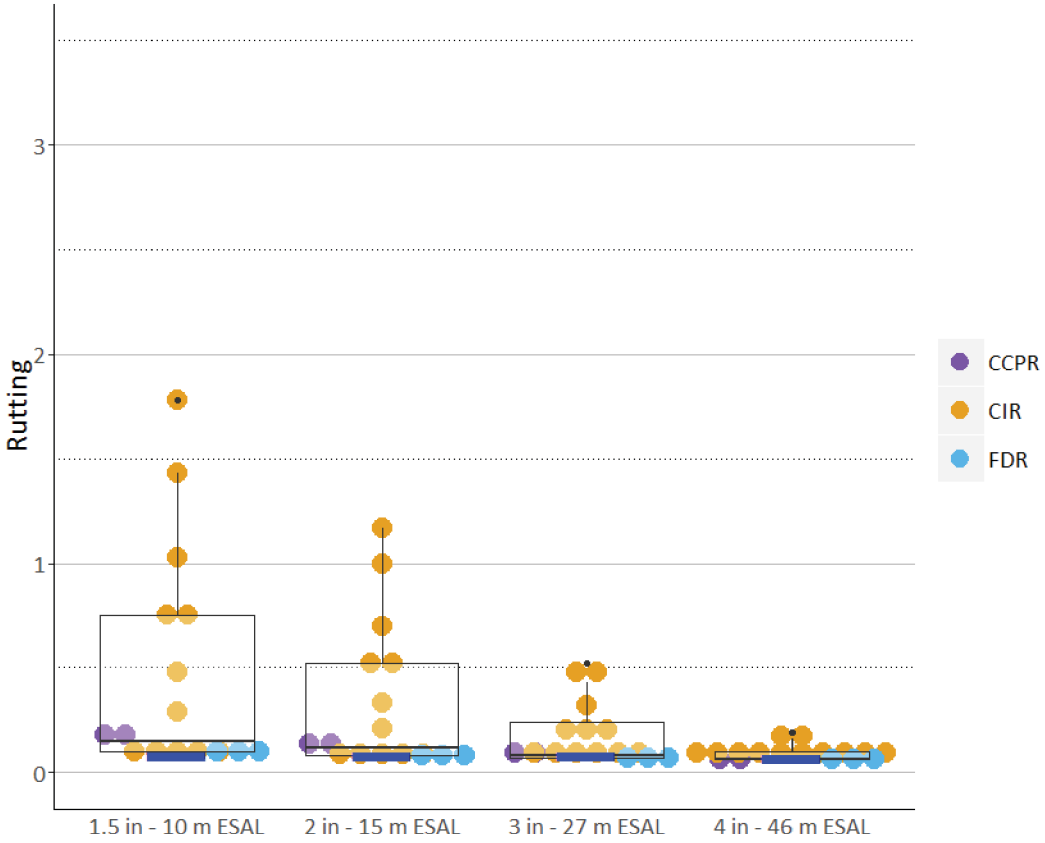

Figure 53. Predicted rutting: Maryland weather.

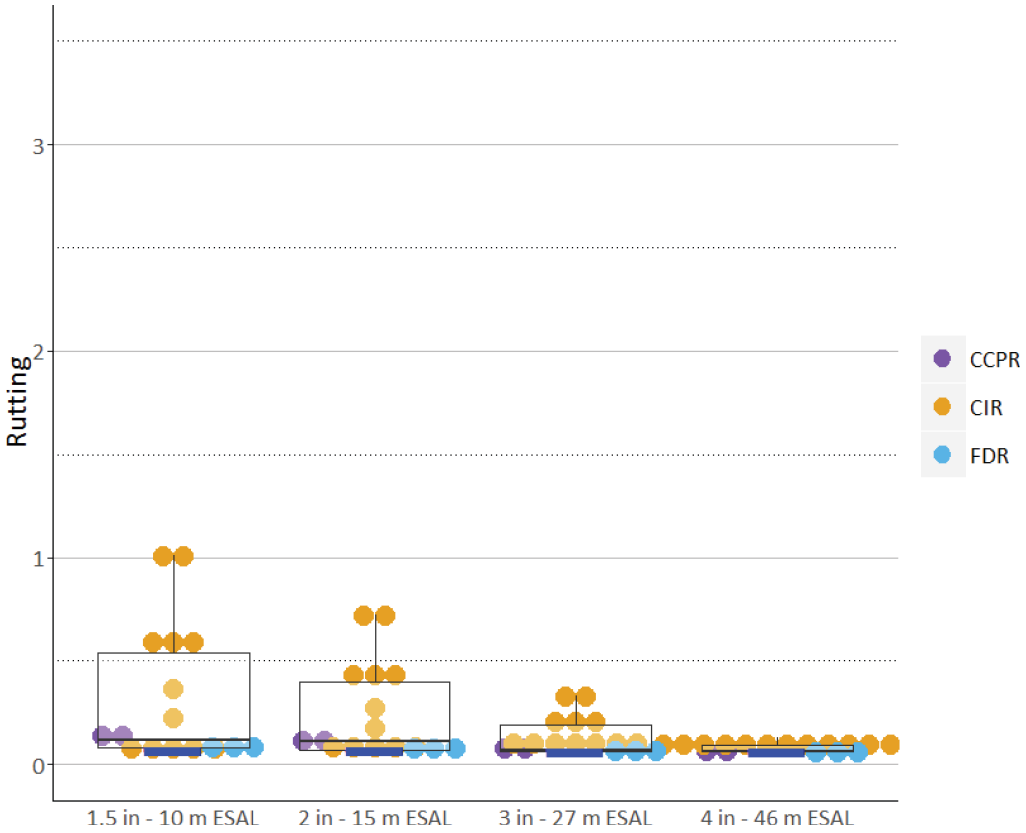

Figure 54. Predicted rutting: Minnesota weather.

wearing course thickness. It can be concluded that, as long as HMA wearing course thickness is above some threshold—approximately 2 in. to 3 in.—the cold-recycled inlay sections exhibit predicted rutting performance comparable to that of conventional HMA inlay sections.

Figures 52 through 54 also show that the range and mean values of predicted rutting for the cold-recycled inlay sections decreases with decreasing temperature, as was expected. The mean predicted rutting under all three weather conditions is acceptable, except perhaps for the thinnest wearing course (1.5 in.). The average values of predicted asphalt concrete rutting for the temperate Maryland weather conditions for the 1.5 in., 2 in., 3 in., and 4 in. wearing course thicknesses were 0.44 in., 0.31 in., 0.16 in., and 0.084 in., respectively. The last two values are well below this study's assumed default design limit of 0.25 in. For the thinner (1.5 in. and 2 in.) wearing courses, the rutting performance can still be considered reasonably good, considering that the traffic applied to these sections was quite high. Although cold-recycled rehabilitation had historically been most commonly used on low volume roads, the results from the present analyses suggest that with a wearing course thickness of more than 2 in., these cold-recycled materials can be used successfully in higher traffic roads. As discussed previously, the five projects with poor rutting performance also had substandard laboratory RLPD behavior. Good quality cold-recycled materials that exhibit satisfactory laboratory RLPD behavior should exhibit satisfactory predicted rutting performance similar to that of conventional HMA mixes.

The five projects with the highest predicted rutting along with selected performance criteria are summarized in Table 23. The arrows in the table indicate whether the respective property fell at the high end or low end of the range of values as compared to the other cold-recycled materials. The results suggest that a higher slope of the RLPD permanent strain versus load cycles is most

Table 23. Projects with highest predicted rutting.

Project	Type	Stabilizer	E* Lower Shelf	RLPD Intercept	RLPD Slope
13-1111	CIR	Foam			↑
14-1026	CIR	Emulsion	↓	↑	↑
14-1055	CIR	Emulsion	↓		↑
13-1112	CIR	Emulsion		↑	↑
14-1025	CIR	Foam		↑	↑

correlated with higher predicted rutting, followed by the RLPD intercept and, in two cases, by the E* lower shelf. Project 13-1111 (a CIR project with foamed asphalt as the recycling agent and exhibiting the highest rutting) had a very high k_3 value (exponent on N) at 0.53, double the average value of 0.27 for all cold-recycled materials in this study (see Table 22). This project also had a very high k_2 value (exponent on T) at 4.51, nearly three times the average value of 1.59. (Project 14-1002, although also having high k_3 and k_2 values, had an exceptionally low k_1 value.) Among all of the cold-recycled mixtures that could be analyzed using the Pavement ME Design software, the five materials listed in Table 23 were among the top six with respect to the highest k_3 values and among the top nine with respect to the highest k_2 values. Interestingly, four of the five projects listed in Table 23 included no chemical additive.

CHAPTER 7

Conclusions

This study measured and evaluated the dynamic modulus and RLPD characteristics from field-produced and field-cured bituminously stabilized cold-recycling mixtures. Dynamic modulus and RLPD properties are inputs to the mechanistic-empirical pavement design methodology embodied in the AASHTOWare Pavement ME Design software. Before this study, little was known regarding appropriate dynamic modulus and RLPD values for cold-recycled materials for use as inputs to mechanistic-empirical pavement design. This study has developed an initial catalog of these properties for bituminously stabilized FDR, CIR, and CCPR cold-recycled materials.

In addition to providing representative values, the investigations examined whether significant differences existed in the dynamic modulus values of FDR, CIR, and CCPR mixtures using different recycling/stabilizing agents and chemical additives. The investigation included statistical analyses of dynamic modulus data at 10 Hz and temperatures of 4.4°C, 21.1°C, and 37.8°C, as well as an evaluation of data envelopes developed from the master curves. The principal conclusions regarding stiffness that were derived from these investigations include the following:

- All three recycling processes had a similar range of dynamic modulus values at intermediate and high reduced frequencies. This conclusion was supported by the statistical testing and is similar to the trend observed by Diefenderfer, Bowers, and Diefenderfer (2015) based on FWD testing. Many highway agencies specify lower structural values (whether layer coefficients or moduli) for FDR than for CIR and CCPR; these lower values may be too conservative.
- FDR showed less temperature dependency and higher stiffness at low reduced frequencies (or higher temperatures), as supported by the statistical testing. Given that CIR and CCPR are composed mostly or entirely of RAP, whereas FDR is composed of RAP and material from an unbound layer, this finding suggests that the existing RAP binder may play a role in the temperature-dependent stiffness properties of CIR and CCPR.
- The master curve data envelopes exhibited much overlap between emulsified asphalt versus foamed asphalt as stabilizing/recycling agents, and no significant difference was shown by the statistical tests. Visual observation of the master curve data envelopes suggests that recycled mixtures using foamed asphalt as the stabilizing/recycling agent may be slightly stiffer at higher temperatures, whereas recycled mixtures using emulsified asphalt as the stabilizing/recycling agent may be slightly stiffer at lower temperatures.
- Visual observation of the master curve data envelopes showed that the presence of a chemical additive generally increased the dynamic modulus values of the recycled mixtures as compared to mixtures with no chemical additive present. When separating the recycling process, the recycling/stabilizing agent, and presence and kind of chemical additive, the statistical tests showed significant differences.
- Visual observation of the master curve data envelopes showed that the presence of a chemical additive generally reduced the recycled materials' stiffness temperature dependency. When evaluating the master curve fitting parameters, no significant difference was shown in the

70 Material Properties of Cold In-Place Recycled and Full-Depth Reclamation Asphalt Concrete

alpha (α) parameter over the total reduced frequency range; however, a significant difference was observed in the gamma (γ) parameter with respect to the effect of lime on CIR specimens using emulsion. This statistical evaluation was based on a limited data set due to an insufficient number of specimens.
- No significant difference was found when comparing the use of hydraulic cement versus lime as a chemical additive at 21.1°C and 37.8°C; however, only the CIR process had projects that used both hydraulic cement and lime as a chemical additive.
- The presence of chemical additives was found to be beneficial with respect to stiffness even though the materials used for testing were 12–24 months old. This finding suggests that the benefits of chemical additives last beyond the initial performance period.
- No strong correlations were found between mixture characteristics (e.g., volumetrics, gradation, density) and stiffness. This finding may be a consequence of the small number of mixtures given the large range of processing types, stabilizing agents, and chemical additives.

The investigations also examined whether significant differences existed in the RLPD properties of FDR, CIR, and CCPR mixtures using different recycling/stabilizing agents and chemical additives. The investigations evaluated data envelopes representing accumulated permanent strain versus load cycle. The principal conclusions regarding RLPD properties derived from these investigations include the following:

- All three recycling processes had similar RLPD characteristics as defined by visual observation of their data envelopes. CIR and CCPR specimens were found to behave very similarly. FDR specimens were found to exhibit lower permanent deformations than CCPR and CIR specimens in some cases. This finding is consistent with the trends in the dynamic modulus envelopes.
- Emulsified asphalt and foamed asphalt stabilizers performed similarly based on visual observation of RLPD data envelopes. This finding is consistent with the trends in the dynamic modulus envelopes.
- Visual observation of the RLPD data envelopes showed that the presence of chemical additives generally increased the mixture's resistance to permanent deformation. In particular, cement reduced the amount of permanent deformation exhibited by the recycled materials.
- The presence of chemical additives was found to be beneficial with respect to rutting susceptibility even though the materials used for testing were 12–24 months old. This finding suggests that the benefits of chemical additives last beyond the initial performance period.
- No clear correlation was found between the slope and intercept values of the power-law RLPD curve and density. This result is most likely a consequence of the small number of mixtures given the large range of processing types, stabilizing agents, and chemical additives.
- The findings suggest that the acceptable COV from AASHTO TP 79 does not adequately reflect the typical variation seen in recycled materials. The allowable variation needs further study for cold-recycled materials.

Predicted performance was evaluated for all of the cold-recycled materials considered in this study. Two baseline pavement scenarios were considered: (1) a rehabilitated pavement having a cold-recycled inlay and an asphalt surface wearing course and (2) a rehabilitated pavement having a HMA recycled inlay and an asphalt surface wearing course. Three wearing course thicknesses with appropriate traffic levels and three climate scenarios were evaluated. All performance predictions were performed using AASHTOWare Pavement ME Design software (Version 2.0) with Level 1 dynamic modulus and RLPD property inputs for the cold-recycled inlay, the HMA inlay, and the asphalt surface wearing course. The investigation examined rutting as the principal distress mode. Conclusions drawn from the rutting predictions for the cold-recycled mixtures considered in this study include the following:

- The predicted rutting performance of the cold-recycled sections generally fell within acceptable ranges. Thirty percent of the analysis cases exhibited poor rutting performance, and these

were mostly sections with only a thin HMA surface wearing course. Predicted rutting decreased significantly as the wearing course thickness increased to 3 in. and 4 in.

- Predicted rutting for the cold-recycled inlay scenarios decreased as the HMA surface wearing course thickness increased. As the cold-recycled layer is pushed deeper into the pavement structure, the behavior approached that of the HMA inlay reference scenario.
- The temperature susceptibility (k_2) and traffic (k_3) exponents in the *MEPDG* rutting model have direct and major impact on the predicted rutting. These exponents are based on the laboratory-measured RLPD plastic strain response and on the resilient strains. Cold-recycled materials that exhibited poor laboratory RLPD behavior (e.g., high k_3, high k_2) also exhibited poor predicted rutting performance.
- The AMPT used for laboratory testing in this study did not report the resilient strains during RLPD testing, so these strains were estimated based on the measured unconfined dynamic modulus modified to correct for the influence of confining stresses in the RLPD test. It is recommended that future testing use an AMPT that directly reports the resilient strains in the RLPD test. Alternatively, the dynamic modulus tests could be performed under confined rather than unconfined conditions so that the appropriate resilient strains can be estimated more accurately.

Rehabilitated pavement sections having good quality cold-recycled materials and a moderately thick HMA surface wearing course (e.g., 2 in. thick or thicker) exhibited predicted pavement performance comparable to that of conventional HMA rehabilitated sections.

References

AASHTO. *Mechanistic–Empirical Pavement Design Guide: A Manual of Practice* (2nd ed.). American Association of State Highway and Transportation Officials, Washington, D.C., 2015.

ARRA. *Basic Asphalt Recycling Manual. Publication No. FHWA-HIF-14-001*. Annapolis, MD: Asphalt Recycling and Reclaiming Association, 2014.

Asphalt Academy. *Technical Guideline: Bitumen Stabilised Materials, 2nd Edition*. Pretoria, South Africa, 2009.

Bemanian, S., P. Polish, and G. Maurer. Cold In-Place Recycling and Full-Depth Reclamation Projects by Nevada Department of Transportation: State of the Practice. In *Transportation Research Record: Journal of the Transportation Research Board, No. 1949.* Transportation Research Board of the National Academies, Washington, D.C., 2006, pp. 54–71.

Biligiri, K. P., K. Kaloush, and J. Uzan. Evaluation of Asphalt Mixtures' Viscoelastic Properties Using Phase Angle Relationships. *The International Journal of Pavement Engineering, 11*(2), 2010, 143–152. https://doi.org/10.1080/10298430903033354

Bonaquist, R. F., D. W. Christensen, and W. Stump III. *NCHRP Report 513: Simple Performance Tester for Superpave Mix Design: First-Article Development and Evaluation.* Transportation Research Board of the National Academies, Washington, D.C., 2003.

Bonaquist, R. F. *NCHRP Report 629: Ruggedness Testing of the Dynamic Modulus and Flow Number Tests with the Simple Performance Tester.* Transportation Research Board of the National Academies, Washington, D.C., 2008.

Bowers, B. F., B. K. Diefenderfer, and S. D. Diefenderfer. Evaluation of Dynamic Modulus in Asphalt Paving Mixtures Utilizing Small-Scale Specimen Geometries. *Electronic Journal of the Association of Asphalt Paving Technologists, 84*, 2015, 497–526.

Cross, S. A., and Y. Jakatimath. Evaluation of Cold In-Place Recycling for Rehabilitation of Transverse Cracking on US 412. Report No. AA-5-11816, Oklahoma State University, Stillwater, OK, 2007.

Diefenderfer, B. K., and S. D. Link. Temperature and Confinement Effects on the Stiffness of a Cold Central-Plant Recycled Mixture. Proceedings: *12th International Society for Asphalt Pavements Conference on Asphalt Pavements*, Raleigh, N.C., 2014. https://doi.org/10.1201/b17219-199

Diefenderfer, B. K., and B. F. Bowers. AAPT/ISAP International Forum: An Agency Perspective on In-Place Pavement Recycling. *Electronic Journal of the Association of Asphalt Paving Technologists, 84*, 2015, 633–657.

Diefenderfer, B. K., B. F. Bowers, and S. D. Diefenderfer. Asphalt Mixture Performance Characterization Using Small-Scale Cylindrical Specimens. Report No. 15-R26, Virginia Center for Transportation Innovation and Research, Charlottesville, 2015.

Diefenderfer, B. K., B. F. Bowers, C. W. Schwartz, A. Farzaneh, and Z. Zhang. *Dynamic Modulus of Recycled Pavement Mixtures. Transportation Research Record: Journal of the Transportation Research Board, No. 2575*, 2016, Transportation Research Board of the National Academies, Washington, D.C., 19–26.

Diefenderfer, B. K., M. D. Sanchez, D. H. Timm, and B. F. Bowers. Structural Study of Cold-Central Plant Recycling Sections at the NCAT Test Track. Report No. 17-R9, Virginia Transportation Research Council, 2017.

Jenkins, K. J., F. M. Long, and L. J. Ebels. Foamed Bitumen Mixes = Shear Performance? *The International Journal of Pavement Engineering, 8*(2), 2007, 85–98. https://doi.org/10.1080/10298430601149718

Khosravifar, S., C. W. Schwartz, and D. G. Goulias. Mechanistic Structural Properties of Foamed Asphalt Stabilized Base Materials. *The International Journal of Pavement Engineering, 16*(1), 2015, 27–38. https://doi.org/10.1080/10298436.2014.893330

Khosravifar, S., I. Haider, A. Afsharikia, and C. W. Schwartz. Application of Time-Temperature Superposition to Develop Master Curves of Cumulative Plastic Strain in Repeated Load Permanent Deformation Tests. *The International Journal of Pavement Engineering, 16*(3), 2015, 214–223. https://doi.org/10.1080/10298436.2014.937810

Kim, Y. R., Y. Seo, M. King, and M. Momen. Dynamic Modulus Testing of Asphalt Concrete in Indirect Tension Mode. *Transportation Research Record: Journal of the Transportation Research Board*, *No. 1891,* Transportation Research Board of the National Academies, Washington, D.C., 2004, pp. 163–173.

Kim, Y. R., H. Lee, and M. Heitzman. Dynamic Modulus and Repeated Load Tests of Cold In-Place Recycling Mixtures using Foamed Asphalt. *Journal of Materials in Civil Engineering, 21*(6), 2009, 279–285. https://doi.org/10.1061/(ASCE)0899-1561(2009)21:6(279)

Li, X., and N. Gibson. Using Small-Scale Specimens for AMPT Dynamic Modulus and Fatigue Tests. *Electronic Journal of the Association of Asphalt Paving Technologists, 82*, 2013, 579–615.

Pellinen, T. K., M. W. Witczak, and R. F. Bonaquist. Asphalt Mix Master Curve Construction Using Sigmoidal Fitting Function With Non-Linear Least Squares Optimization. *Proceedings of 15th Engineering Mechanics Division Conference* (June 4, 2002, Columbia University, New York), American Society of Civil Engineers, Reston, VA, 2004, pp. 83–101.

Pellinen, T. K., S. Xiao, and S. Y. Raval. Dynamic Modulus Testing of Thin Pavement Cores. *Journal of ASTM International, 3*(4), West Conshohocken, PA, 2006, 144–157. https://doi.org/10.1520/JAI12258

Schwartz, C. W., and S. Khosravifar. *Design and Evaluation of Foamed Asphalt Base Materials.* Final Report, Project No. SP909B4E. Maryland Department of Transportation, State Highway Administration, Baltimore, MD, 2013.

Seo, Y., O. El-Haggan, M. King, S. J. Lee, and Y. R. Kim. Air Void Models for the Dynamic Modulus, Fatigue Cracking, and Rutting of Asphalt Concrete. *Journal of Materials in Civil Engineering, 19*(10), American Society of Civil Engineers, Reston, VA, 2007, 874–883. https://doi.org/10.1061/(ASCE)0899-1561(2007)19:10(874)

Stroup-Gardiner, M. *NCHRP Synthesis of Highway Practice 421: Recycling and Reclamation of Asphalt Pavements Using In-Place Methods.* Transportation Research Board of the National Academies, Washington, D.C., 2011. https://doi.org/10.17226/14568

Thenoux, G., A. Gonzalez, and R. Dowling. Energy Consumption Comparison for Different Asphalt Pavements Rehabilitation Techniques Used in Chile. *Resources, Conservation and Recycling, 49*(4), Elsevier, 2007, 325–339. https://doi.org/10.1016/j.resconrec.2006.02.005

Von Quintus, H. L., J. Mallela, R. Bonaquist, C. W. Schwartz, and R. L. Carvalho. *NCHRP Report 719: Calibration of Rutting Models for Structural and Mix Design.* Transportation Research Council of the National Academies, Washington, D.C., 2012. https://doi.org/10.17226/22781

Witczak, M. W., K. Kaloush, T. Pellinen, M. El-Basyouny, and H. L. Von Quintus. *NCHRP Report 465: Simple Performance Test for Superpave Mix Design.* TRB, National Research Council, Washington, D.C., 2002.

Yun, T., B. S. Underwood, and Y. R. Kim. Time-Temperature Superposition for HMA with Growing Damage and Permanent Strain in Confined Tension and Compression. *Journal of Materials in Civil Engineering, 22*(5), American Society of Civil Engineers, Reston, VA, 2010, 415–422. https://doi.org/10.1061/(ASCE)MT.1943-5533.0000039

Zhao, Y., H. Liu, and W. Liu. (2013). Characterization of Linear Viscoelastic Properties of Asphalt Concrete Subjected to Confining Pressure. *Mechanics of Time-Dependent Materials, 17*(3), Springer Netherlands, 2013, 449–463. https://doi.org/10.1007/s11043-012-9196-7

APPENDIX

Deviations from AASHTO TP 79-15

Deviations from AASHTO TP 79-15, Standard Method of Test for Determining the Dynamic Modulus and Flow Number for Asphalt Mixtures using the Asphalt Mixture Performance Tester (AMPT)

9. Procedure A – Dynamic Modulus Test

9.1.2. The air void contents were not measured prior to testing as the specimens were fabricated from field cores.

9.5.2. Test results were not excluded if any existed that were outside the data quality statistics requirements shown in Table 1.

9.7.1.1. Test results were not excluded if any were outside the single-operator precision values shown in Table 3.

10. Procedure B – Flow Number Test

10.1.2. The air void contents were not measured prior to testing as the specimens were fabricated from field cores.

10.6.1.1. Test results were not excluded if any were outside the single-operator precision values shown in Table 5.

X3. Use of Small Test Specimens

X3.1.1. The specimens used during this study had a diameter of 50 mm and a height of 110 mm. End platens were fabricated to match the specimen diameter.

Abbreviations and acronyms used without definitions in TRB publications:

A4A	Airlines for America
AAAE	American Association of Airport Executives
AASHO	American Association of State Highway Officials
AASHTO	American Association of State Highway and Transportation Officials
ACI–NA	Airports Council International–North America
ACRP	Airport Cooperative Research Program
ADA	Americans with Disabilities Act
APTA	American Public Transportation Association
ASCE	American Society of Civil Engineers
ASME	American Society of Mechanical Engineers
ASTM	American Society for Testing and Materials
ATA	American Trucking Associations
CTAA	Community Transportation Association of America
CTBSSP	Commercial Truck and Bus Safety Synthesis Program
DHS	Department of Homeland Security
DOE	Department of Energy
EPA	Environmental Protection Agency
FAA	Federal Aviation Administration
FAST	Fixing America's Surface Transportation Act (2015)
FHWA	Federal Highway Administration
FMCSA	Federal Motor Carrier Safety Administration
FRA	Federal Railroad Administration
FTA	Federal Transit Administration
HMCRP	Hazardous Materials Cooperative Research Program
IEEE	Institute of Electrical and Electronics Engineers
ISTEA	Intermodal Surface Transportation Efficiency Act of 1991
ITE	Institute of Transportation Engineers
MAP-21	Moving Ahead for Progress in the 21st Century Act (2012)
NASA	National Aeronautics and Space Administration
NASAO	National Association of State Aviation Officials
NCFRP	National Cooperative Freight Research Program
NCHRP	National Cooperative Highway Research Program
NHTSA	National Highway Traffic Safety Administration
NTSB	National Transportation Safety Board
PHMSA	Pipeline and Hazardous Materials Safety Administration
RITA	Research and Innovative Technology Administration
SAE	Society of Automotive Engineers
SAFETEA-LU	Safe, Accountable, Flexible, Efficient Transportation Equity Act: A Legacy for Users (2005)
TCRP	Transit Cooperative Research Program
TDC	Transit Development Corporation
TEA-21	Transportation Equity Act for the 21st Century (1998)
TRB	Transportation Research Board
TSA	Transportation Security Administration
U.S.DOT	United States Department of Transportation

TRANSPORTATION RESEARCH BOARD
500 Fifth Street, NW
Washington, DC 20001

ADDRESS SERVICE REQUESTED

The National Academies of
SCIENCES • ENGINEERING • MEDICINE

The nation turns to the National Academies of Sciences, Engineering, and Medicine for independent, objective advice on issues that affect people's lives worldwide.
www.national-academies.org

ISBN 978-0-309-44671-6
90000
9 780309 446716